The Abdus Salam International Centre for Theoretical Physics

United Nations Educational, Scientific and Cultural Organization

IAEA

2165-8

International MedCLIVAR-ICTP-ENEA Summer School on the Mediterranean Climate System and Regional Climate Change

13 - 22 September 2010

Aerosol climate interactions

SOLMON Fabien

The Abdus Salam International Centre
ESP
Trieste
ITALY

Strada Costiera 11, 34151 Trieste, Italy - Tel.+39 040 2240 111; Fax +39 040 224 163 - sci_info@ictp.it

Aerosol climate interactions

F. Solmon (ESP ICTP)

Aerosol - climate interactions

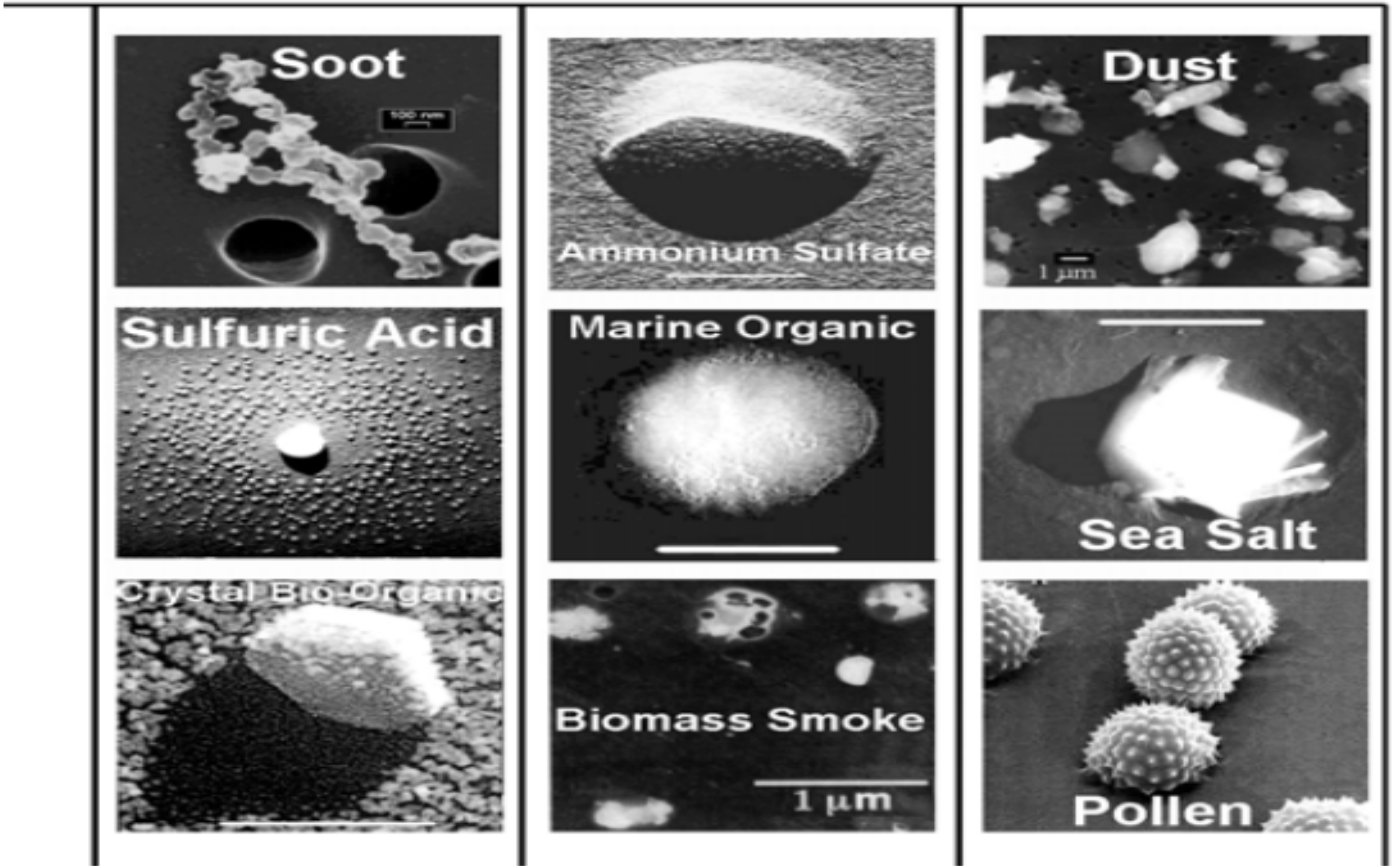

Source variability

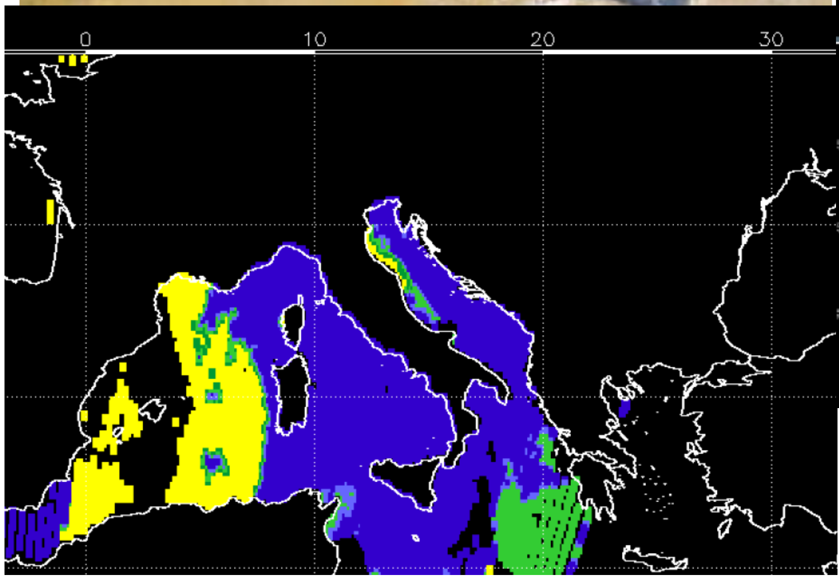

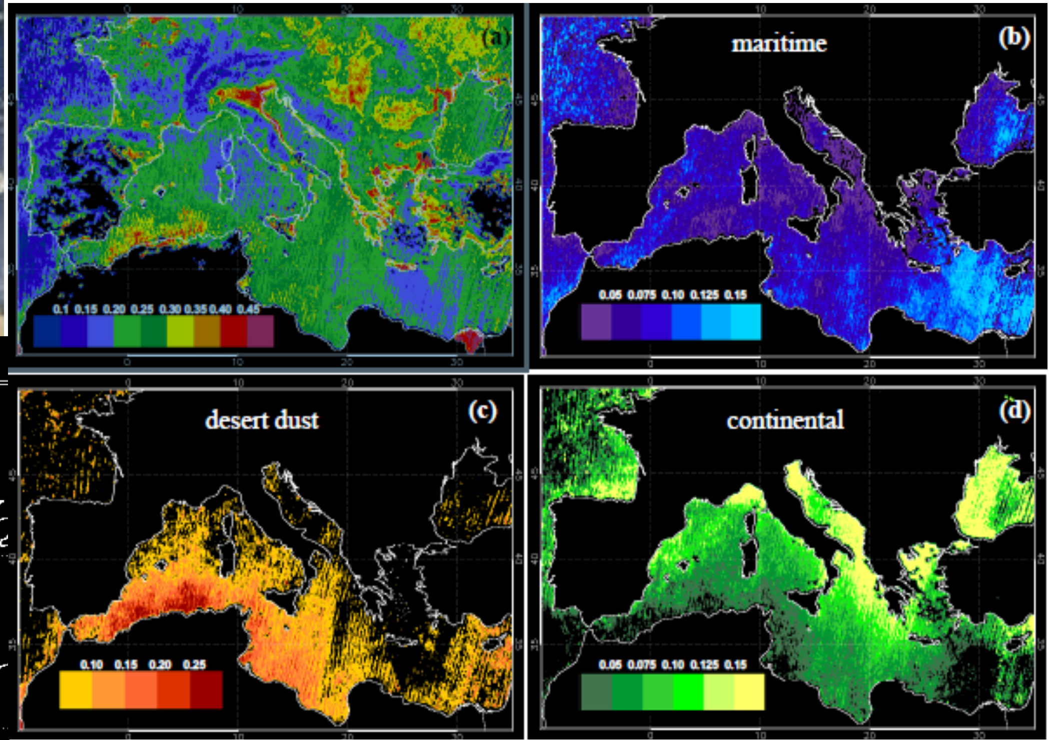

JJA 2001

Barnaba and Gobi 2004

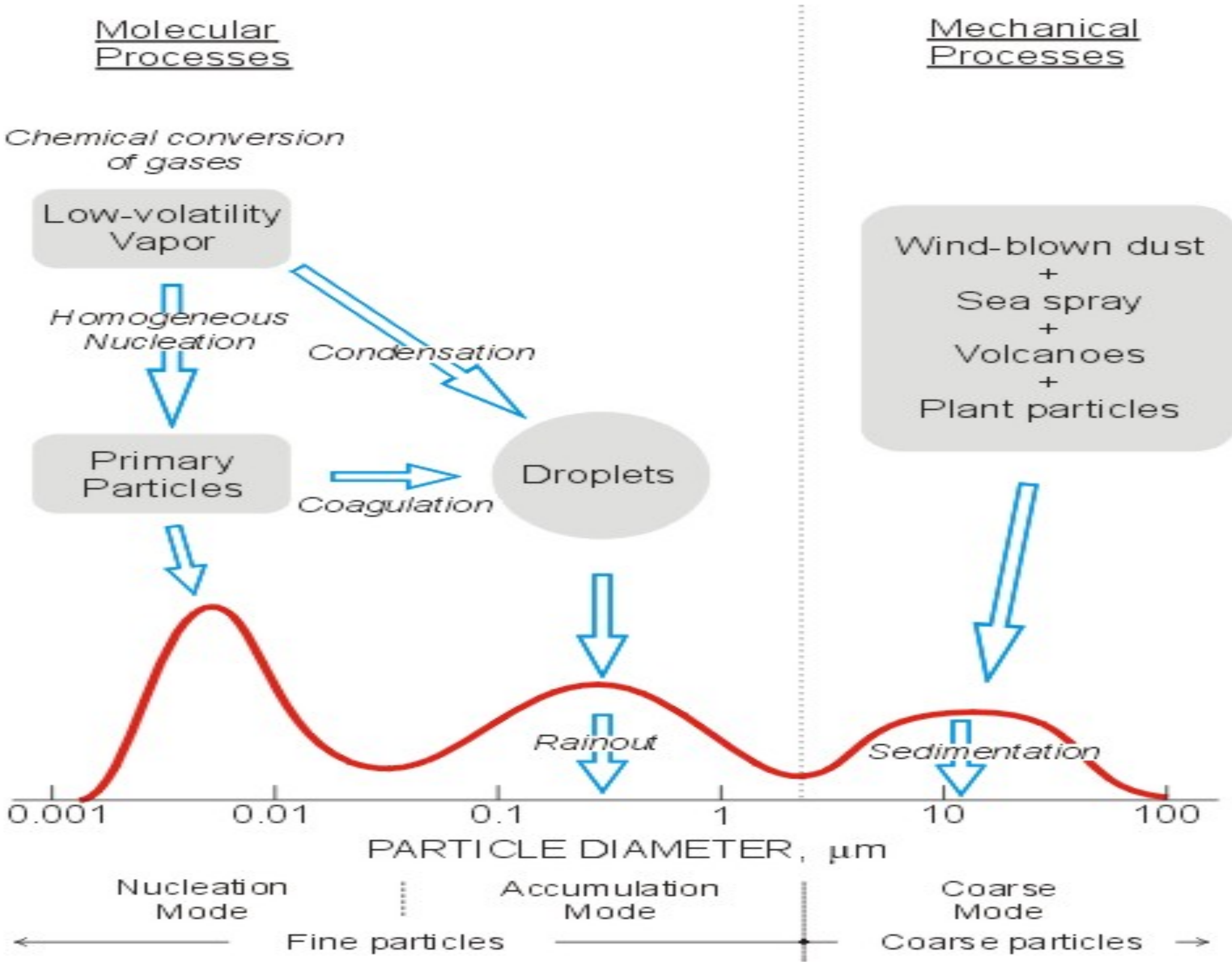
Molecular Processes
Mechanical Processes
Chemical conversion of gases
Low-volatility Vapor
Homogeneous Nucleation
Condensation
Primary Particles
Coagulation
Droplets
Wind-blown dust
+
Sea spray
+
Volcanoes
+
Plant particles
Rainout
Sedimentation
0.001
0.01
0.1
1
10
100
PARTICLE DIAMETER, µm
Nucleation Mode
Accumulation Mode
Coarse Mode
Fine particles
Coarse particles

Aerosol/radiation interactions(Mie theory)

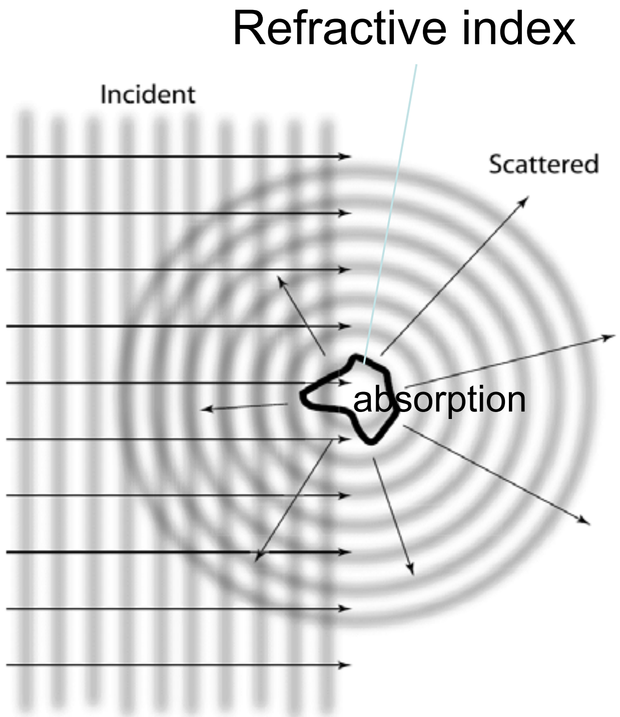

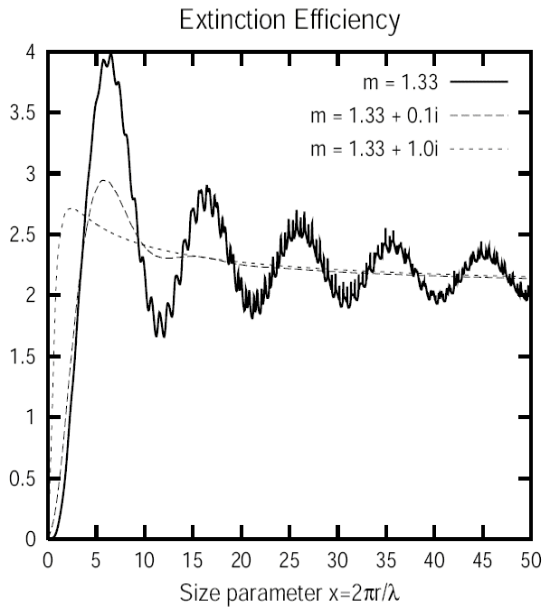

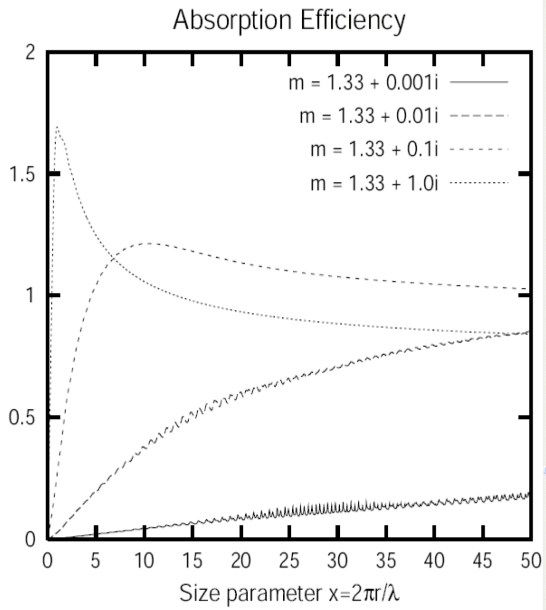

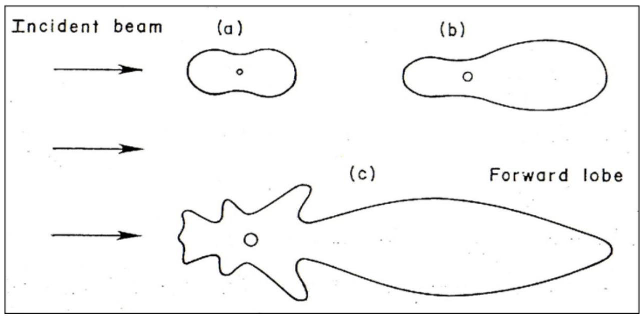

Scatter regimes as a function of 2r= (a)
2r= << 1, (b)2r= 1 (c) 2r= > 1

In modelling we use integrated optical properties over the size distribution.
Kext (m2/g) , SSA, g

Direct effect

Dust Short Wave radiative forcing

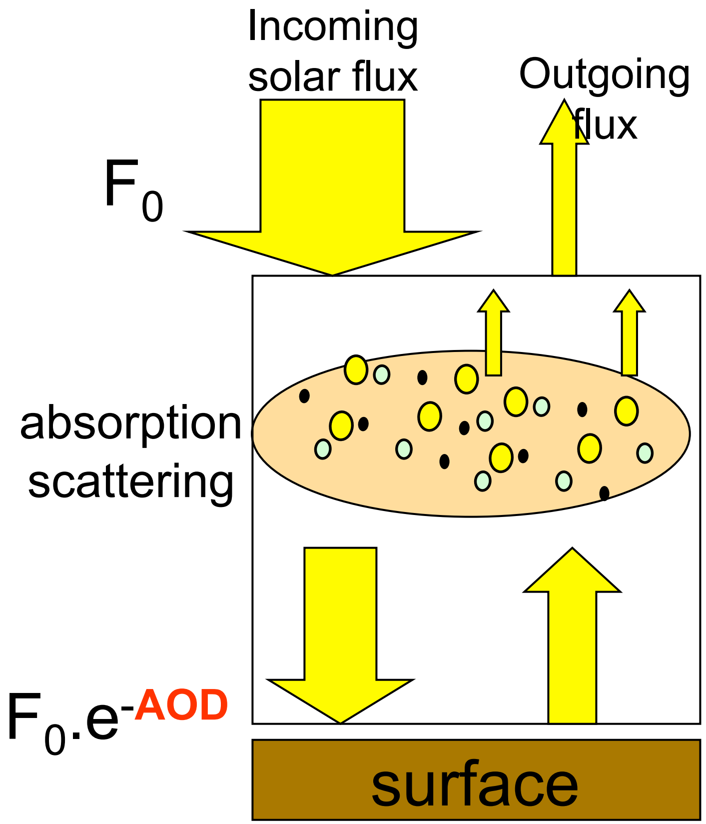

Aerosol optical depth AOD describes the aerosol extinction due to the sum of absorption and scattering effects.

⇨ **TOA SW Radiative forcing** : difference of outgoing fluxes without and with aerosol

All other atmospheric and surface variables being fixed.

> 0. = warming of the system

< 0. = cooling of the system

⇨ **SRF SW Radiative forcing :** difference of net flux at the surface

Always < 0. = cooling of the surface

Dust Long Wave radiative forcing

Atmospheric layers absorb and emit (grey body) in thermal radiation range.
Radiative equilibrium between layers

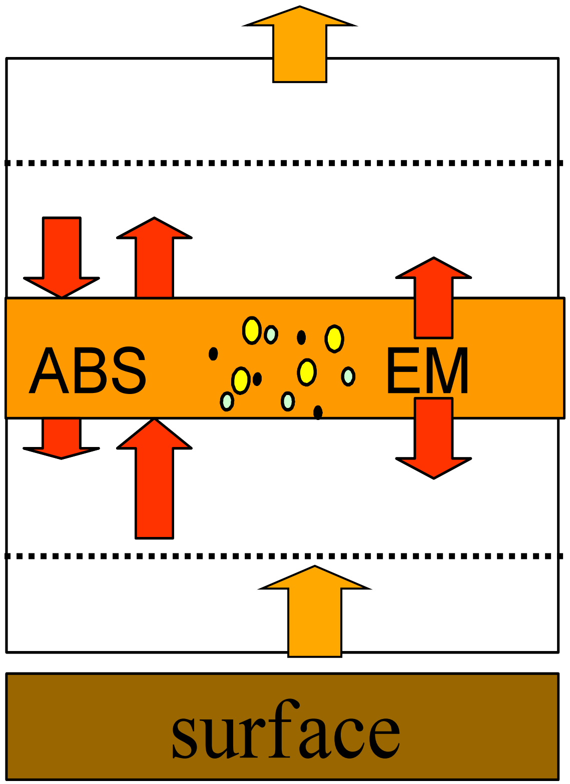

TOA LW Radiative forcing : difference of outgoing fluxes without and with aerosol

All other atmospheric and surface variables being fixed

SRF LW Radiative forcing : difference of net flux at the surface

Always > 0. = relative warming of the surface …

Indirect effects …

Aerosol /cloud interactions

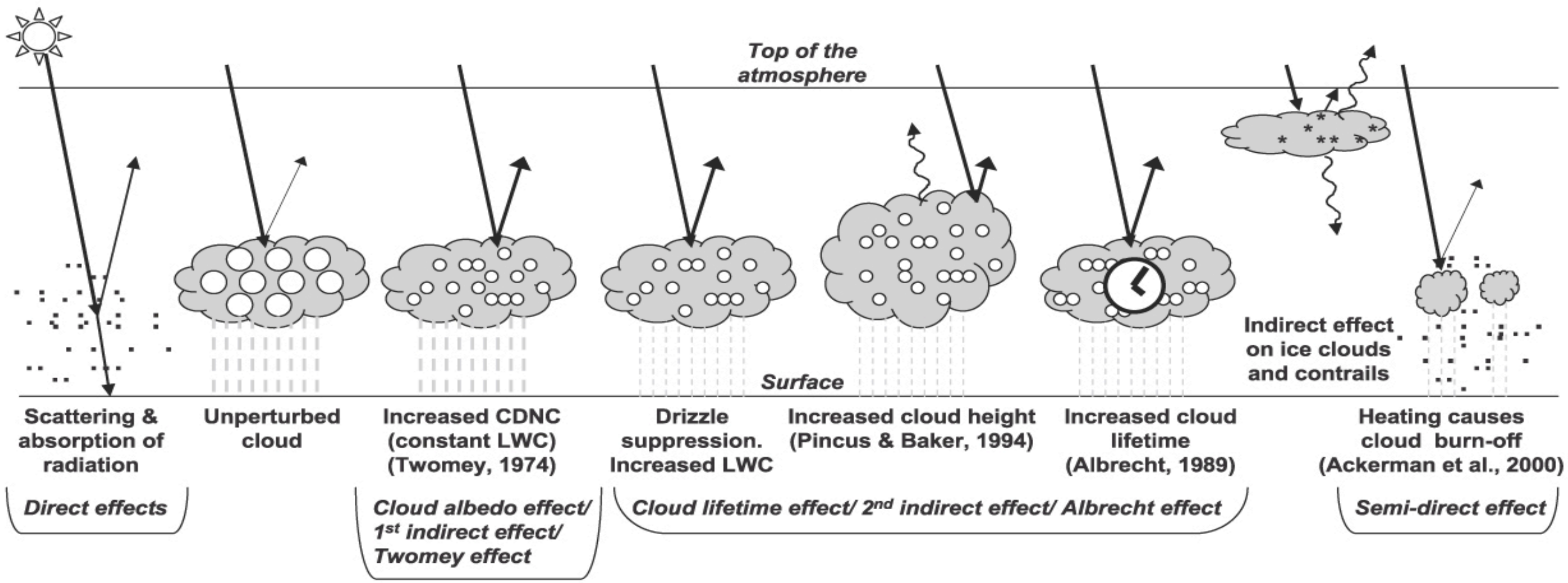

Aerosol deposition on snow

Impact on climate via biogeochemical effects

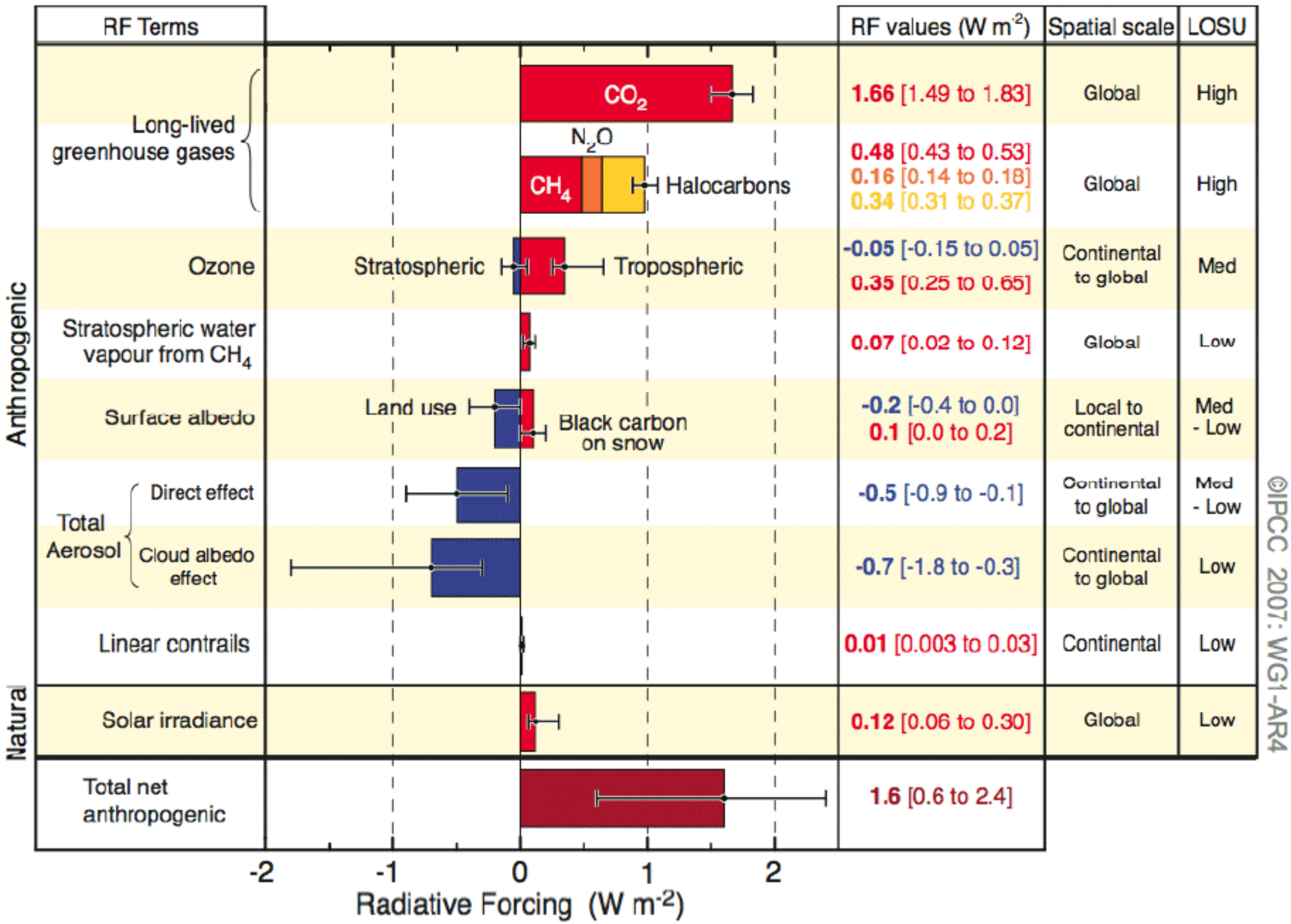
RF Terms
RF values (W m-2)
Spatial scale
LOSU
Anthropogenic
Long-lived greenhouse gases
CO2
1.66 [1.49 to 1.83]
Global
High
N2O
CH4
Halocarbons
0.48 [0.43 to 0.53]
0.16 [0.14 to 0.18]
0.34 [0.31 to 0.37]
Global
High
Ozone
Stratospheric
Tropospheric
-0.05 [-0.15 to 0.05]
0.35 [0.25 to 0.65]
Continental to global
Med
Stratospheric water vapour from CH4
0.07 [0.02 to 0.12]
Global
Low
Surface albedo
Land use
Black carbon on snow
-0.2 [-0.4 to 0.0]
0.1 [0.0 to 0.2]
Local to continental
Med - Low
Total Aerosol
Direct effect
-0.5 [-0.9 to -0.1]
Continental to global
Med - Low
Cloud albedo effect
-0.7 [-1.8 to -0.3]
Continental to global
Low
Linear contrails
0.01 [0.003 to 0.03]
Continental
Low
Natural
Solar irradiance
0.12 [0.06 to 0.30]
Global
Low
Total net anthropogenic
1.6 [0.6 to 2.4]
-2
-1
0
1
2
Radiative Forcing (W m-2)
©IPCC 2007: WG1-AR4

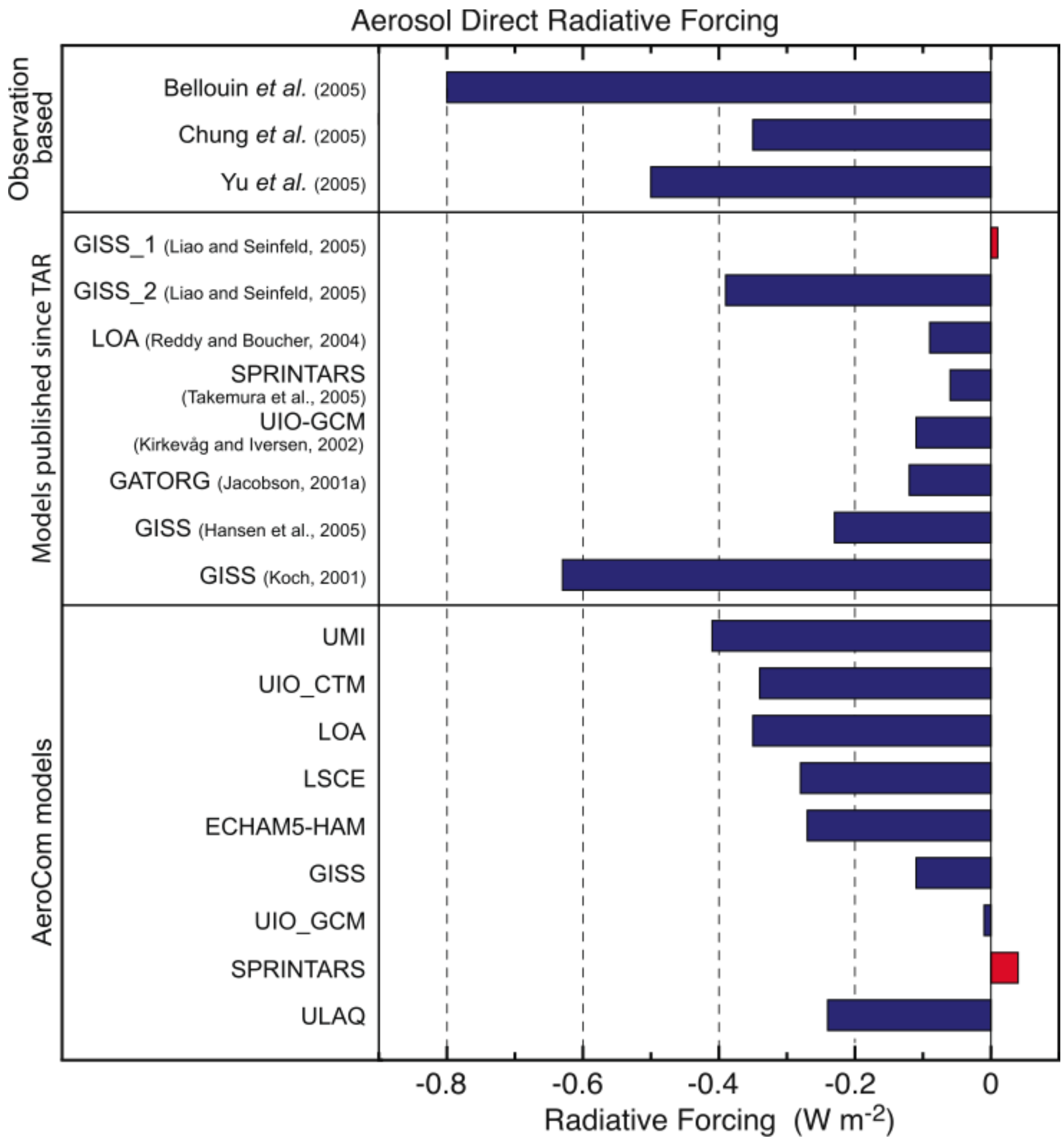
Aerosol Direct Radiative Forcing
Observation based
Bellouin et al. (2005)
Chung et al. (2005)
Yu et al. (2005)
Models published since TAR
GISS_1 (Liao and Seinfeld, 2005)
GISS_2 (Liao and Seinfeld, 2005)
LOA (Reddy and Boucher, 2004)
SPRINTARS (Takemura et al., 2005)
UIO-GCM (Kirkevåg and Iversen, 2002)
GATORG (Jacobson, 2001a)
GISS (Hansen et al., 2005)
GISS (Koch, 2001)
AeroCom models
UMI
UIO_CTM
LOA
LSCE
ECHAM5-HAM
GISS
UIO_GCM
SPRINTARS
ULAQ
-0.8
-0.6
-0.4
-0.2
0
Radiative Forcing (W m-2)

Incremental development of climate/earth system models

Example of studies:

Global dimming (global vs local) :Slide from P.Alpert

Aerosol regional climate effect over China

Dust impact on west African regional climate

Importance of atmospheric processing of aerosol, biogeochemical implications

Geophys. Res. Lett., 32, L17802, doi:10.1029/2005GL023320, 2005.

1. Global Dimming or Local Dimming?

Effect of Urbanization on Sunlight Availability

Alpert, P. (1), Kishcha, P. (1), Kaufman, Y.J. (2) and Schwarzbard, R. (1)

More recent findings based on global gridded population density,
that strengthen our point, will be added

Background

- It was suggested by Stanhill & Cohen (2001) that “Global Dimming”, i.e. significant global decrease of surface solar radiation, took place during 1950s-1980s.
- Also supported by others, e.g., Gilgen et al (1998), Liepert (2002), Cohen et al (2004).
- This finding was based on several hundreds of pyranometer measurements, distributed world-wide, most are archived in the GEBA data-base, Switzerland, (Thanks to Gilgen et al).
- Climate simulations suggest that direct, semi-direct and indirect aerosol effects on clouds & interaction with GHG forcing could explain the solar dimming, Liepert et al (2004).

Motivation

- It is the purpose of our study to show that the solar dimming was dominated by large urban sites.
- Since most of the globe has sparse population, this suggests that the solar dimming was# of local or regional scale- NOT global.

- #*Comment:* *Our study is in line with recent studies showing a reversal of the trend to "Brightening", since the late 1980s, Wild et al. (2005), Pinker et al. (2005).*

1st Class Pyranometer for measuring solar radiation

Pyranometers are deployed in some weather stations throughout the world

Radiation fluxes (1964 – 1989) in the equatorial regions

$15^oS – 15^oN$

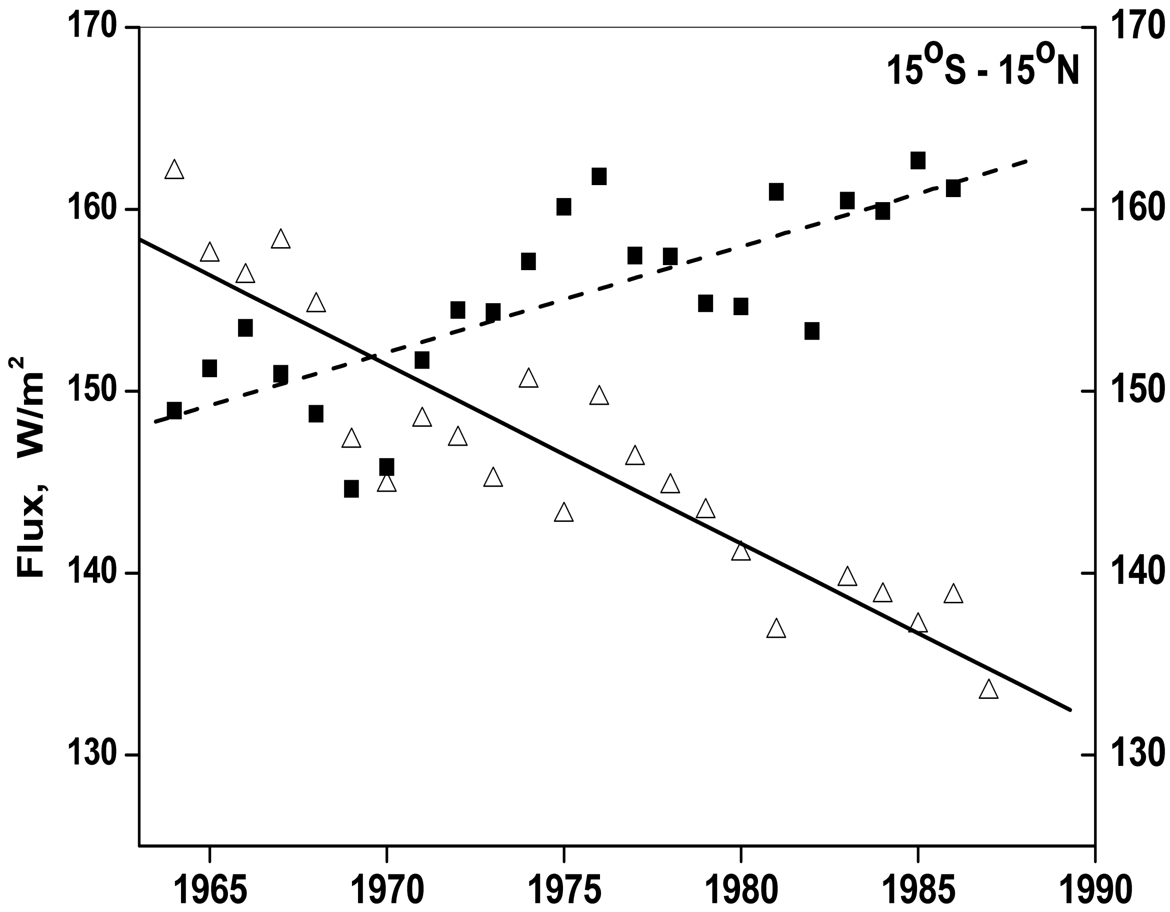

Notice, opposite trend to dimming, i.e. brightening, for sparsely populated sites

Highly populated sites –higher than 100,000 persons/site

Annual radiation fluxes (1964 – 1989) for

10°- 40° N

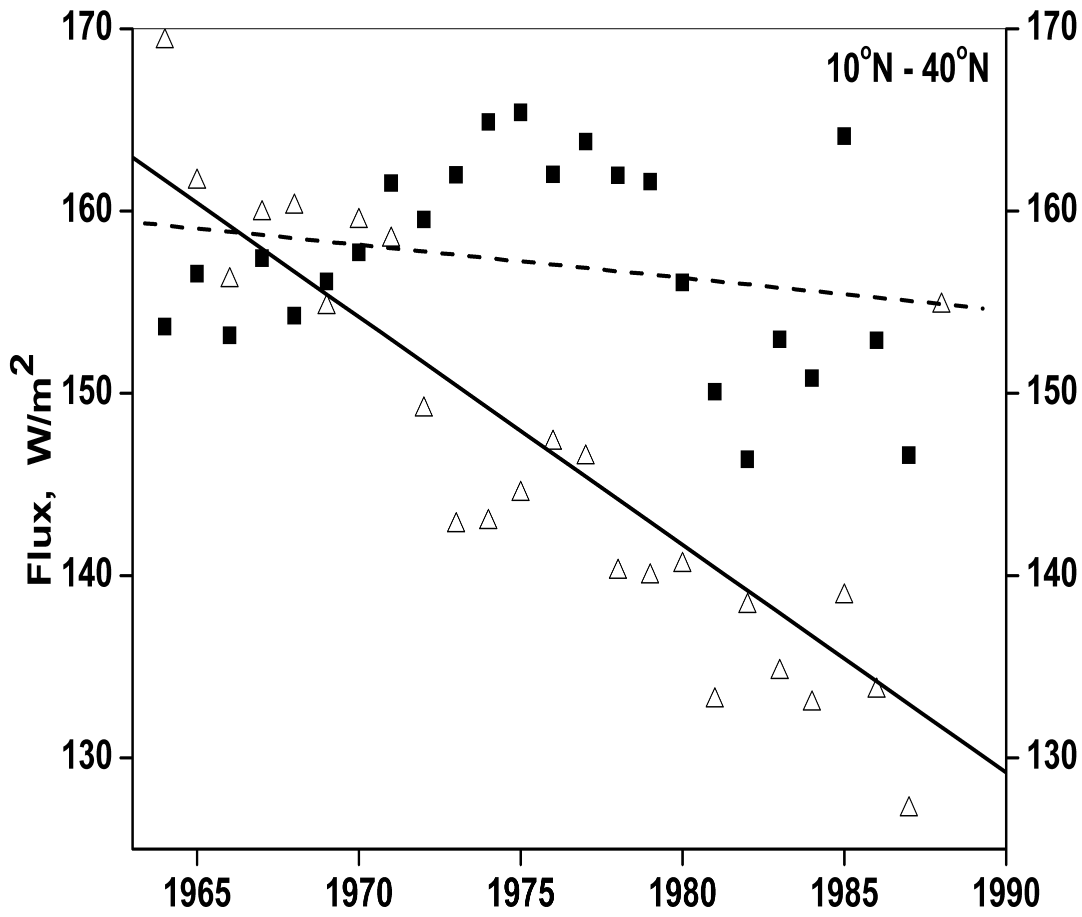

The sharpest is the mid-latitude decline of **-1.25 W/m²/yr** for the highly populated sites.
Compared to **-0.18 & not-significant** for the non-populated sites.

1964-1989 slopes averaged for populated & sparsely-populated sites' groups for some latitudinal zones

Latitudinal zone	Number of sites used	Slope W/m^2/yr	Goodness-of-fit R^2	Significance level p
	All sites			
Global scale	318	-0.27	0.43	<0.001
	Highly populated sites			
Global scale	144	-0.43	0.52	<0.001
15ºS – 15ºN	27	-0.98	0.84	<0.001
10ºN – 40ºN	37	-1.25	0.68	<0.001
40ºN – 70ºN	84	-0.19	0.27	<0.010
	Sparsely populated sites			
Global scale	174	-0.16	0.18	<0.040
15ºS – 15ºN	21	0.58	0.58	<0.001
10ºN – 40ºN	31	-0.18	0.05	Not significant
40ºN – 70ºN	117	-0.27	0.35	<0.002

Population changes (dP) & surface radiation decline (dI)

Numbers (percentages) of sites with negative and positive relative flux changes (dI)# for four population interval changes (dP)

dI	dP interval, million				
	All	< 0	0≤ & <0.1	0.1≤ & <0.5	≥0.5
All values	121	16	21	56	28
< 0	80 (66%)	8 (50%)	11 (52%)	39 (70%)	22 (79%)
≥ 0	41 (34%)	8 (50%)	10 (48%)	17 (30%)	6 (21%)

Conclusion: The percentage of sites with negative flux changes steadily increases with population change

#The relative flux changes dI between the 10-year periods: 1980-1989 and 1964-1973, respectively:

$$dI = (I(80 \div 89) - I(64 \div 73)) \cdot 100\% / I(64 \div 73)$$

Large industrial/ urban areas like N. Italy, SE England, N. Germany can be noticed

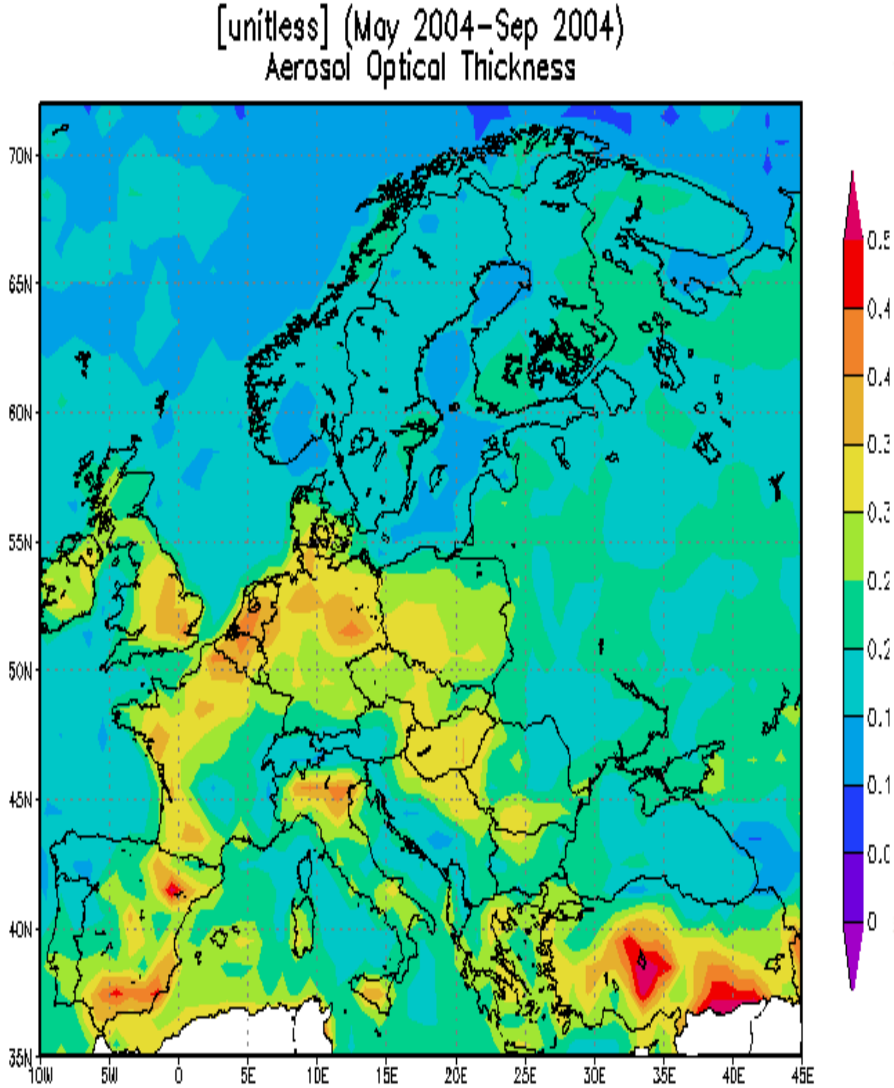

Population density over Europe

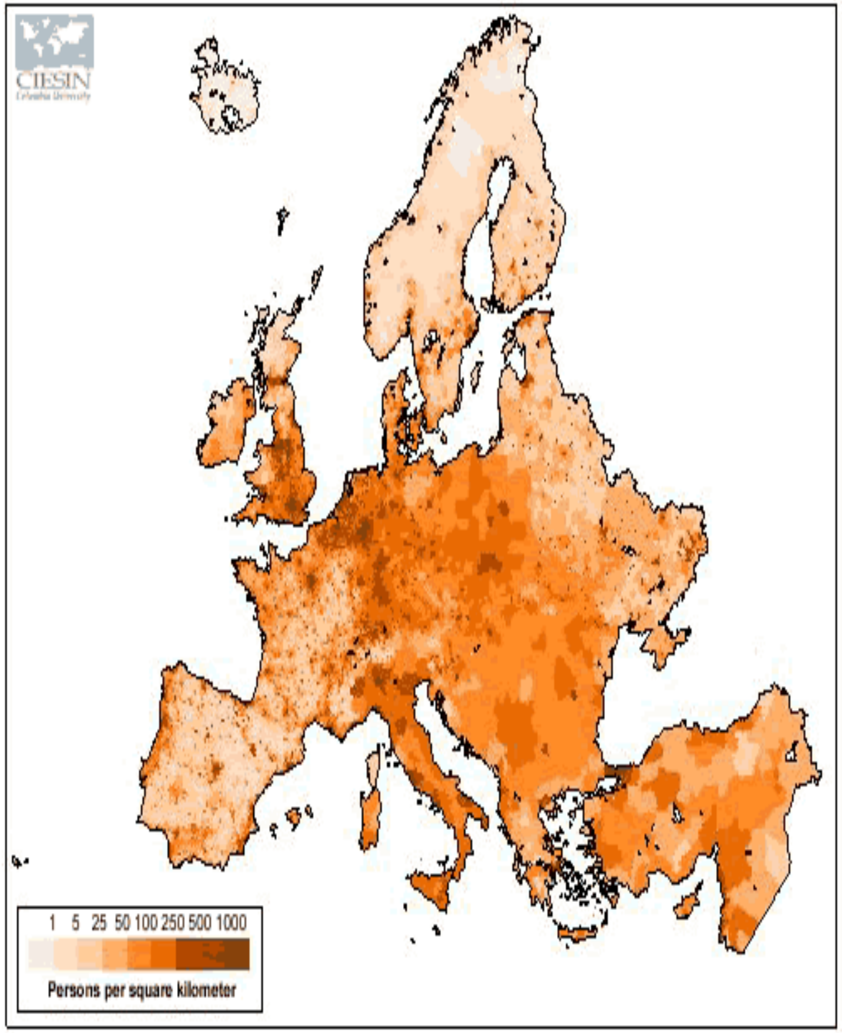

Summary

- The solar dimming phenomenon is significantly dominated by large cities' pollution.
- Since most of the globe has sparse population, this suggests that solar dimming is basically of a local nature- NOT GLOBAL.
- The dimming is sharpest for the sites at 10°N-40°N with great industrial activity.
- In the equatorial regions brightening was observed for sparsely populated sites between 1964 and 1989.
- Other urban development effects on solar radiation besides aerosols also exist: heat island,surface albedo, forest removal etc.

Global Land Area (%) with increasing Population Density, P (in person/km^2)

Population density, (P, person/km^2)	0< P <0.1	0.1< P <1	1< P <10	10< P <100	100< P <1000	1000< P <10000	10000< P <50000	P> 50000
Land Area (% of global land)	23.7	21.8	25.9	20.7	7.44	0.51	0.01	0.0002

92%

0.6%

99.4%

Ref.: Gridded Population of the World Version 3 (GPWv3, 2005). Center for International Earth Science Information Network (CIESIN), Columbia University; and Centro Internacional de Agricultura Tropical (CIAT). 2005.

P. Alpert and P. Kishcha, "Quantification of the effect of urbanization on solar dimming", Geophys. Res. Lett., 35, L08801, doi:10.1029/2007GL033012, 2008.

Effect of Urbanization on Solar Dimming

obtained for all 317 globally-distributed sites (1964-1989)

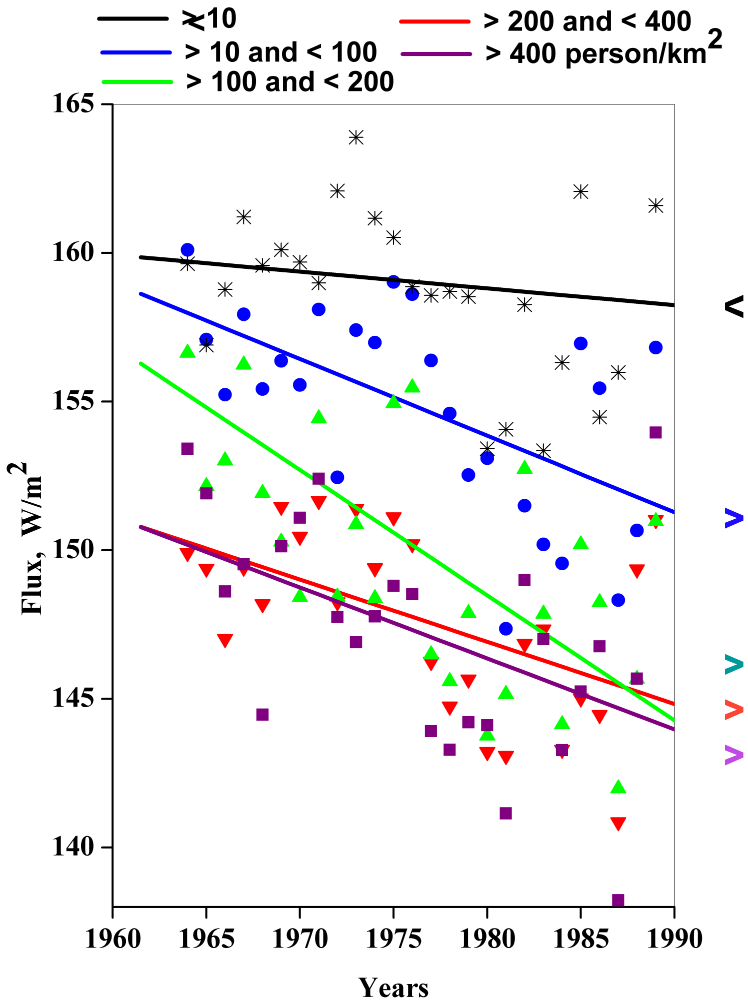

Population density	Surface solar radiation trend	Number of pyranometer sites	Significance level
< 10	-0.05 W/m²/yr	44	Not signific.
> 10 & < 100	-0.26 W/m²/yr	109	0.002
> 100 & < 200	-0.32 W/m²/yr	56	0.001
> 200 & < 400	-0.22 W/m²/yr	53	0.007
> 400	-0.24 W/m²/yr	55	0.013

Dimming is essentially dominated by anthropogenic emissions: a decline in surface solar radiation became sharper at sites with population density increasing up to 200 persom/km²;

Some saturation was observed at highly-populated sites: the trend at sites with population density > 200 persom/km² was less pronounced than that at sites with a lower population density.

Effect of Urbanization on Solar Dimming

obtained for 201 pyranometer sites distributed from 40°N to 70°N (1964-1989)

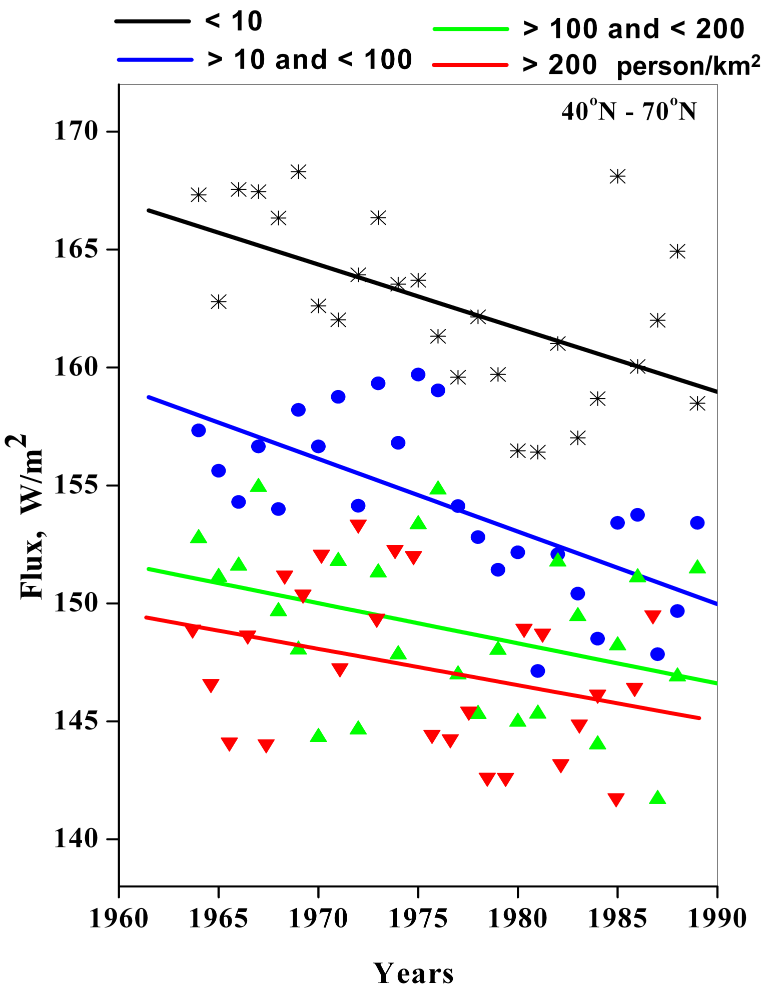

Population density	Surface solar radiation trend	Number of pyranometer sites	Significance level
< 10	-0.27 W/m²/yr	29	0.003
> 10 & < 100	-0.31 W/m²/yr	67	0.003
> 100 & < 200	-0.17 W/m²/yr	40	Not signific.
> 200	-0.14 W/m²/yr	65	Not signific.

Dimming was observed even at sparsely-populated sites with population density < 10 persom/km²;
Dimming was less pronounced at highly-populated sites (> 100 persom/km²) than that at sparsely-populated sites (< 10 persom/km²).

Effect of Increasing Population Density on Solar Dimming obtained for all 318 globally-distributed sites (1964-1989)

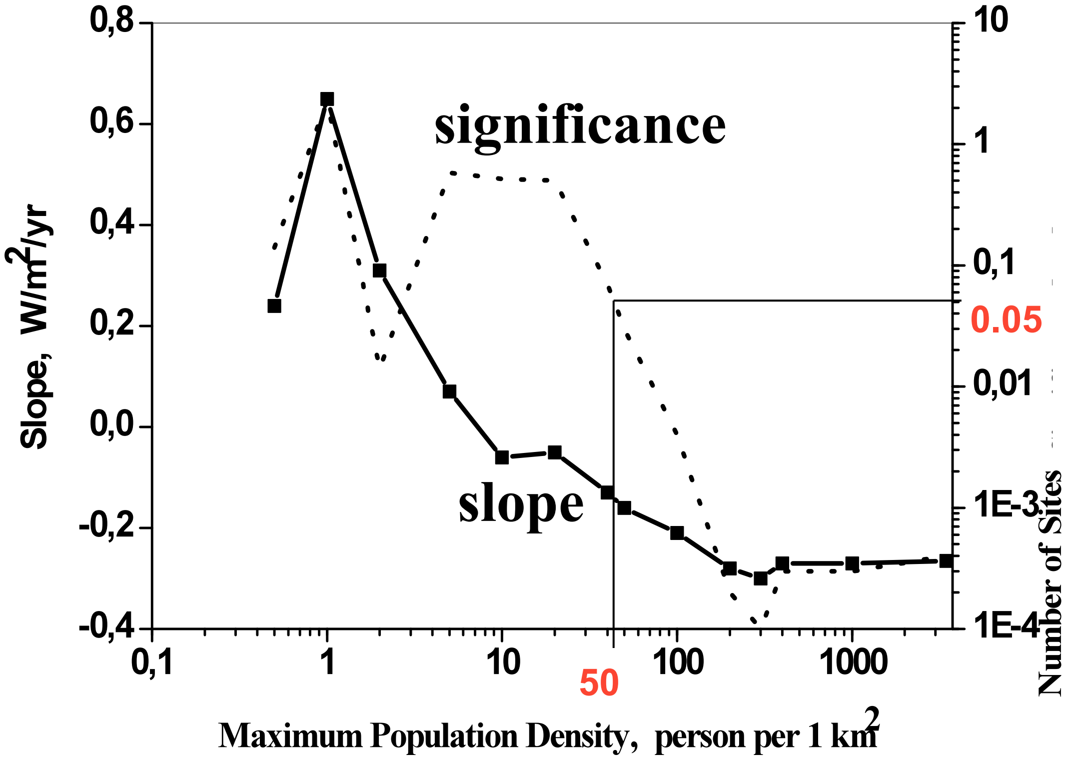

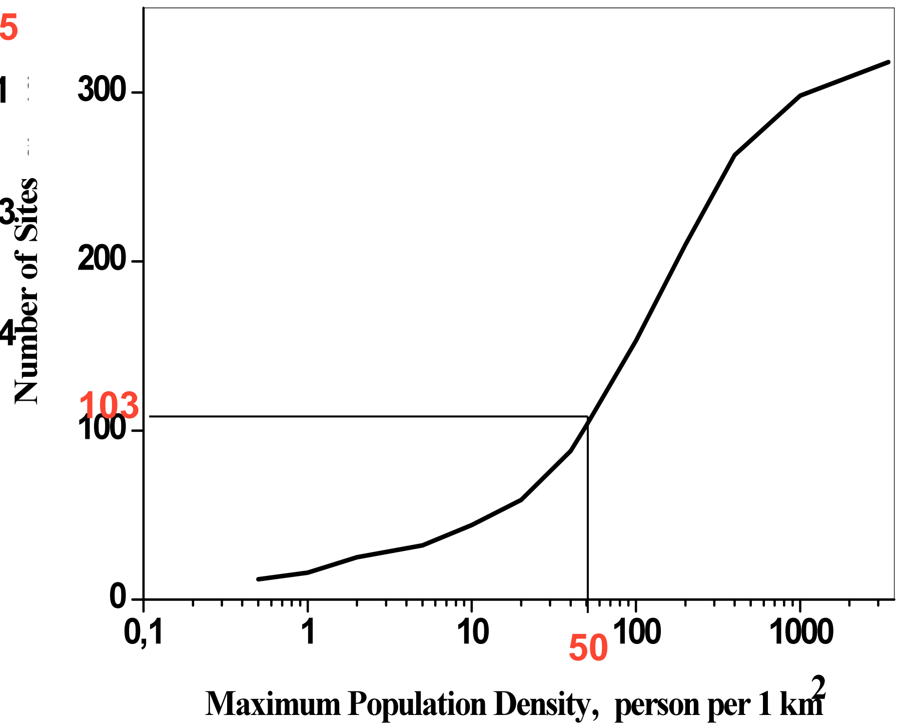

Dimming becomes totally significant from -0.16 to -0.27 W/m2/yr when maximum population density is higher than 50 person/km^2.

Effect of Increasing Population Density on Solar Dimming

obtained only for 208 sites at latitudes higher than 40°N

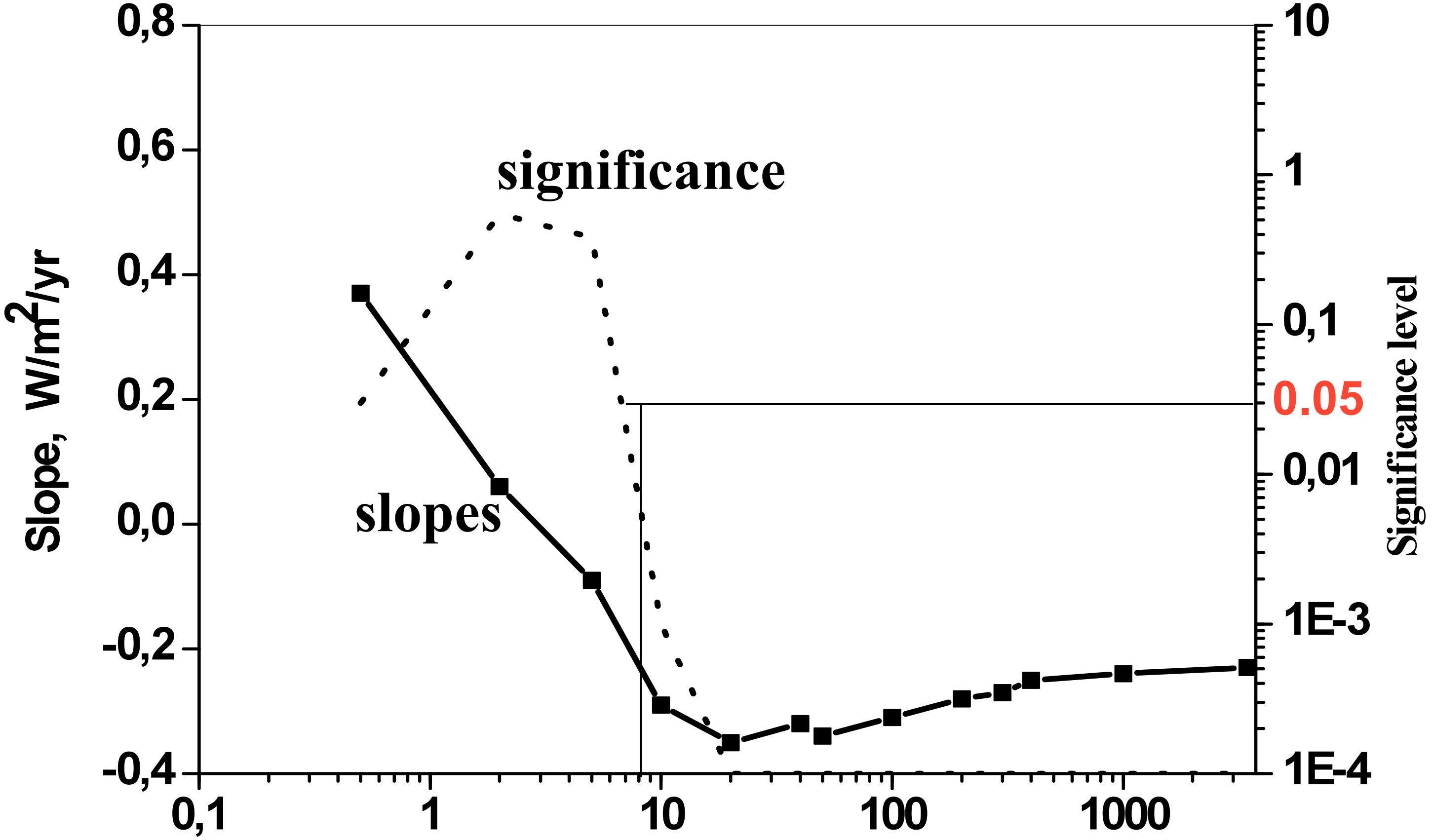

At middle latitudes dimming becomes totally significant when maximum population density is higher than about **10 person/km²**.

Aerosol regional climate effect over China

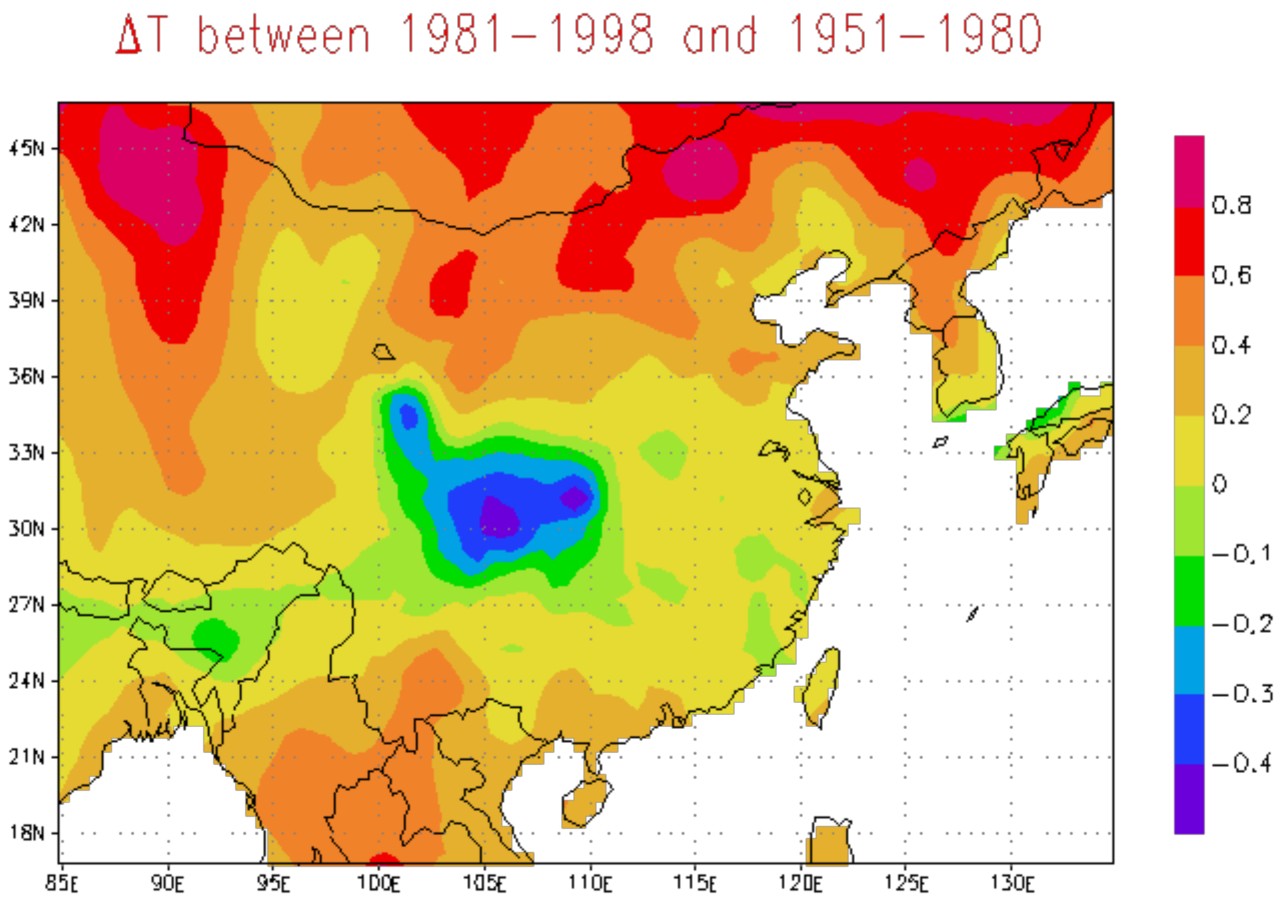

Change of observed mean temperature (°C) in China

Qian and Giorgi (2000)

A modelling approach …

Regional Climate Model

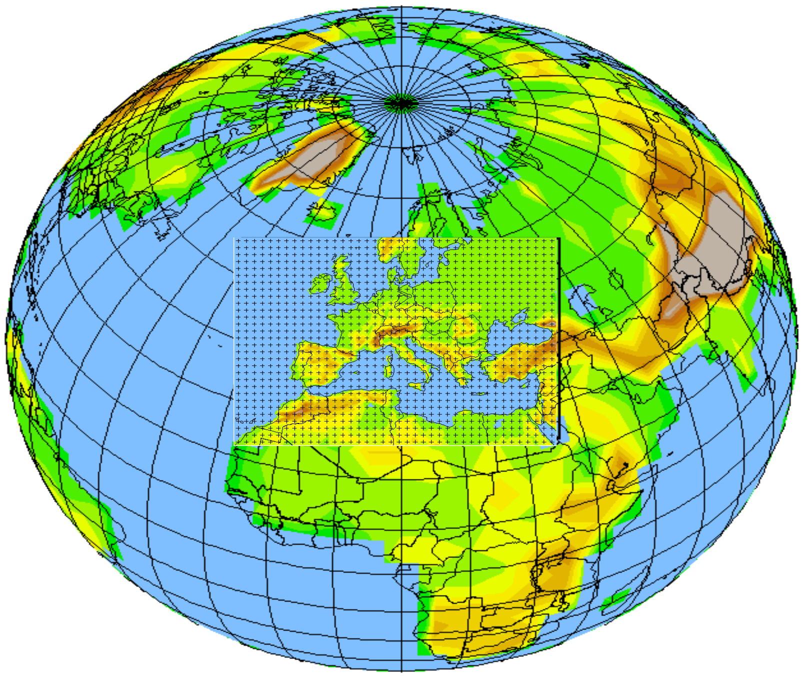

High resolution limited area models adapted to climatic simulations.

Forced by analysis or GCM outputs.

RegCM (ICTP/UNESCO, Trieste, it)

Giorgi and Mearns (1999), RegCM special issue of JGR (1999)

…

RegCNET

Special Issue of Theor., Apl., Clim., sep 2006

Aerosols in RegCM3

- **Tracer model / RegCM3**

$$\frac{\partial \chi}{\partial t} = -\overline{V} \cdot \nabla \chi + F_H + F_V + T_{CUM} + S_\chi - R_{w,ls} - R_{w,cum} - D_{dep} + \sum Q_p - Q_l$$

Transport | Primary Emissions | Removal terms | Physico – chemical transformations

- **Particles and chemical species considered**

SO_2	SO_4^{--}	BC (soot)		OC (total organic carbon)		DUST (4 bins)			
Aqueous and gazeous conversion (Qian et al., 2001)		*Hydrophilic (20% at emission)*	*Hydrophobic* (80%at emission)	*Hydrophilic (50%at emission)*	*Hydrophobic(50%at emission)*	0.01-1 µm	1-2.5 µm	2.5-5 µm	5-20 µm

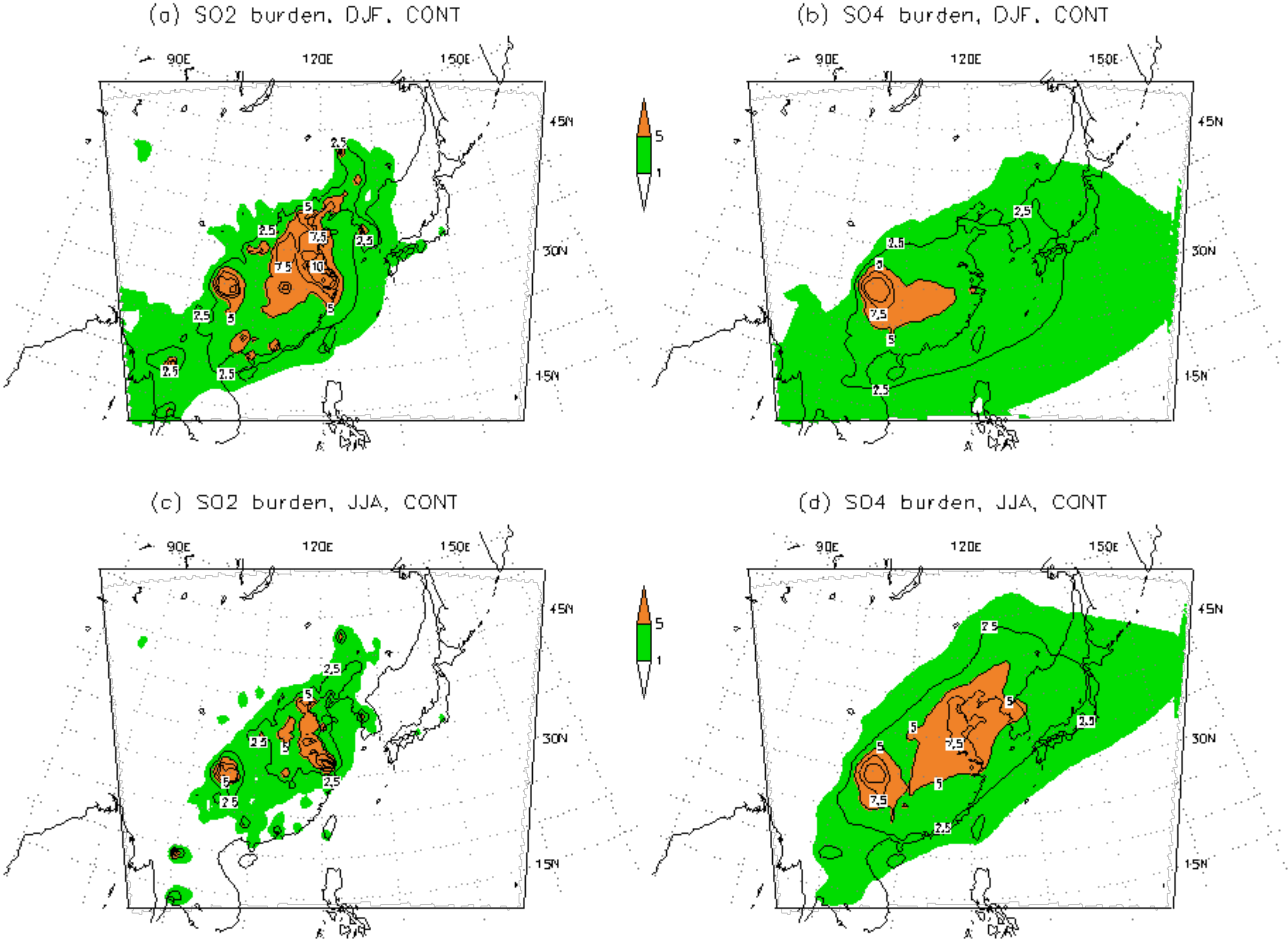
(a) SO2 burden, DJF, CONT
(b) SO4 burden, DJF, CONT
(c) SO2 burden, JJA, CONT
(d) SO4 burden, JJA, CONT
90E
120E
150E
45N
30N
15N
5
1

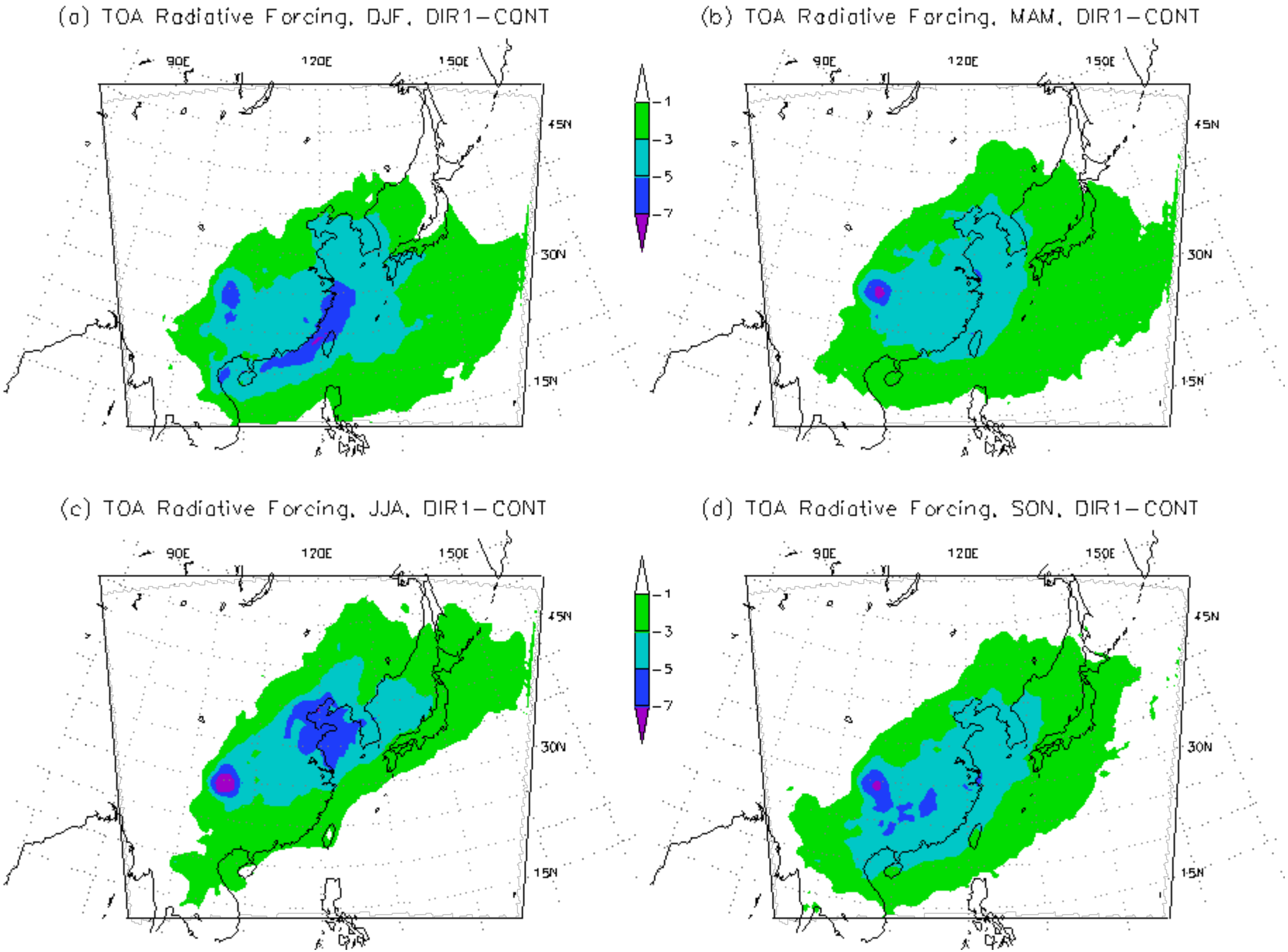
(a) TOA Radiative Forcing, DJF, DIR1-CONT
(b) TOA Radiative Forcing, MAM, DIR1-CONT
(c) TOA Radiative Forcing, JJA, DIR1-CONT
(d) TOA Radiative Forcing, SON, DIR1-CONT
90E
120E
150E
45N
30N
15N
-1
-3
-5
-7

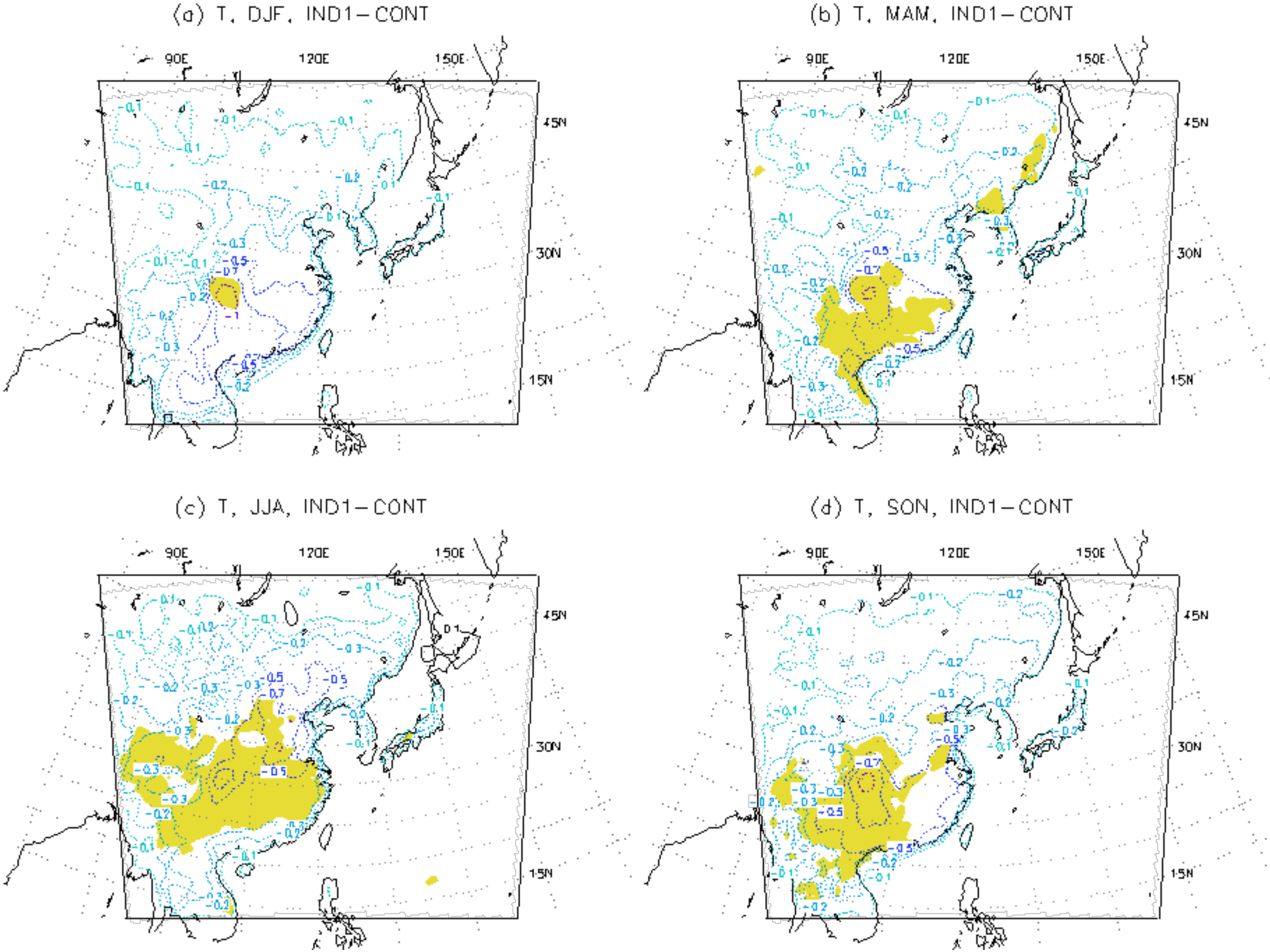
(a) T, DJF, IND1−CONT
(b) T, MAM, IND1−CONT
(c) T, JJA, IND1−CONT
(d) T, SON, IND1−CONT
90E
120E
150E
45N
30N
15N

Climatic impact of saharan dust

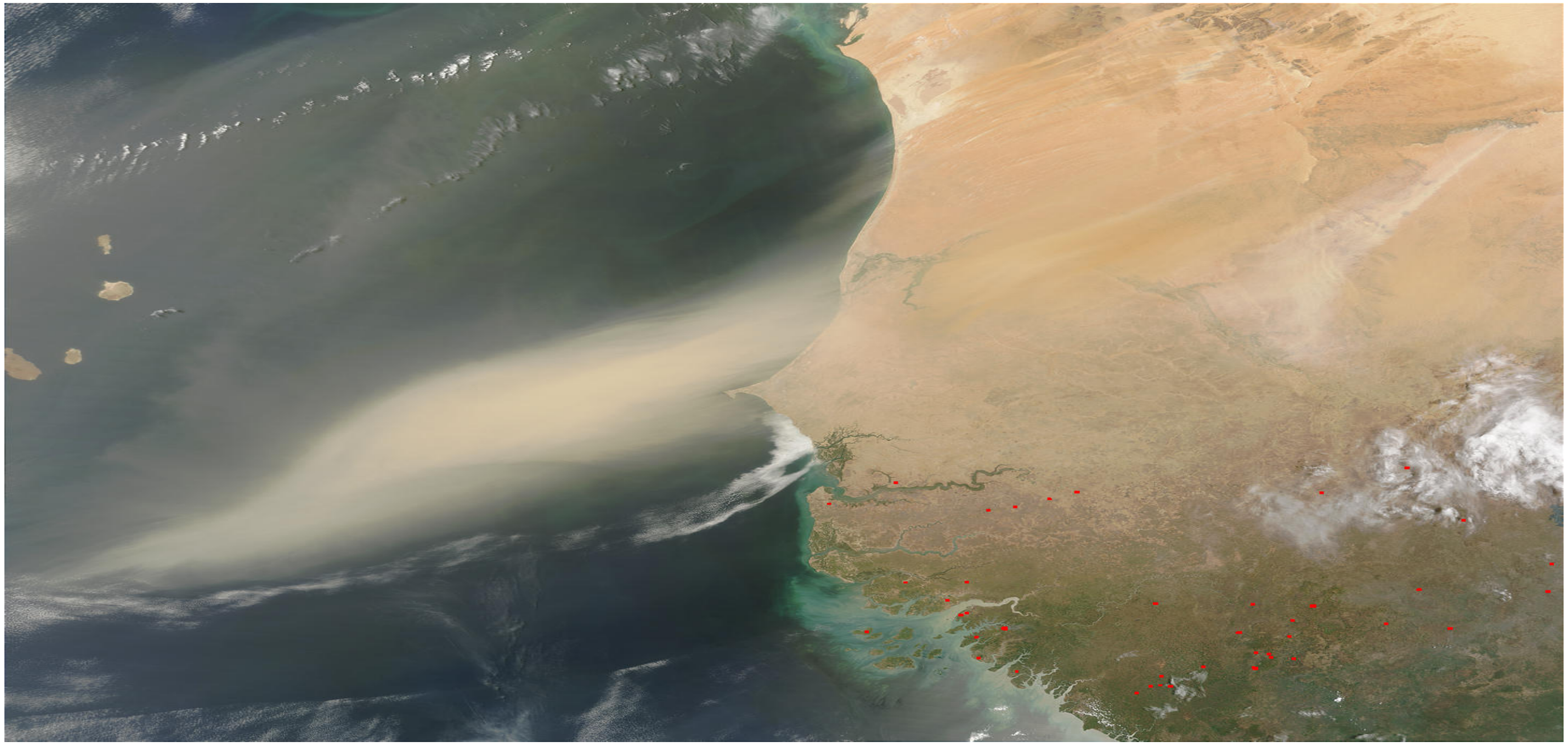

Collab : M. Mallet, N. Elguindi , A.S. Zakey, A . Konaré, F. Giorgi

Key questions :

Role of dust on precipitation in Sahel (positive or negative feedback in drought persistence ?)

Impact of dust on MCS, AEWs, tropical cyclones developments

Paleoclimate

Ecosystems and Health impacts

Many studies have been published recently based on :

Climate models

Mesoscale models (dust event simulations)

Satellite observations

Dust aerosol on-line module in the ICTP RegCM3 model

No cloud microphysics interaction !

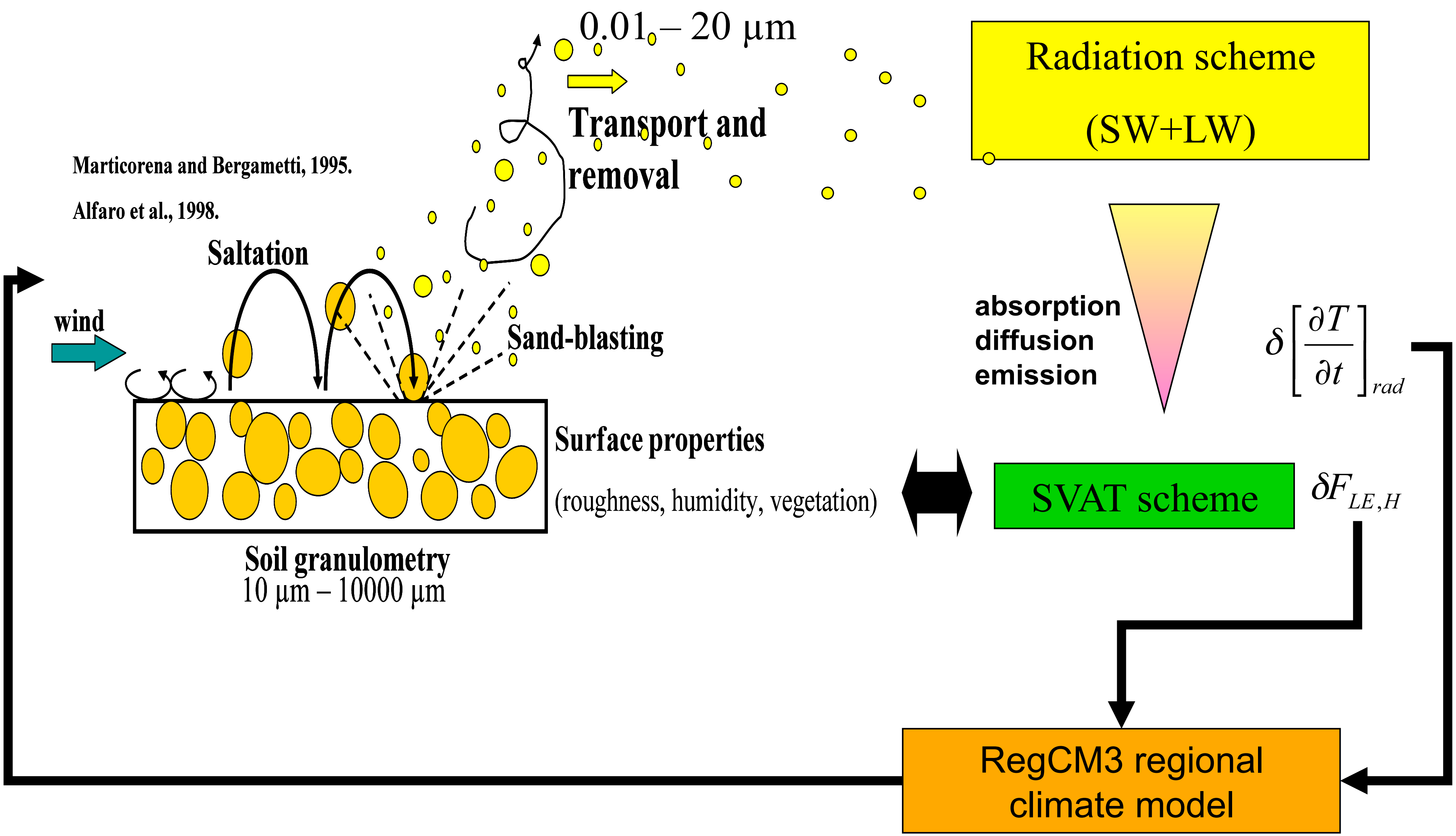

AOD

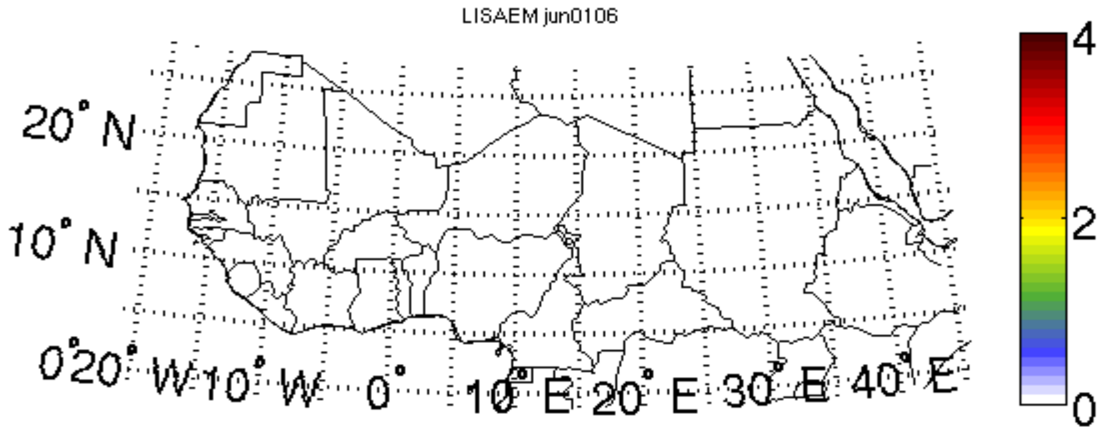

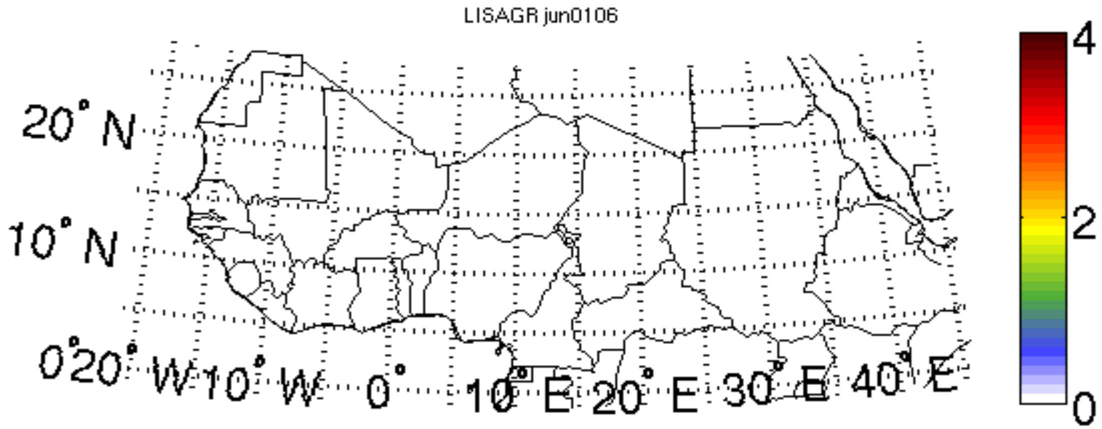

In this study : Grell + FC, Resolution of 60 km !

DUST event March 2006 9-14 (AOD day av)

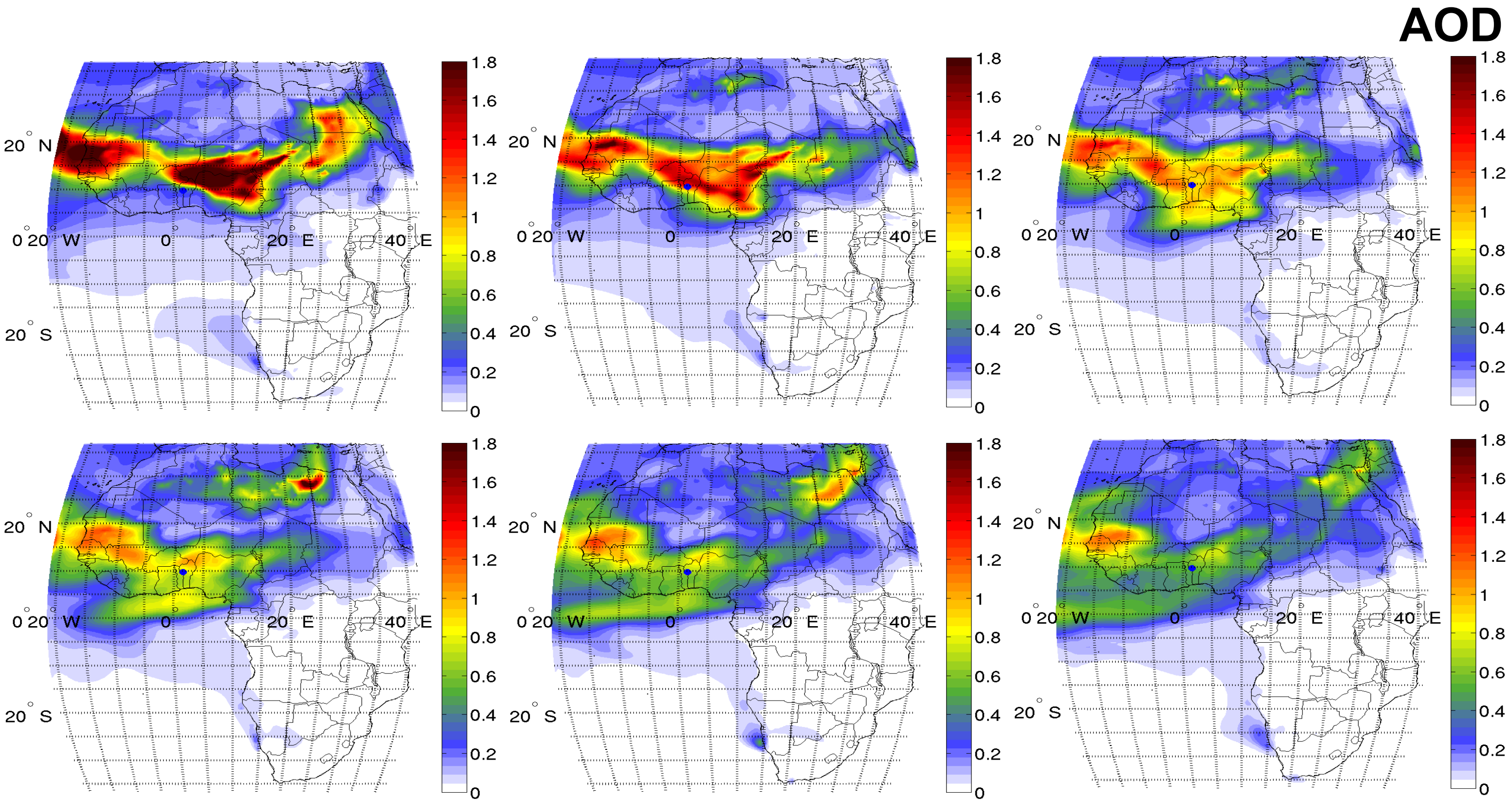

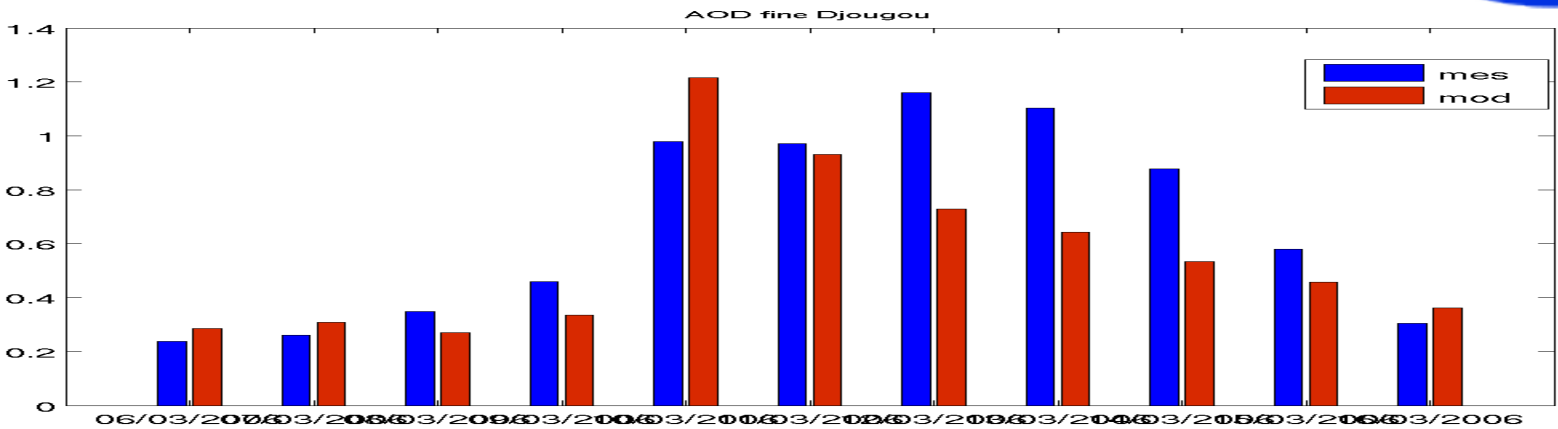

JJA

(2000-2006)

MISR AOD

1.5

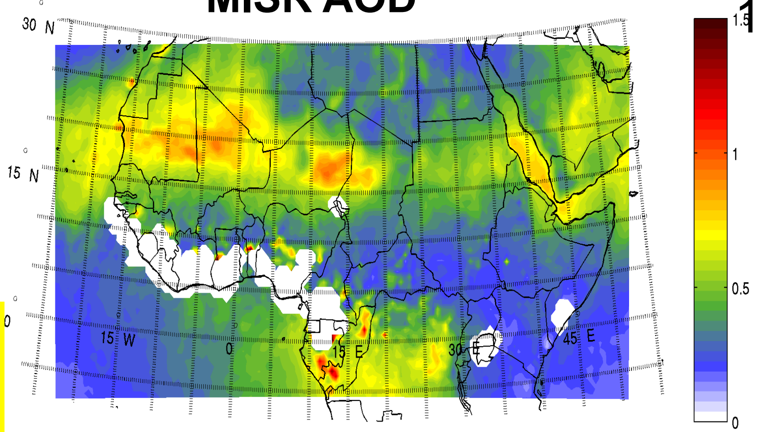

RegCM AOD

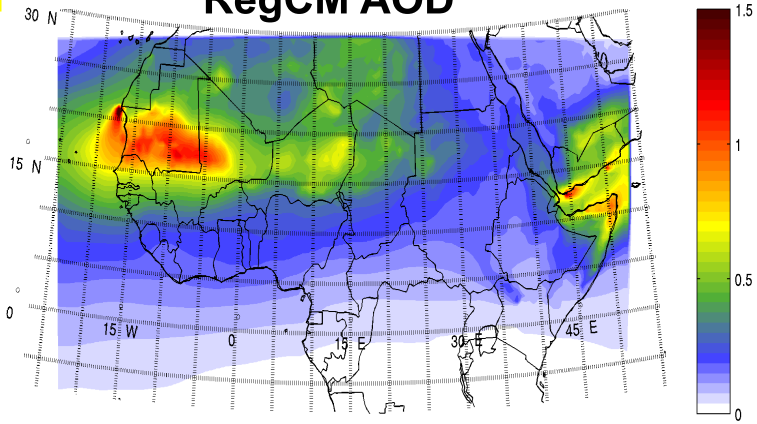

Dust radiative forcings

10

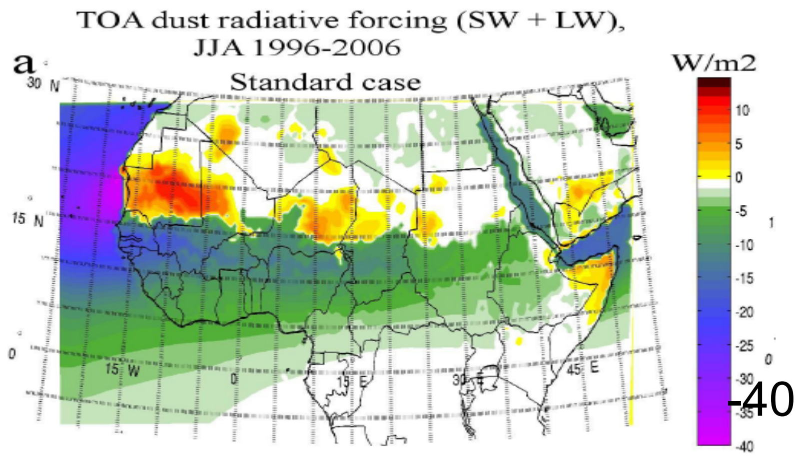

-40

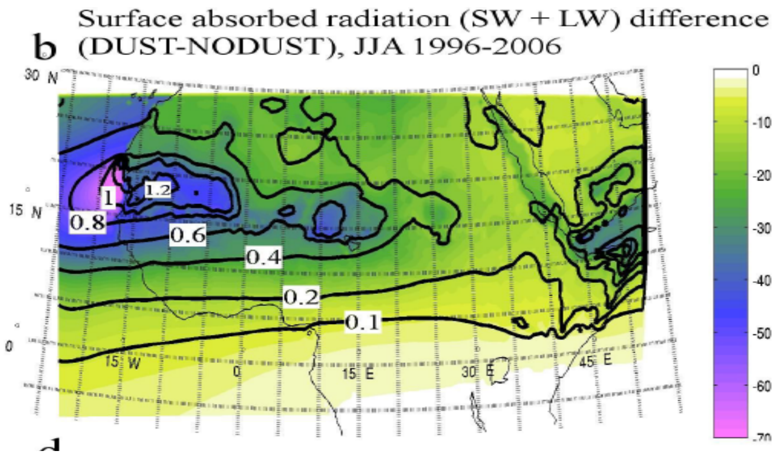

-70

Compares well with Li et al., 2004
(TOA) : -35 W/m2/AOD ,(SRF) -65 W/m2/AOD

Comparison with observations

MISR AOD

JJA

(2000-2006)

RegCM AOD

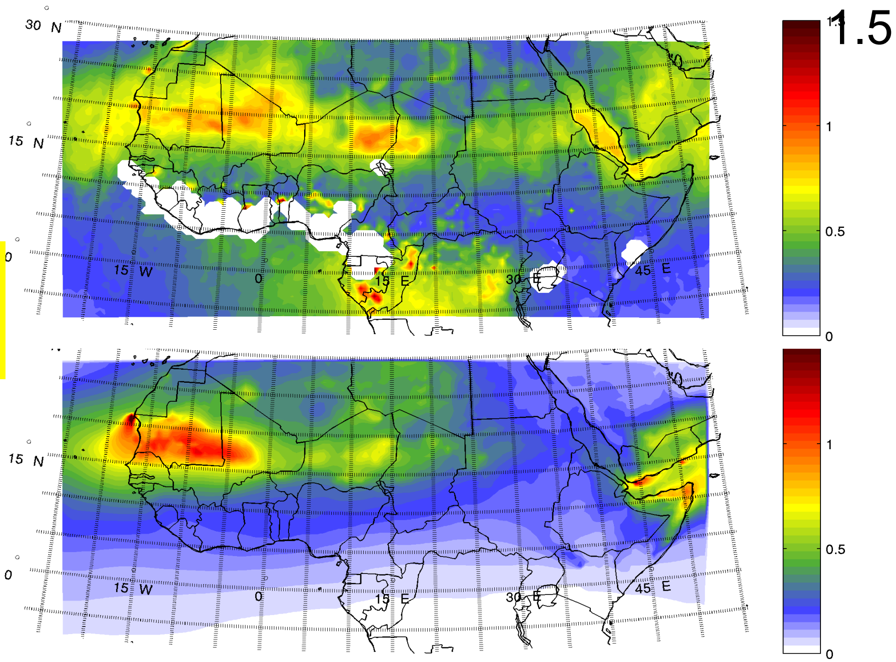

RegCM

Lidar

M'Bour

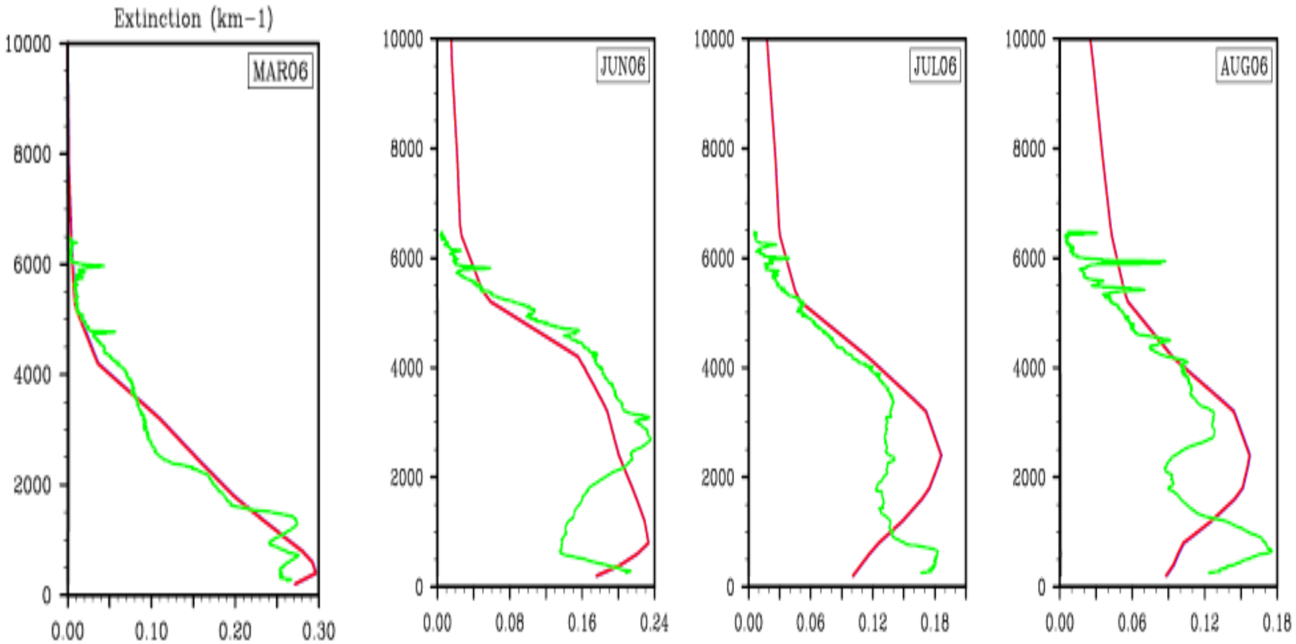

Average dynamical and precipitation response to dust over Sahel

(NODUST, JJA 1996-2006)

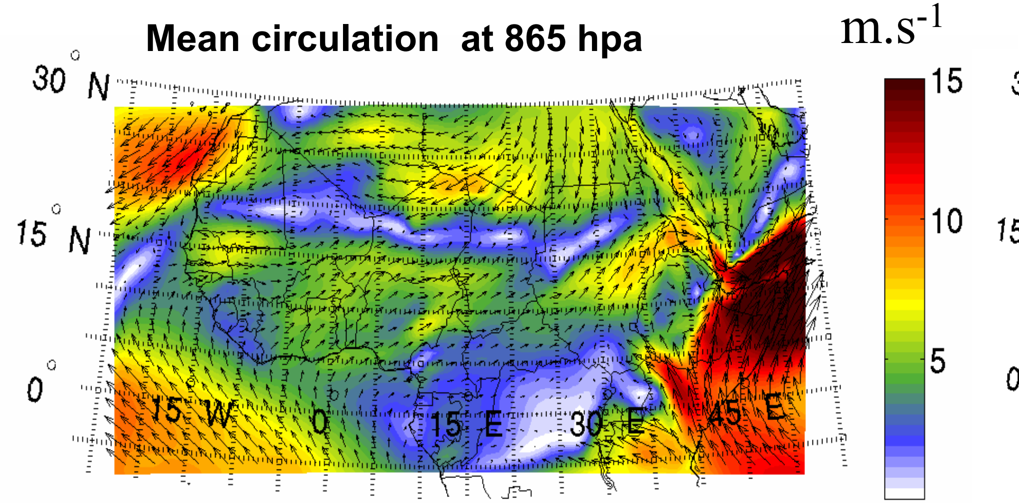

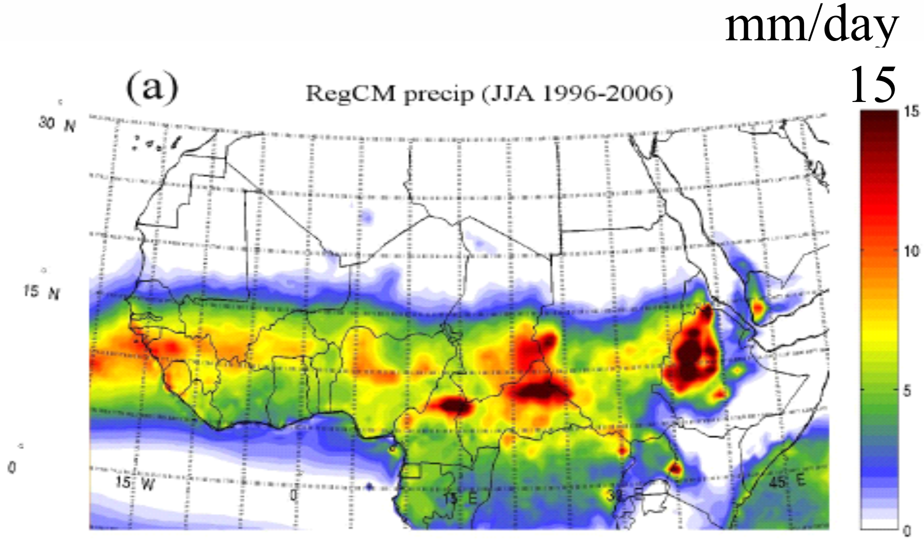

Res = 60 km

(DUST -NODUST, JJA 1996-2006)

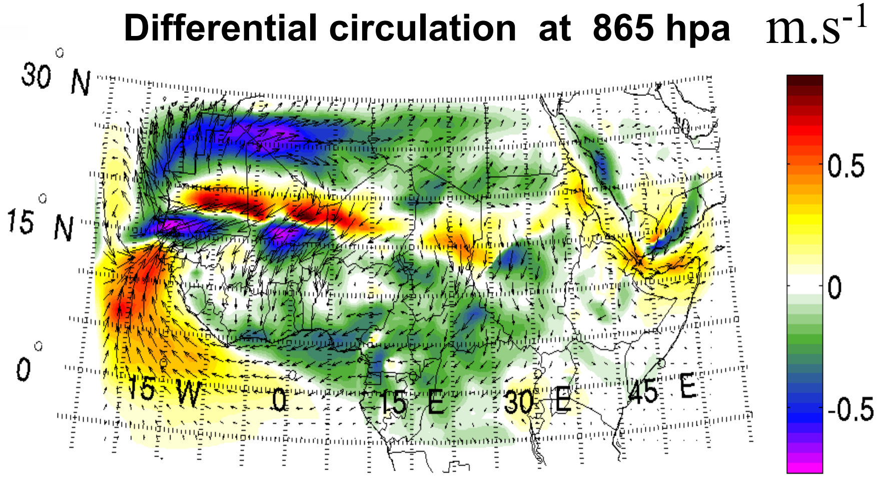

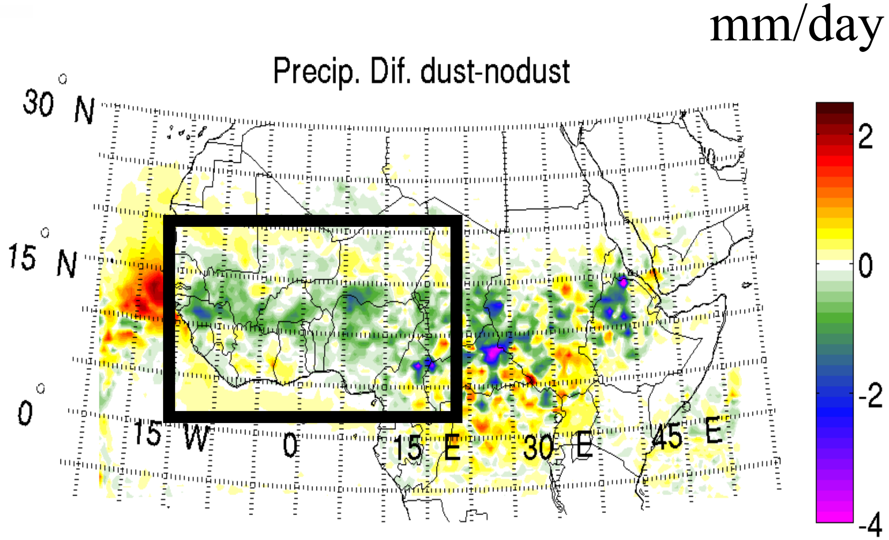

Dust perturbation analysis :

$$\frac{\partial T}{\partial t} = \left[\frac{\partial T}{\partial t}\right]_{adv} + \left[\frac{\partial T}{\partial t}\right]_{adb} + \left[\frac{\partial T}{\partial t}\right]_{conv} + \left[\frac{\partial T}{\partial t}\right]_{rad} + \left[\frac{\partial T}{\partial t}\right]_{trb} + \left[\frac{\partial T}{\partial t}\right]_{cond/prc}$$

$$\delta\left[\frac{\partial T}{\partial t}\right]_{rad} = \left[\frac{\partial T}{\partial t}\right]_{rad}^{dust} - \left[\frac{\partial T}{\partial t}\right]_{rad}^{nodust}$$

...

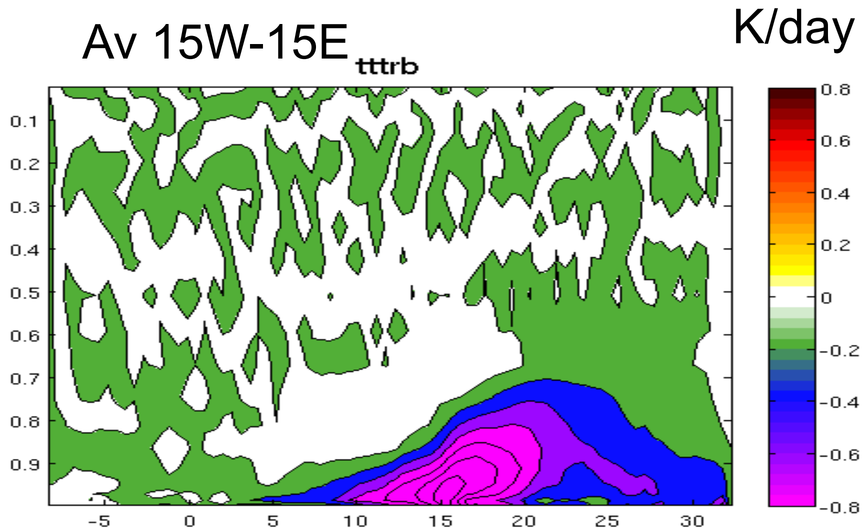

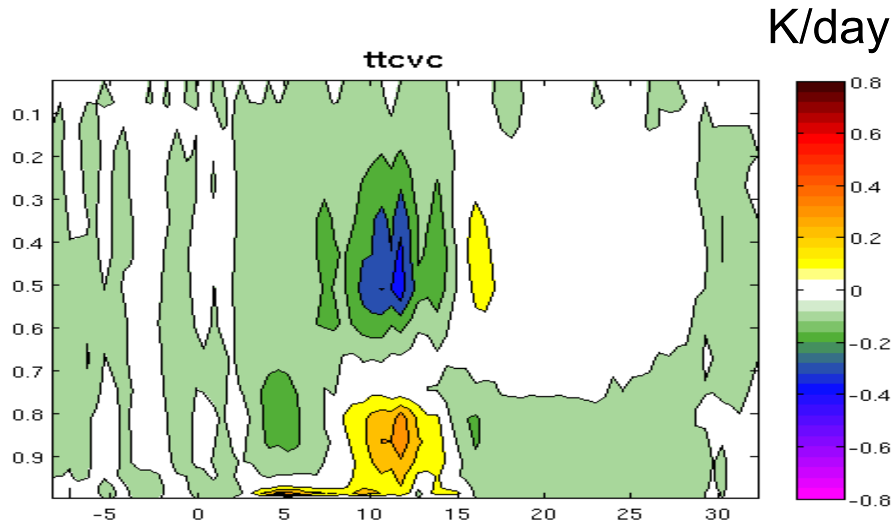

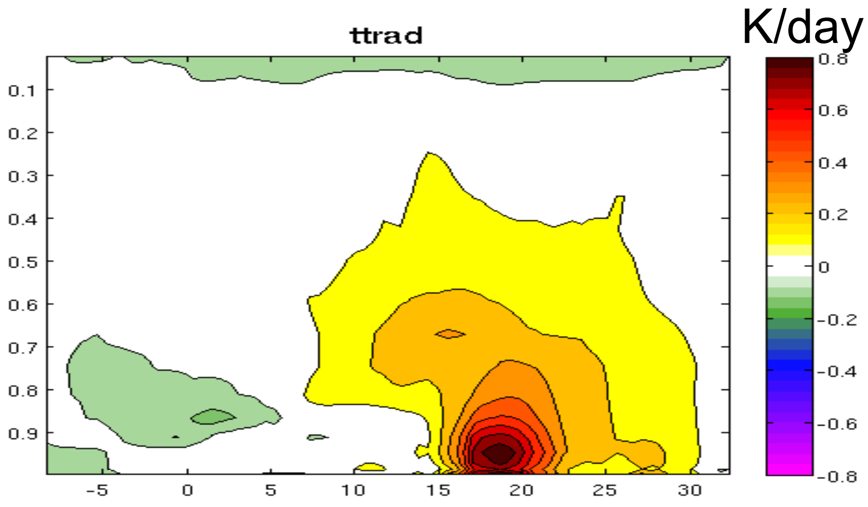

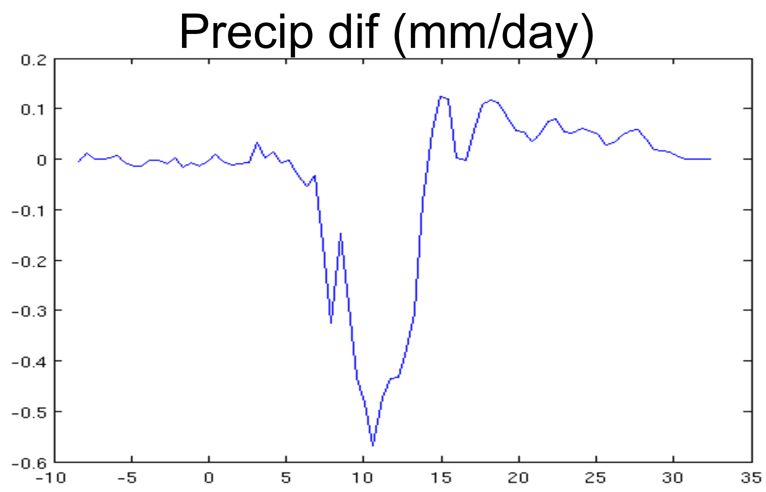

Cloud water, meridional circulation and precip. difference (DUST-NODUST)

15W-15E average

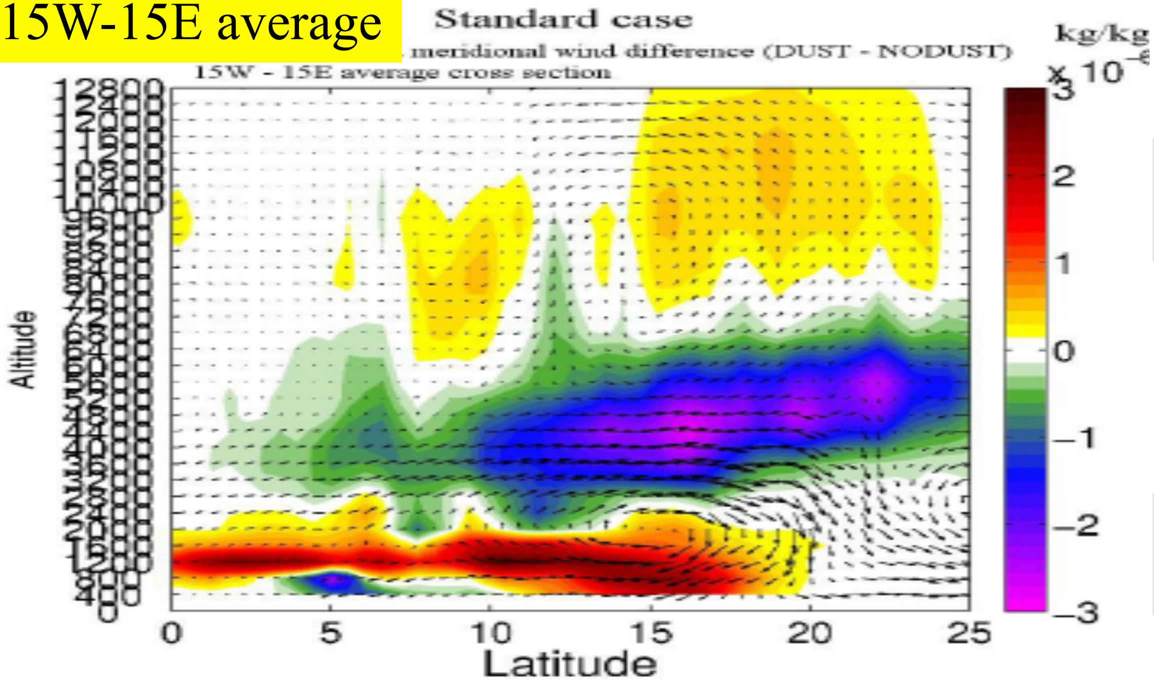

2 : ‘Elevated heat pump’ effect (Lau et al., 2009)

1: Weakening of the ‘monsoon pump’

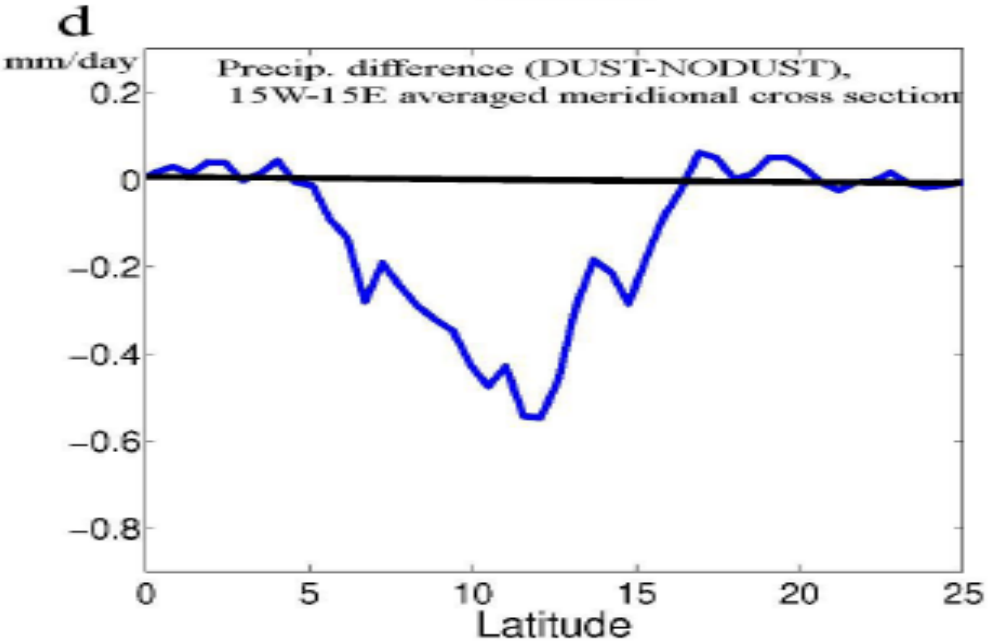

Seasonal evolution of dust impact on precipitation (JJA 1996-2006)

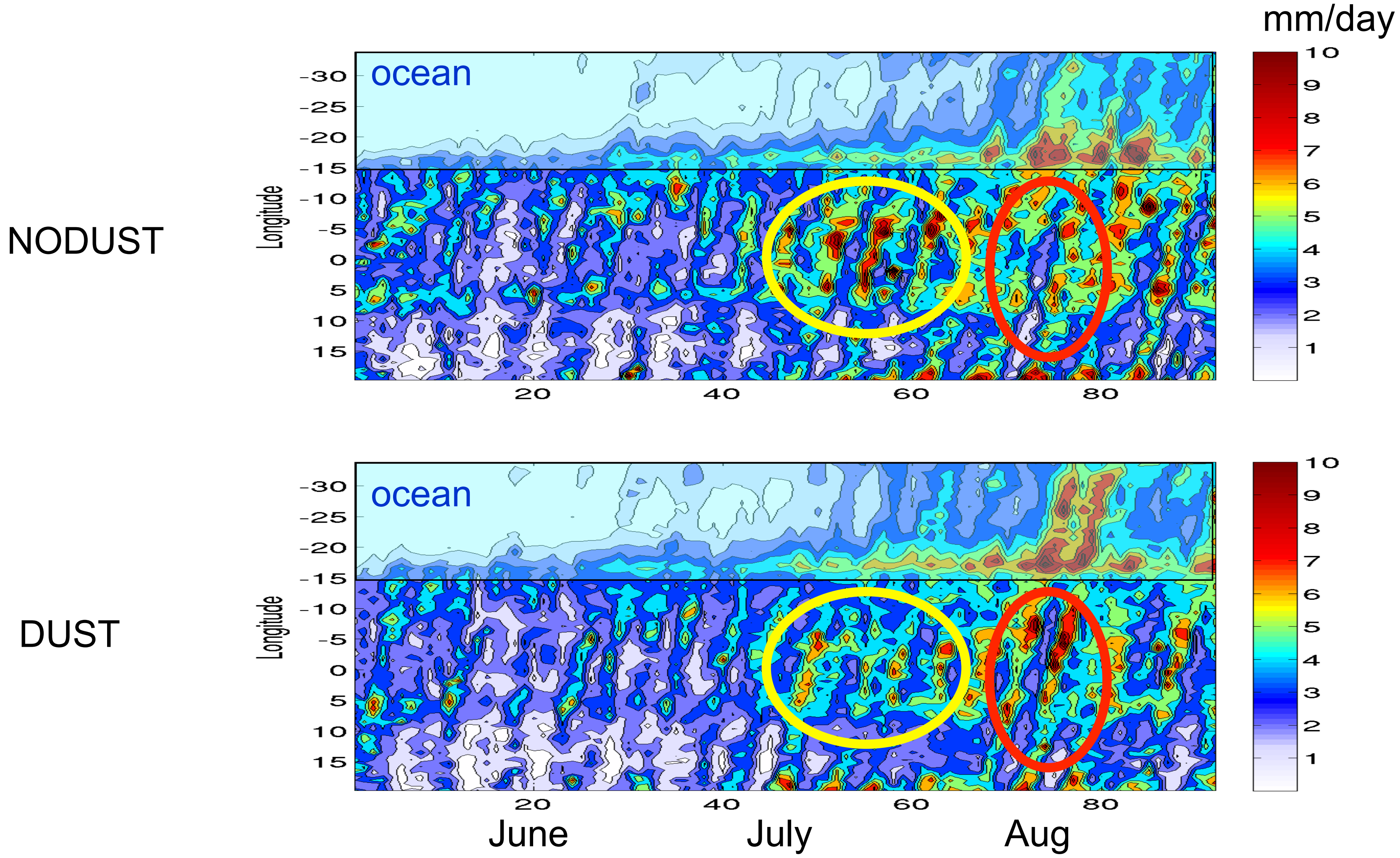

10-22 N meridional average

Response to dust forcing vs. Precipitation bias.

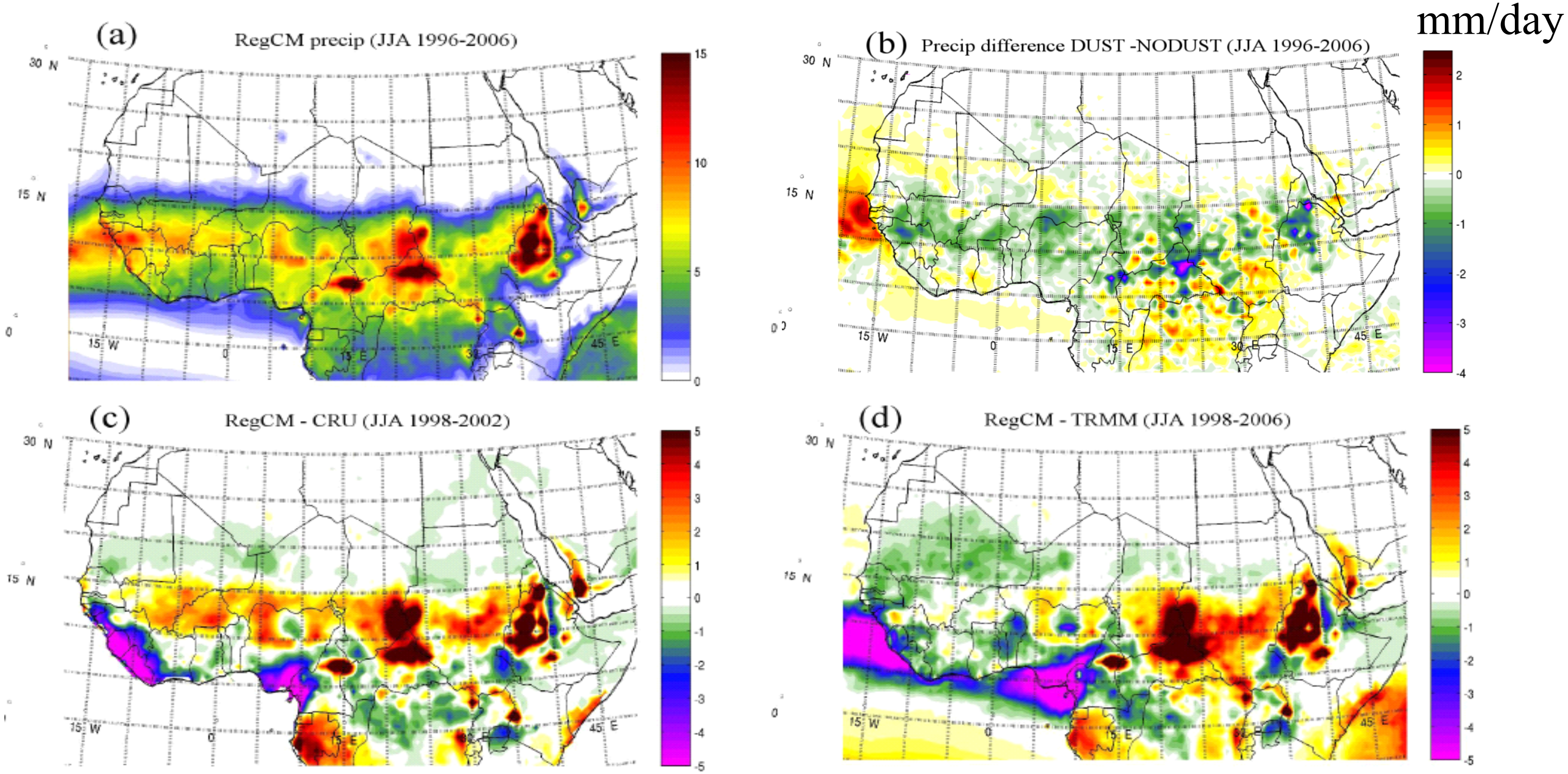

Region (15W-15E average)	5 N – 10 N		10 N – 17 N		17-N 20 N	
OBS	CRU	TRMM	CRU	TRMM	CRU	TRMM
Bias (mm/day and %)	-1.23 (-20.3 %)	-1.23 (-24%)	+1.09 (+20%)	+0.06 (+1.4%)	-0.23 (-41%)	-0.41 (-92%)
(DUST –NODUST) (mm/day and %)	-0.18 (-3.0 %)	-0.19 (-3.8 %)	-0.42 (-7.9%)	-0.28 (-6.1%)	+0.04 (+7.4 %)	+0.05 (+11.3%)
Improvment ?	no	no	yes	yes	yes	yes

Climate sensitivity to dust absorption properties

Variability of measured values of dust SSA values (mineral composition, coating, aerosol size distribution ..) : impacts on the climatic response ?

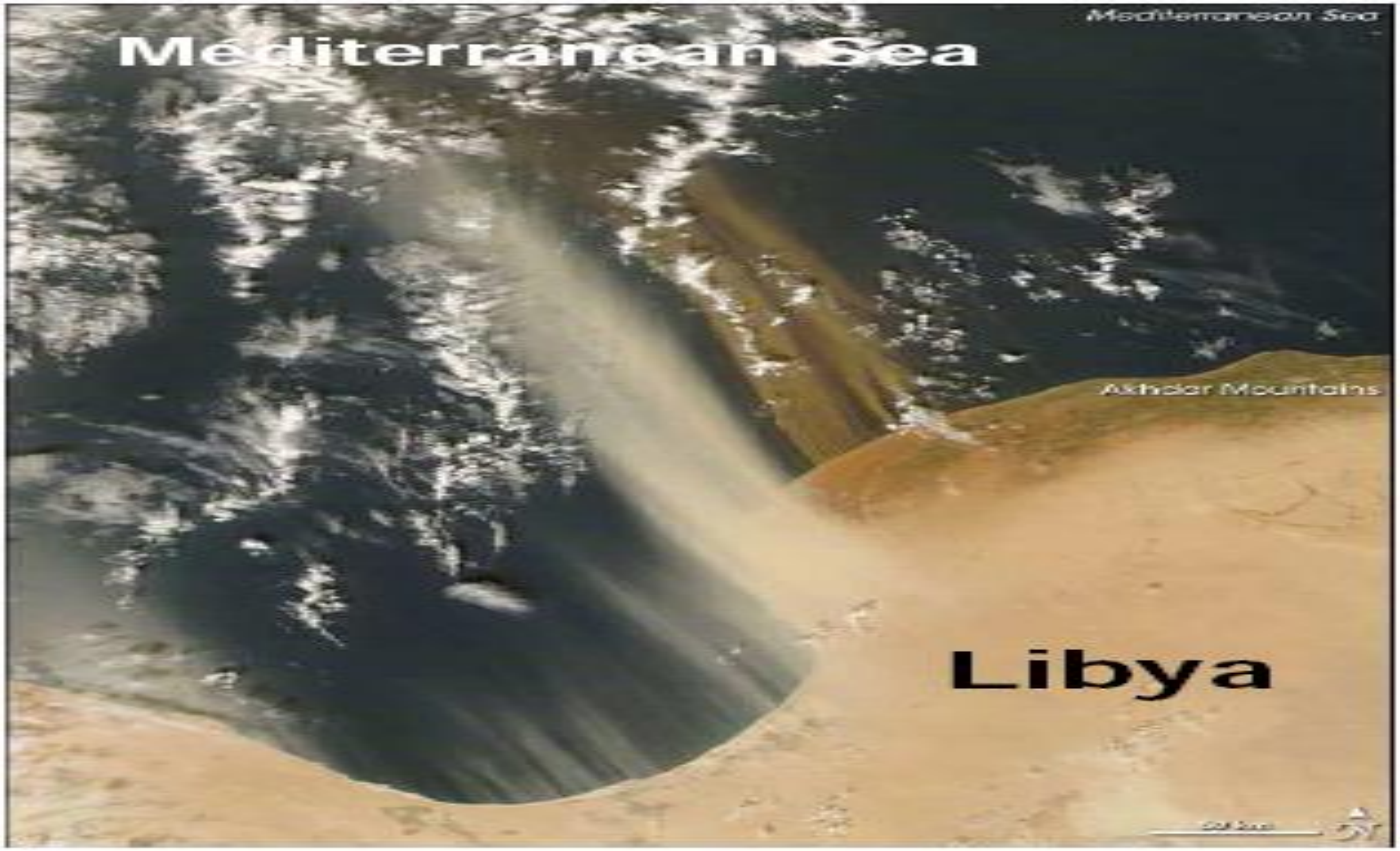

Source NASA

Any evidence of dust climatic signal over Sahel from observation ?

Kluser et al., 2010 (ACPD) propose a statistical study of dust impact on cloud cover property and rain likelihood using MODIS (deep blue) and SEVIRI clouds and dust product.

The observed increase in cloud top temperature in the monsoon season's Harmattan air mass can be explained by suppression of initial convection by boundary layer stabilisation and due to the entrainment of very dry air warmed by solar heating. This effect indicates that strong dust activity during the Sahelian monsoon season significantly affects convective intensity within the region.

Table 1. Net dust effects on cloud cover (δ_{COV}), cloud top temperature (δ_{CTT}), ice phase fraction (δ_{IPF}), liquid phase effective radius ($\delta_{Re(liquid)}$) and warm rain likelihood (δ_{WRL}) within the Harmattan flow of the monsoon season.

sensor	dust load	δ_{COV}	δ_{CTT}	δ_{IPF}	$\delta_{Re(liquid)}$	δ_{WRL}
MODIS	moderate	−20.84%	+14.07 K	−16.90%	−2.39 µm	−0.27
	heavy	−14.73%	+12.06 K	−14.15%	−3.16 µm	−0.35
SEVIRI	moderate	−21.31%	+12.37K	−15.78%	–	–
	heavy	−21.68%	+14.89K	−22.88%	–	–

Conclusion

•**Regional precipitation responses depend on coexisting differential circulations patterns induced by the dust radiative forcing at different tropospheric levels.**

•**Surface and lower troposphere cooling induces a decrease of the monsoon pump intensity whereas atmospheric diabatic warming over the source areas trigger an elevated heat pump effect resulting in enhanced convection and cloud formation in the higher troposphere over the Sahel.**

•**The net regional impact of dust on average precipitation results from these coexisting effects. On average, drying is dominant over Sahelian region except for a limited band over northern Sahel which sees enhanced precipitations. This signal is significant when changing domain and SST conditions. Model precipitation bias is positively impacted when dust are accounted for.**

•**The balance between these effects is very sensitive to the dust SSA which affects the intensity of precipitation decrease vs. increase as well as the latitudinal limit between these two responses.**

•**When SST are prescribed to the model, only diabatic warming is effective over ocean and more convection and precipitation are obtained in the dust outflow region. When SST are allowed to feedback (cooling of mixed layer due to decrease of incoming SW radiation) the response could be of opposite sign due a decrease of latent heat and moisture availability for deep convection. Needs ocean coupling !**

Coexistence of natural and anthropogenic particles at the regional scale

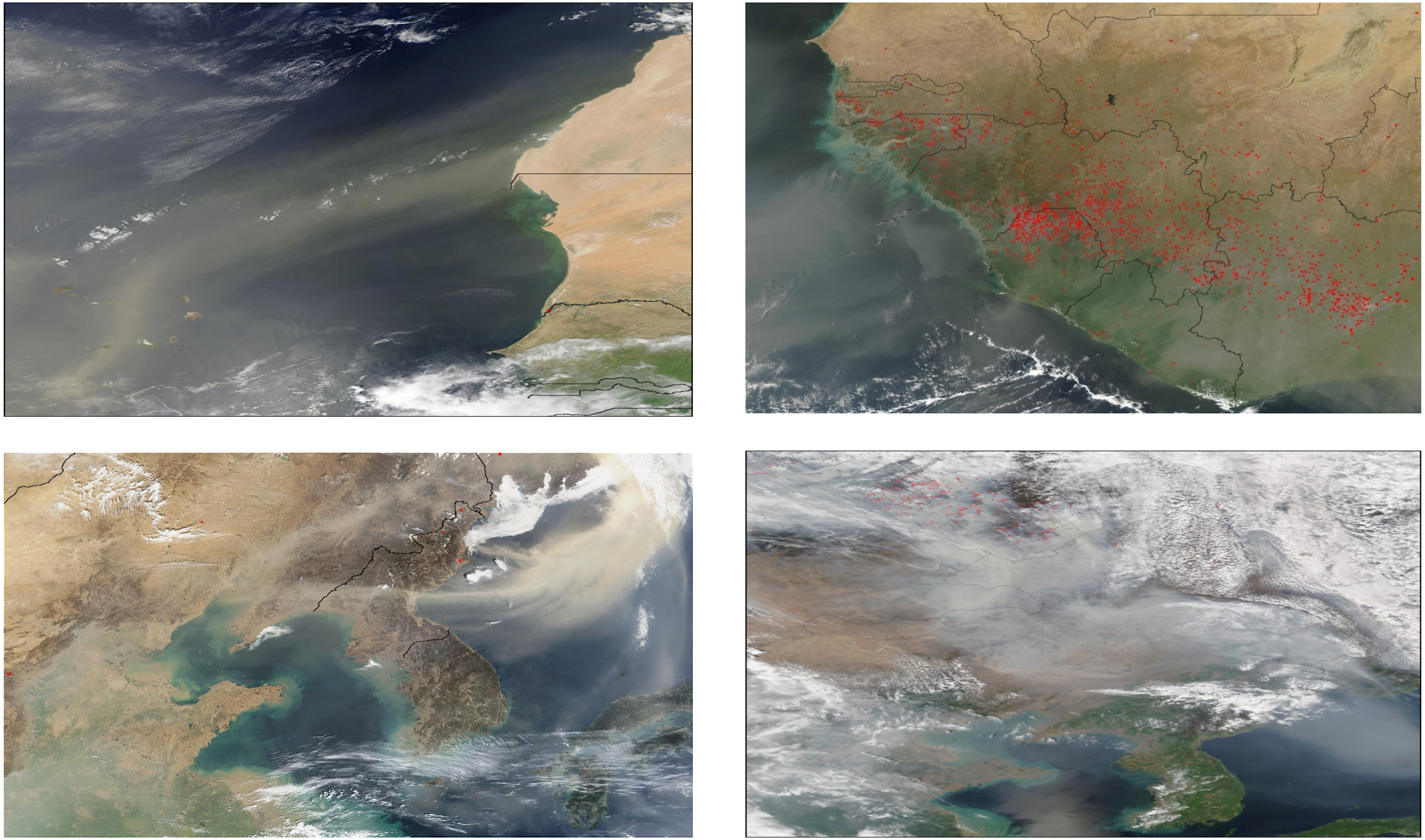

MODIS Land Rapid Response Team, NASA/ GSFC

- Experimental evidence of interactions btw particules and btw gas and particules
- Environmental impacts of the mixing

Coexistence of natural and anthropogenic particles at the regional scale

R. Arimoto et al. / Global and Planetary Change 52 (2006) 23–56

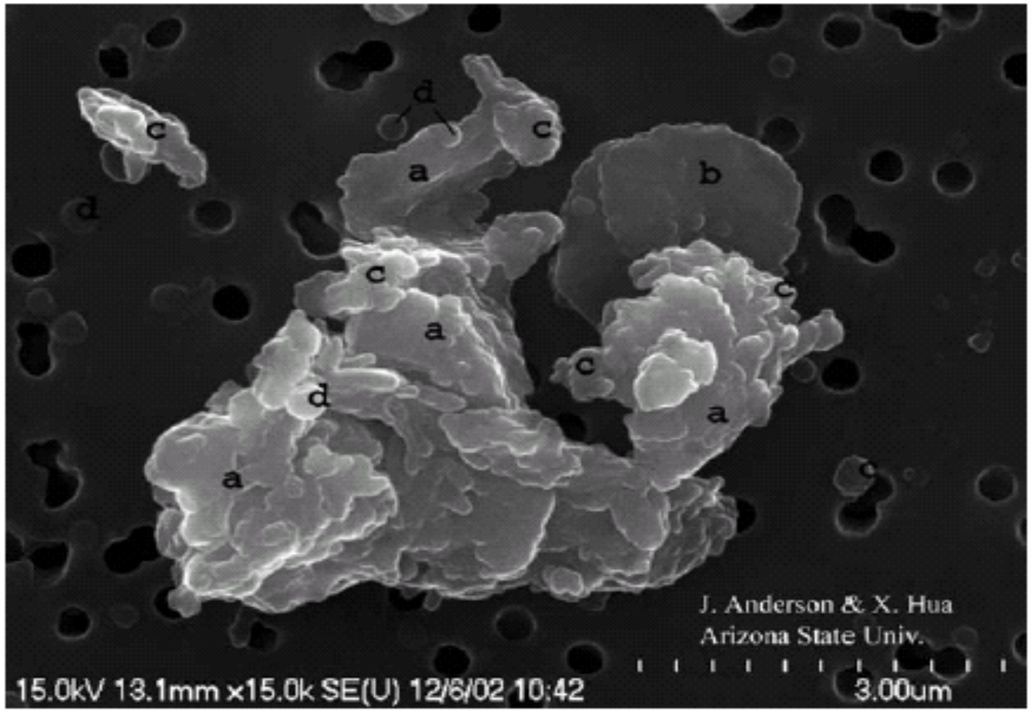

Fig. 9. Field emission SEM image of RF13 sample from 600 m leg over Yellow Sea. Large central particle is a silicate dust/black carbon aggregate consisting of: (a) Ca aluminosilicate, (b) Mg aluminosilicate, (c) black carbon spherule aggregates (soot), (d) separate carbon spheres.

Ex 2 : Biogeochemical (and global climate) perspective.

« Iron cycle in the East Asia outflow, deposition to the North Pacific Ocean »

P. Chuang (UCSC), N. Meskhidze (NCSU)

Iron depositon in High Nutrients Low Chlorophyll regions

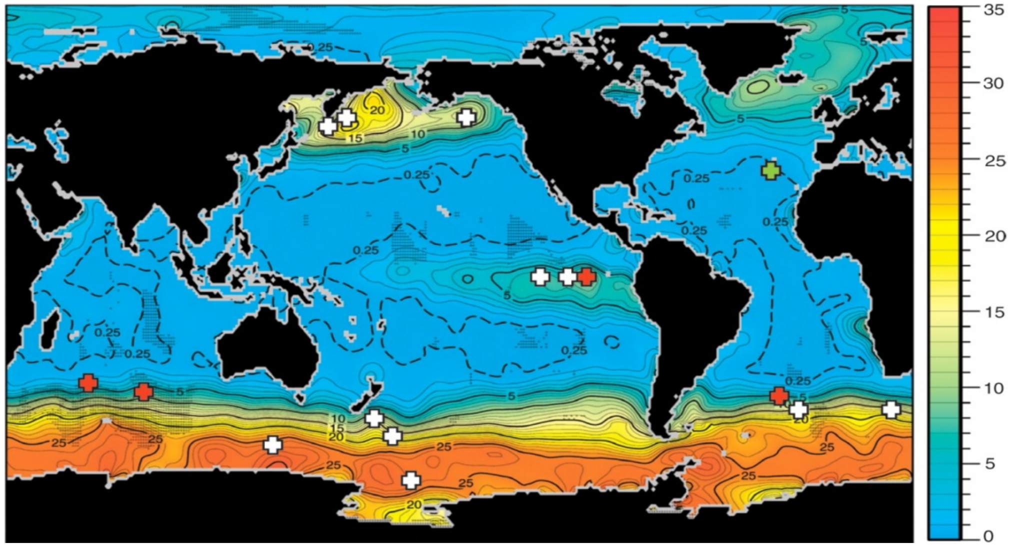

Annual surface mixed layer nitrate concentrations (μmol.l-1)

From Boyd et al., Science, 2007.

Regional Iron Fertilisation experiment in different HNLC:

- **Bloom of biological activity and carbon sequestation**

A 30 to 90 μatm drawdown in surface pCO_2

- **Paleoclimate : 'The Iron hypothesis' (Martin)**
  Kohfeld et al., 2005; Archer et al., 2000; Mahowald et al.,1999 …

The North Pacific HNLC

Source and bioavailability of iron

Atmospheric deposition

Rivers runoff

Upwelling

Dust is considered as a major source of iron for remote ocean

atmospheric processing

Source region

The BODEX team

DIF ~0.5 %

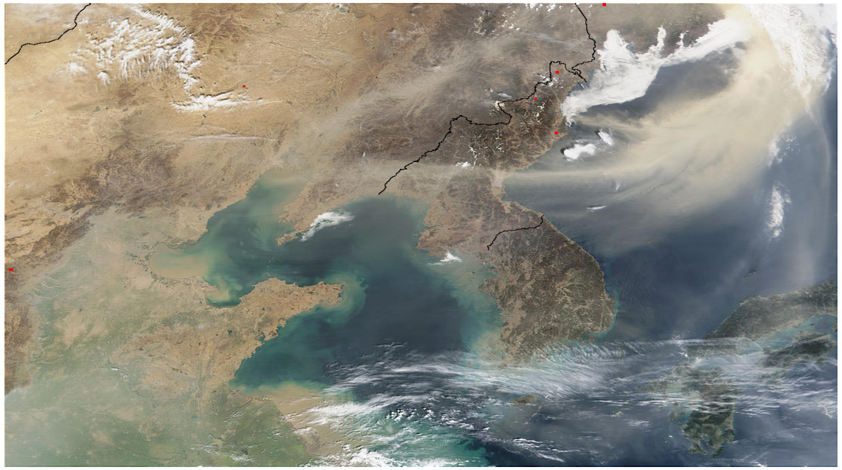

Remote ocean

Unknown scientist

DIF ~0.01-80 %

Low Bioavailability

Dissolved Iron Fraction = (soluble iron) / (total iron)

Higher Bioavailability

Effort to better to characterize DIF evolution in model (e.g Meskhidze et al;, 2005 Fan et al., 2006)

Possible role of anthropogenic coumpounds (North Pacific Ocean).

Iron dissolution modelling

GEOS-CHEM

Meskhidze et al., 2005

O_3

Anthro. aerosols

1: Assume an initial mineral composition for the dust

Table 3. Concentration of Major Minerals in the Soil and Clay Fractions of Surface Soils in the Gobi Desert and in Mineral Dust Originating From These Soils

Mineral	In Soil,[a] % wt		In Mineral Dust and Used as Initial Condition for Model Simulation,[b] % wt
	In Silt	In Clay	
Anhydrite $CaSO_4$	6	0	6
Calcite $CaCO_3$	12	0	11
Albite $NaAlSi_3O_8$	18	8	17
Microcline $KAlSi_3O_8$	8	5	8
Illite[c] $K_{0.6}Mg_{0.25}Al_{2.3}Si_{3.5}O_{10}(OH)_2$	18	42	20
Smectite/Montmorillonite[c] $Na_{0.6}Al_{1.4}Mg_{0.6}Si_4O_{10}(OH)_2 \cdot 4H_2O$	7	15	8
Hematite[d] Fe_2O_3	5	8	5
Quartz SiO_2	21	10	20
Kaolinite $Al_2Si_2O_5(OH)_4$	5	12	5
Total	100	100	100

ISORROPIA

Dissolved iron modelling

- **12 new tracers in GC representing mineral species in the dust mode :**

  $(Fe, Ca, Al, Na, Sil, K, Mg, SO_4^{2-}, NO_3^-, NH_4)_{aq}$, $(CaCO_3)_s$, $(CaSO_4)_s$

Symbol	Chemical Forms Allowed for Species[a]
SO_2[b]	$(SO_2)_g$
S(VI)[c]	$(SO_4^{2-})_{aq}$, $(HSO_4^{2-})_{aq}$, $(FeSO_4^+)_{aq}$, $(AlSO_4^+)_{aq}$, $(CaSO_4)_s$, $(Na_2SO_4)_s$, $(NaHSO_4)_s$, $((NH_4)_2SO_4)$ $(NH_4HSO_4)_s$, $((NH_4)_3H(SO_4)_2)_s$
NO_x[b]	$(NO)_g$, $(NO_2)_g$
N(V)[d]	$(HNO_3)_g$, $(NO_3^-)_{aq}$, $(NH_4NO_3)_s$, $(NaNO_3)_s$
N(-III)[e]	$(NH_3)_g$, $(NH_4^+)_{aq}$, $((NH_4)_2SO_4)_s$, $(NH_4HSO_4)_s$, $((NH_4)_3H(SO_4)_2)_s$, $(NH_4NO_3)_s$
Na[f,g]	$(Na^+)_{aq}$, $(NaCl)_s$, $(NaNO_3)_s$, $(NaHSO_4)_s$, $(Na_2SO_4)_s$
Ca[g,h]	$(Ca^{2+})_{aq}$, $(CaCO_3)_s$, $(CaSO_4)_s$
Fe[g]	$(Fe^{3+})_{aq}$, $(Fe(OH)^{2+})_{aq}$, $(Fe(OH)_2^+)_{aq}$, $(Fe(OH)_3^0)_{aq}$, $(Fe(OH)_4^-)_{aq}$, $(FeSO_4^+)_{aq}$, $(Fe(OH)_3)_s$
Al[i]	$(Al^{3+})_{aq}$, $(Al(OH)^{2+})_{aq}$, $(Al(OH)_2^+)_{aq}$, $(Al(OH)_3^0)_{aq}$, $(Al(OH)_4^-)_{aq}$, $(AlSO_4^+)_{aq}$

Dissolved iron FEDI (oxydation III)

- **Tracers are transported and removed (wet and dry dep) as dust in GC**

- **At the source : FETOT = 3.7 % * DUST ;**

  DIF = FEDI / FETOT = 0.45 % (from obs ACE-ASIA)

Test Case Simulation (2 x 2.5, Full chemistry) : MARCH-APRIL 2001

« HIDU »
High dust regime

« LODU »
Low dust regime

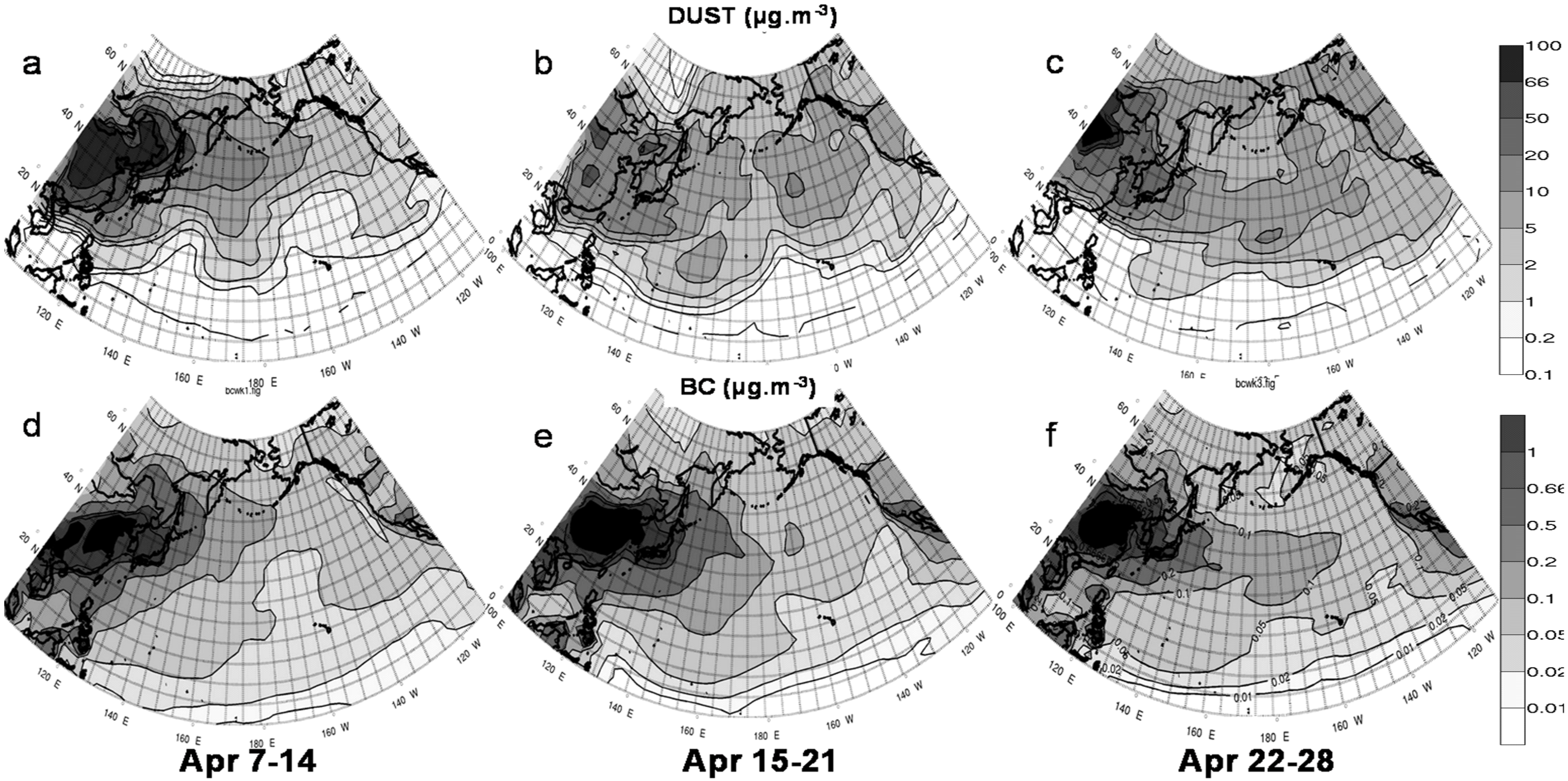

Validation of GC aerosol fields (Heald et al., 2006)

Model / data comparison during april 2001

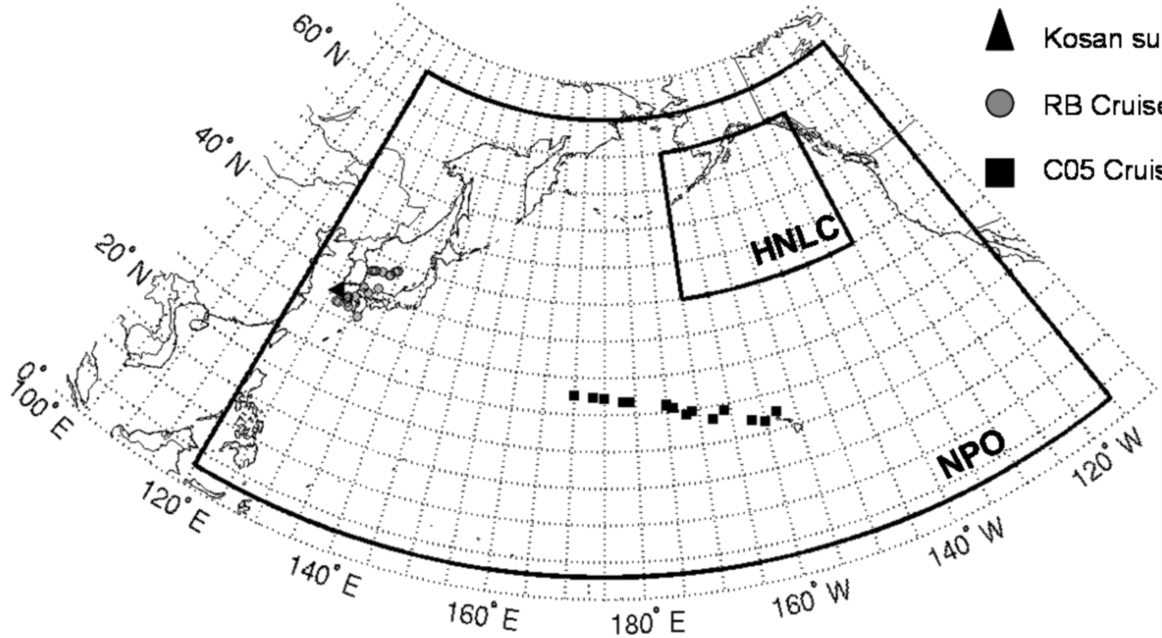

Ace-Asia

Chen et al., 2005

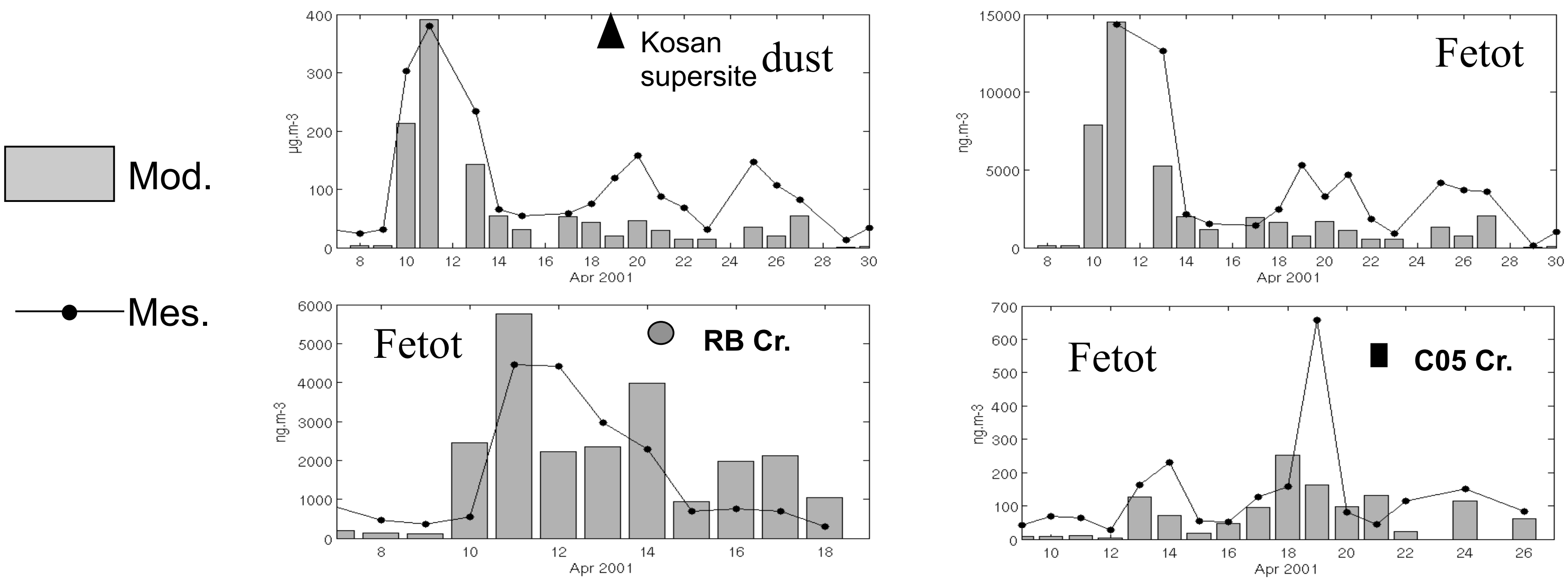

Scavenging of anthropogenic compounds by dust (Kosan)

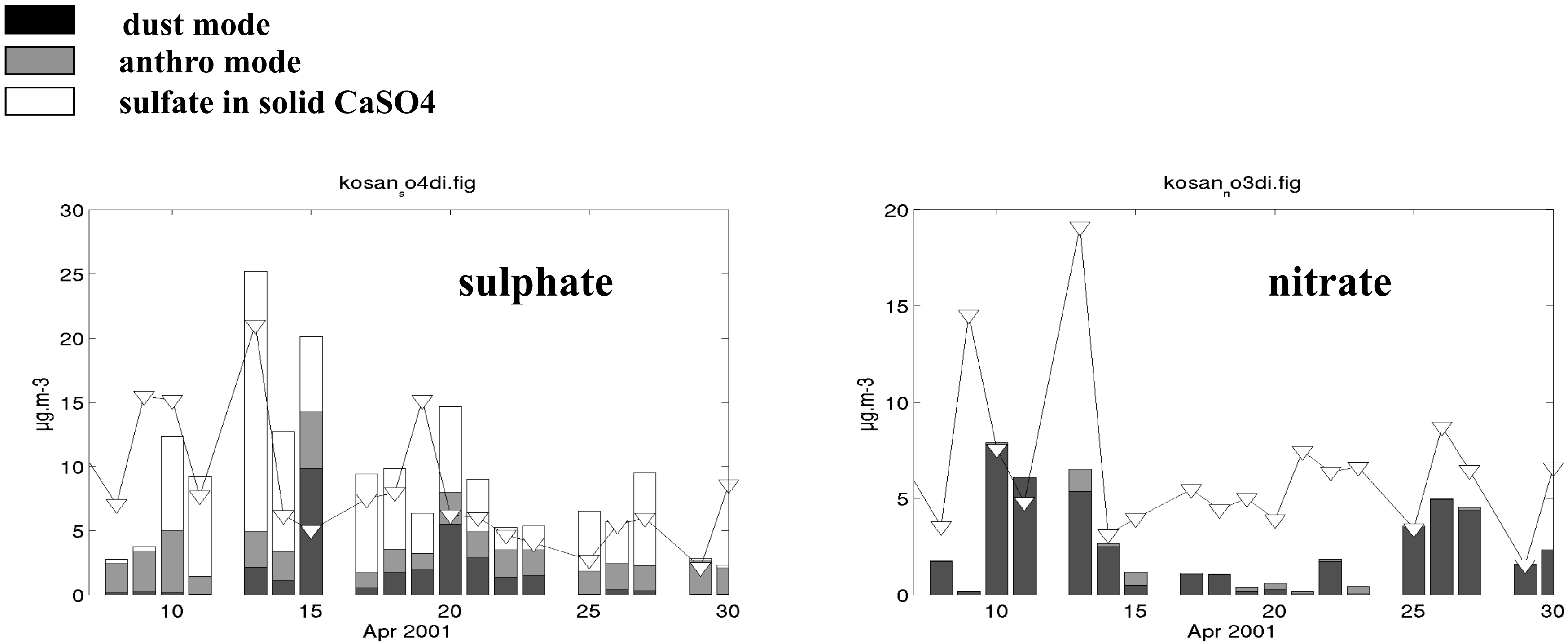

pH and hematite dissolution evolution

$CaCO_3$ dissolution

$CaSO_4$ formation
Carbonate volatilisation

NH_3 solubilisation.

NO_3 volatilisation

SO_4

Self neutralisation

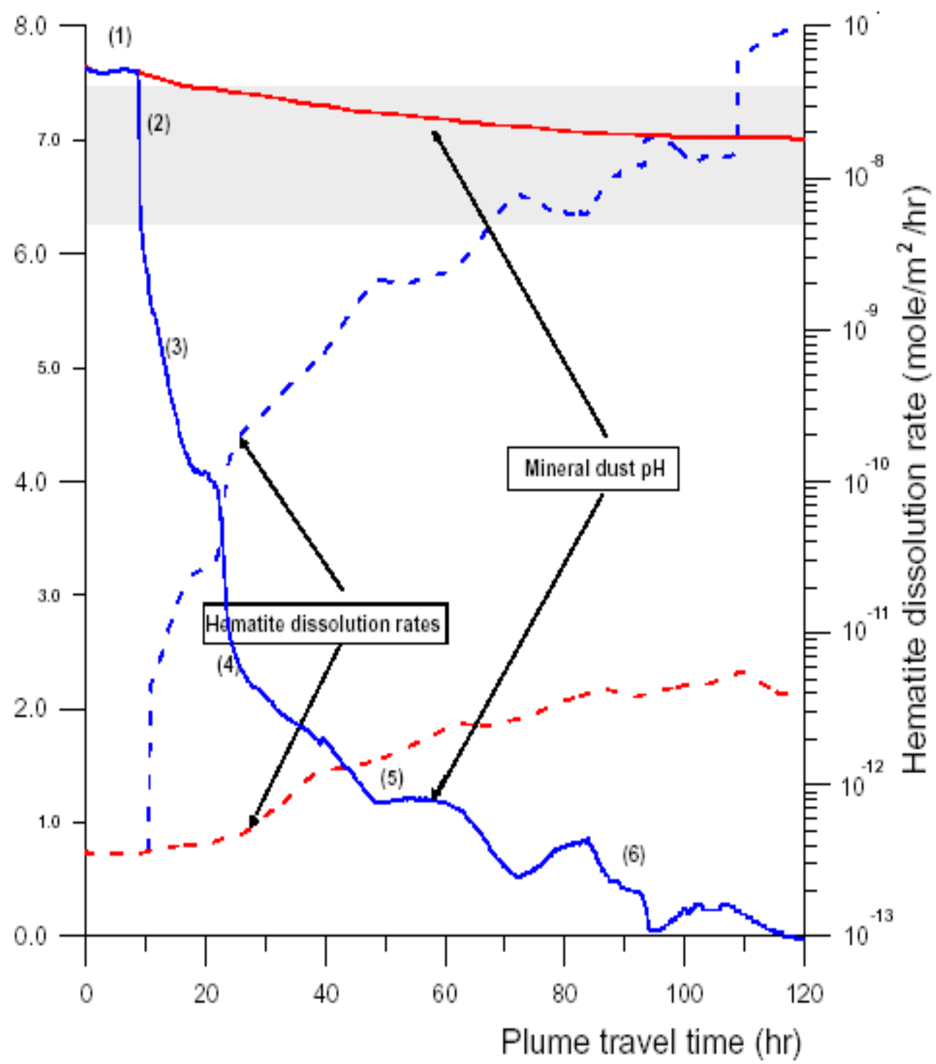

Low dust case

High dust case

From N. Meskhidze

OD Lagrangian Box model

Increasing interaction with acidic compounds

>

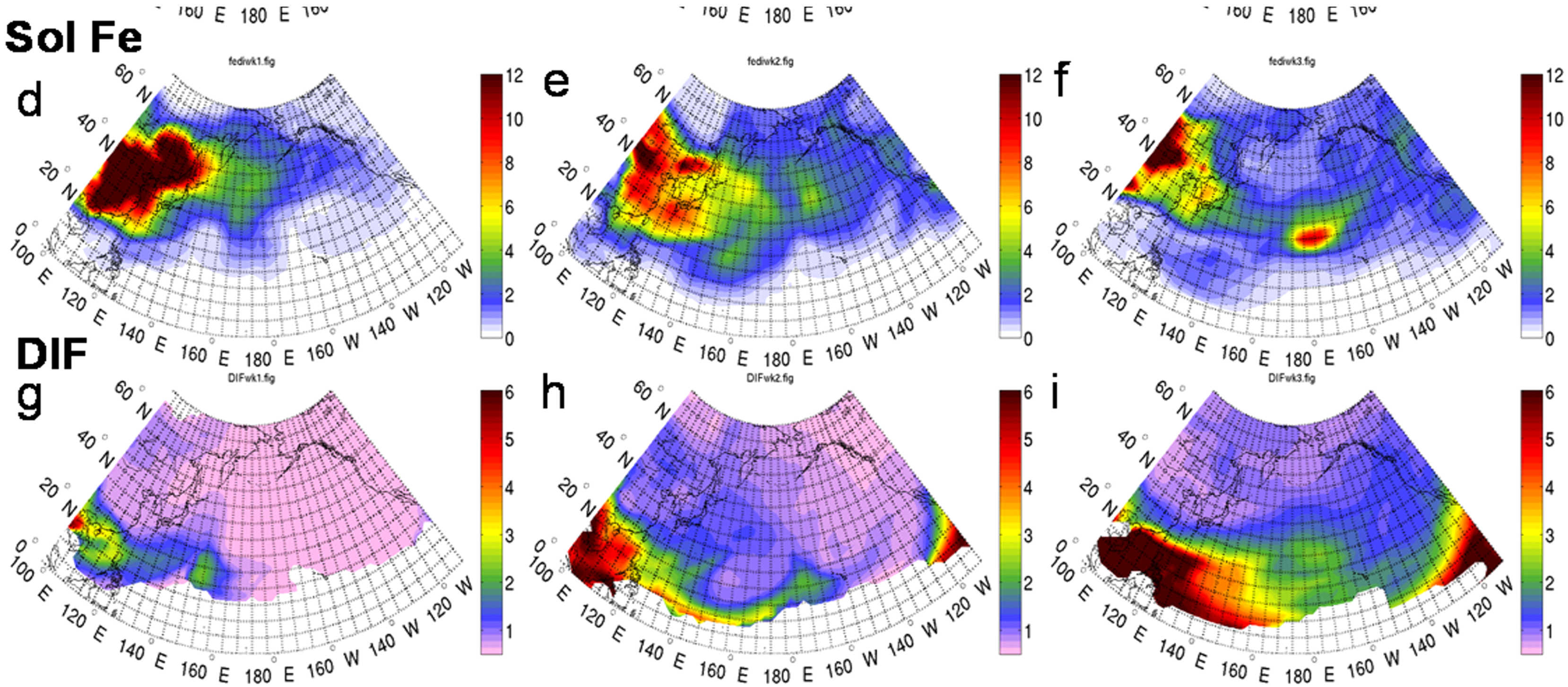

- **Large dust event are not necessarily the most FEDI productive (Solmon et al., 2009, Meskhidze et al., 2005)**

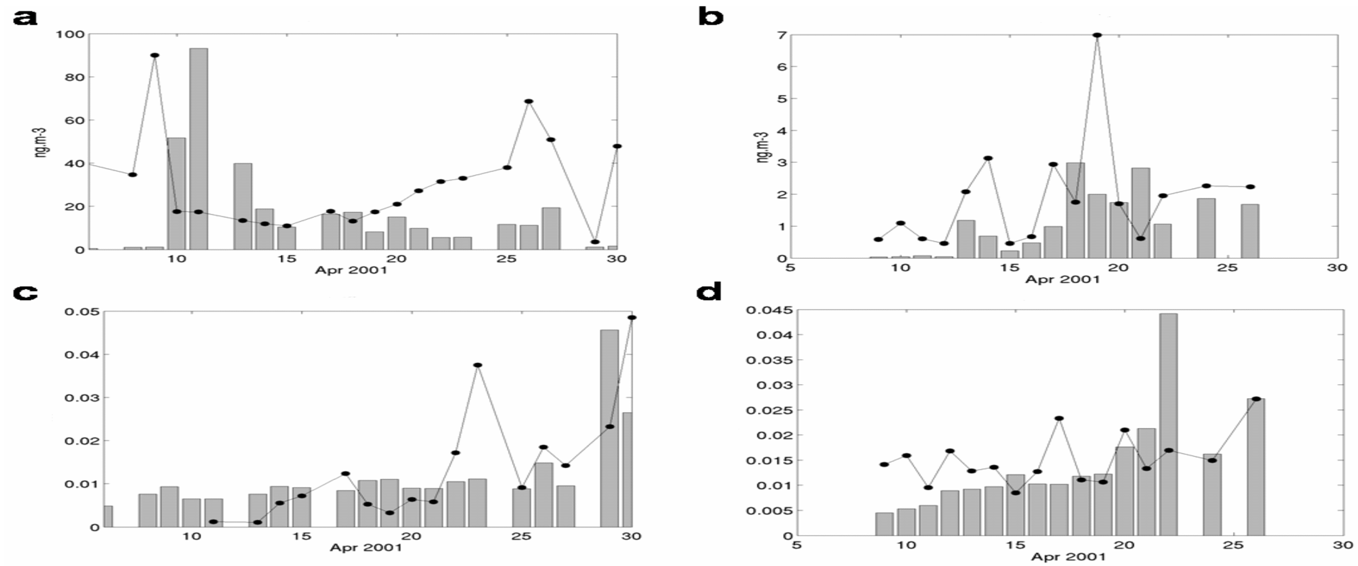

Figure 10: Simulated (bar) vs measured (dot line) soluble iron concentrations in surface and corresponding dissolved iron fraction (unitless) during april 2001. (a) Soluble iron concentration over Kosan ; (b) Soluble iron measured during the C05 cruise. DIF over Kosan. (DIF) during the C05 cruise.

Sensitivity to SO_2 emission doubling.

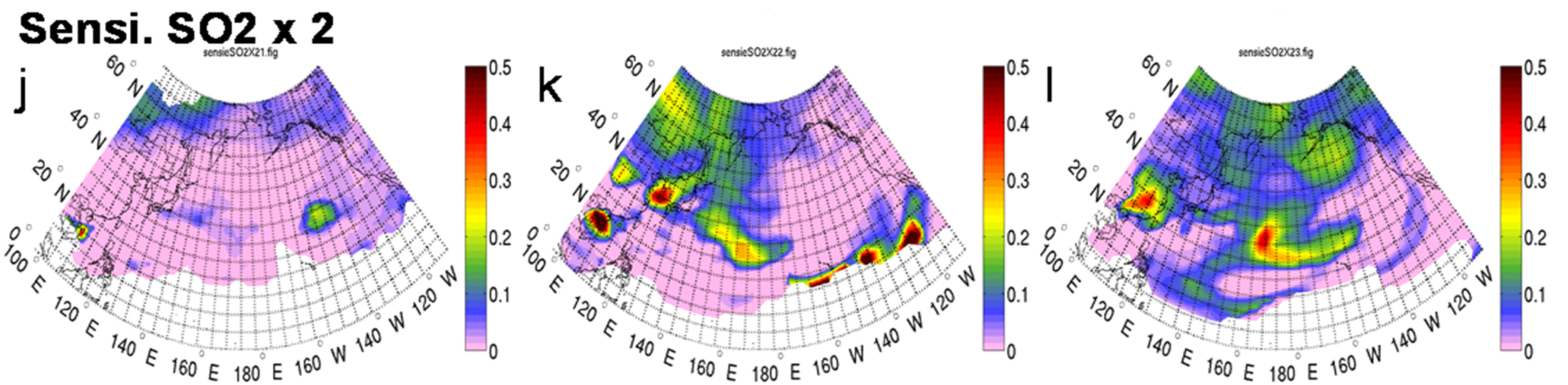

Sensitivity of soluble iron production to a doubling of SO2 sources. Fraction defined as :
(DIF (SO2x2) – DIF) / DIF

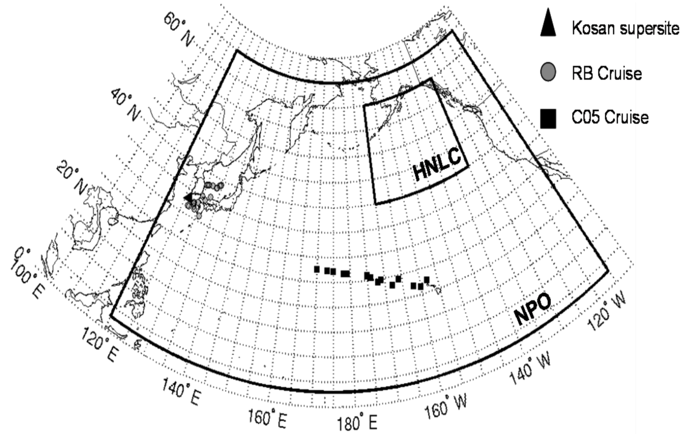

	Soluble Fe deposition (mg.m^{-2}.yr^{-1}) REF	Soluble Fe deposition (mg.m^{-2}.yr^{-1}) SO2 x 2	Relative increase (%)
NPO box (3-65 N; 120E – 115 W)	1.22	1.30	+ 6.4
HNLC box (40-60 N; 170-135 W)	1.05	1.19	+ 13.4

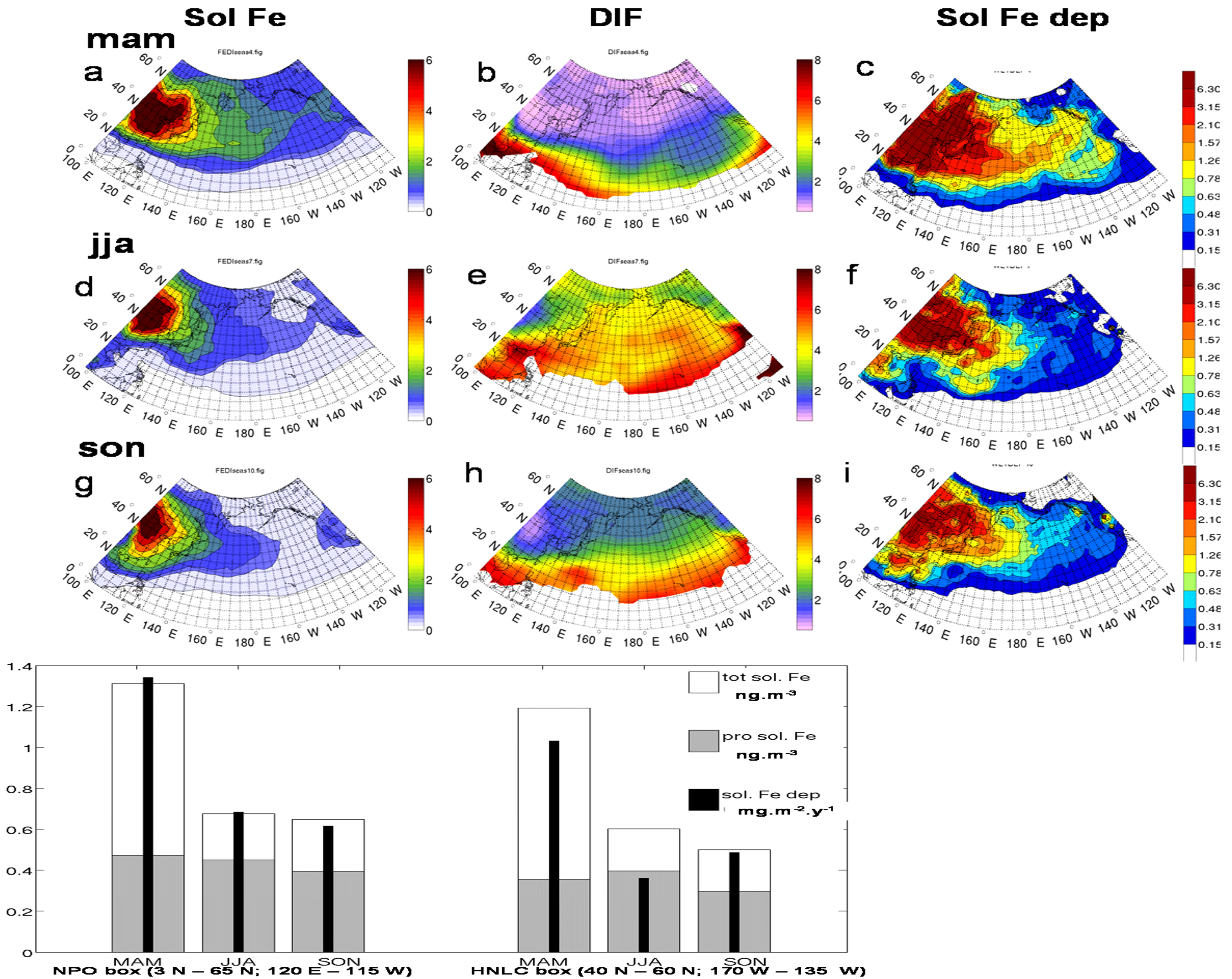

Sol Fe
DIF
Sol Fe dep
mam
jja
son
a
b
c
d
e
f
g
h
i
tot sol. Fe ng.m-3
pro sol. Fe ng.m-3
sol. Fe dep mg.m-2.y-1
MAM
JJA
SON
NPO box (3 N – 65 N; 120 E – 115 W)
HNLC box (40 N – 60 N; 170 W – 135 W)

Conclusions

- **Impact of anthropogenic pollution on soluble iron carried by dusts in the East Asian outflow.** Longer term simulations, further validations (global) and sensitivity studies are required.

- **Importance of chemical buffering effects : low intensity events (more frequent) are more efficient to produce soluble iron compared to big storms.**

  =>Validation and further development of dust/anthro heterogeneous chemistry and aerosol µ-physic in GEOS-CHEM is an important issue for iron modelling.

- **Other mechanisms for dust iron processing and DIF increase (chlorine, iron III photoreduction / dissolution promoted by organic acids in clouds).**

- **Potential importance of continuous anthropogenic emission of soluble iron (Luo et al., 2007). Experimental characterisation of combustion iron and processing is an issue.**

How will soluble iron deposition and ecosystem response evolve in the future ?

Thank you !

Comparison (and contradiction !) with a recent GCM studies …

Lau et al., 2009 (angeo special issue)

K. M. Lau et al.: Response of the atmospheric water cycle to Saharan dust radiative forcing

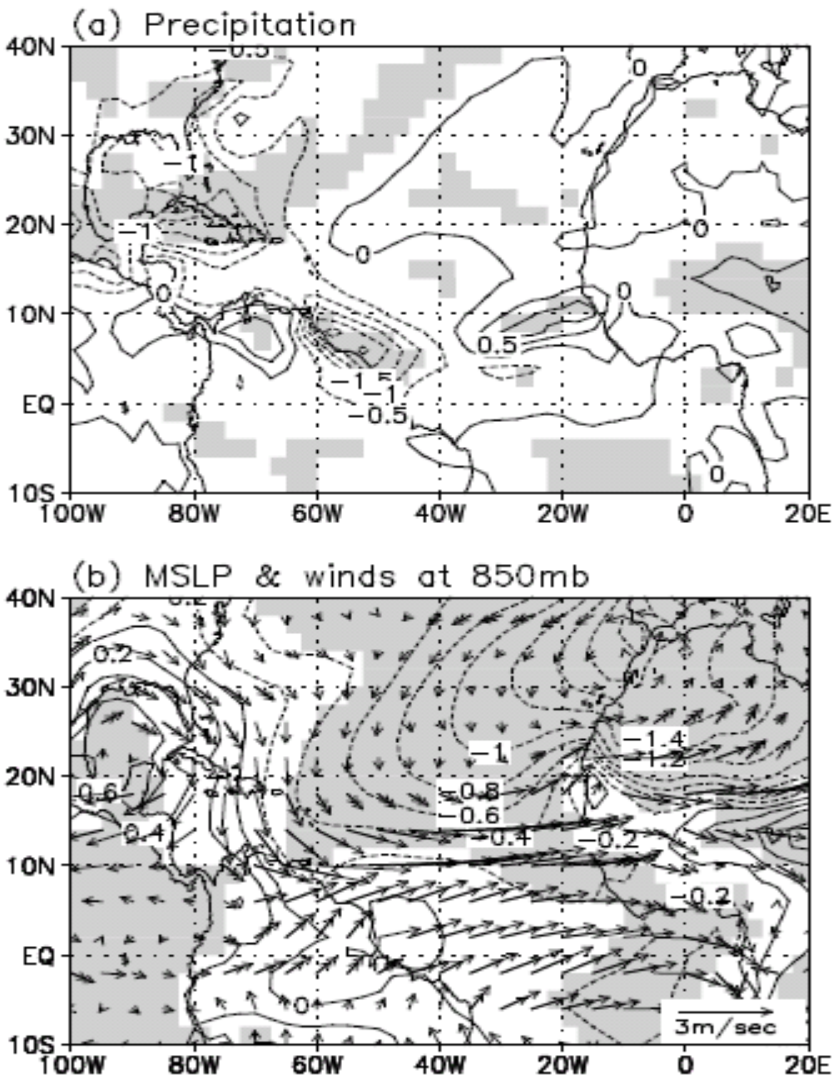

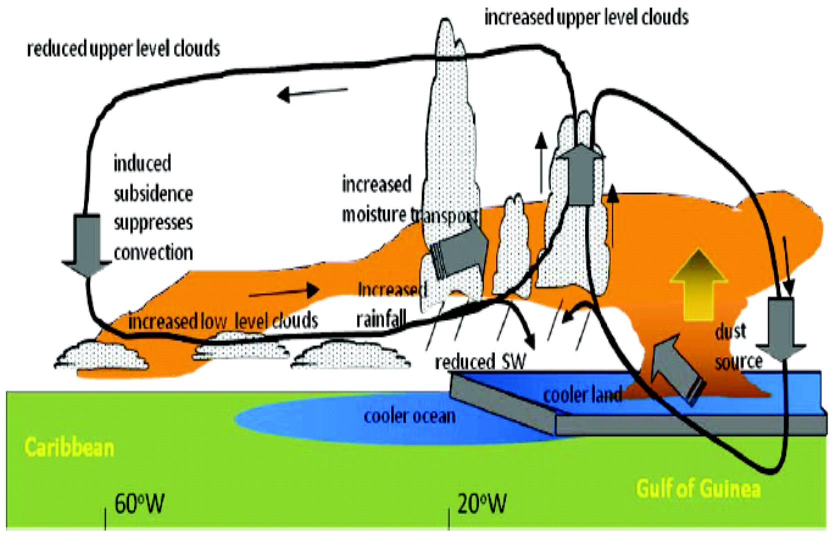

Fig. 10. Schematic diagram showing Saharan dust induced anomalous Walker-type and Hadley-type circulations, and accompanying chan[ges] in components of the atmospheric water and energy cycle, across West Africa, the Atlantic and the Caribbean.

Extended domain, 60 km resolution

JJA 1996-2006

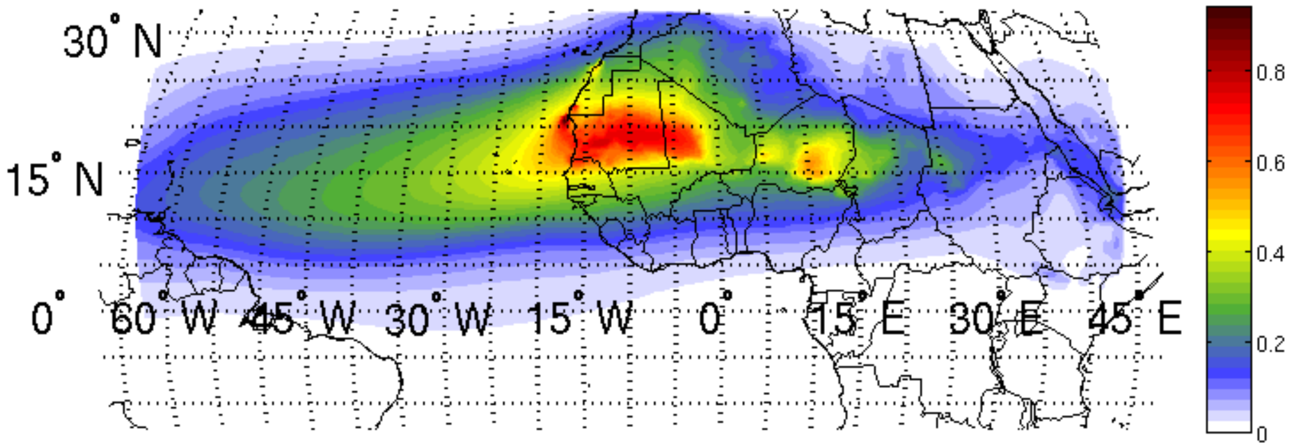

AOD

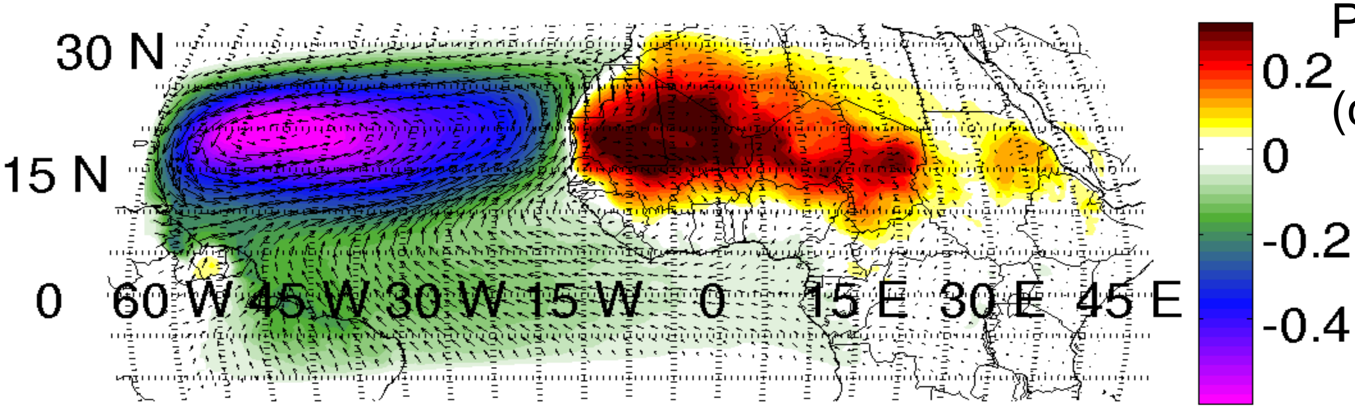

Psea

(cb dust – nodust)

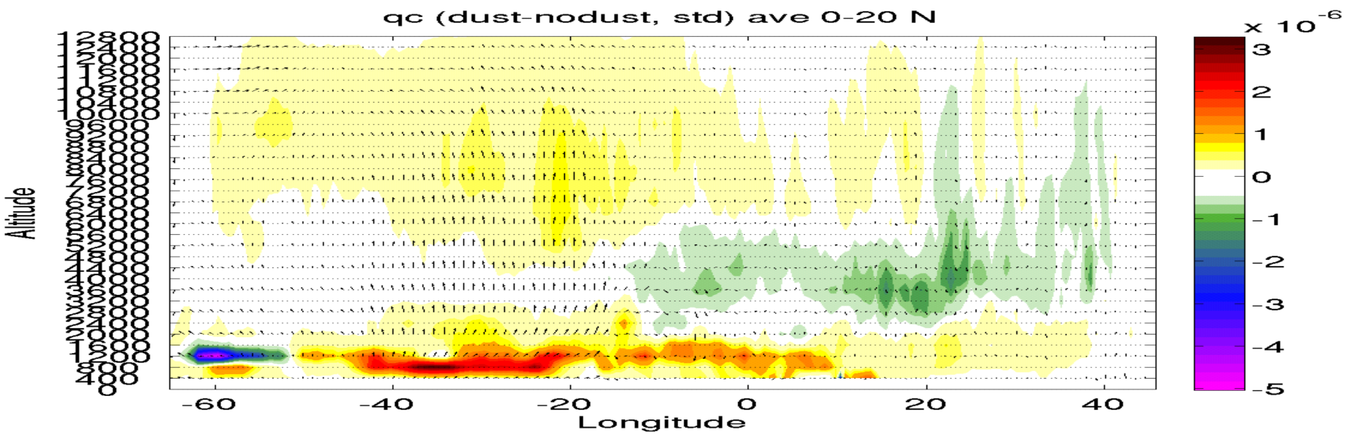

Qc and vertical circulation (dust – nodust)

Does this change precipitation anomaly over Sahel ?

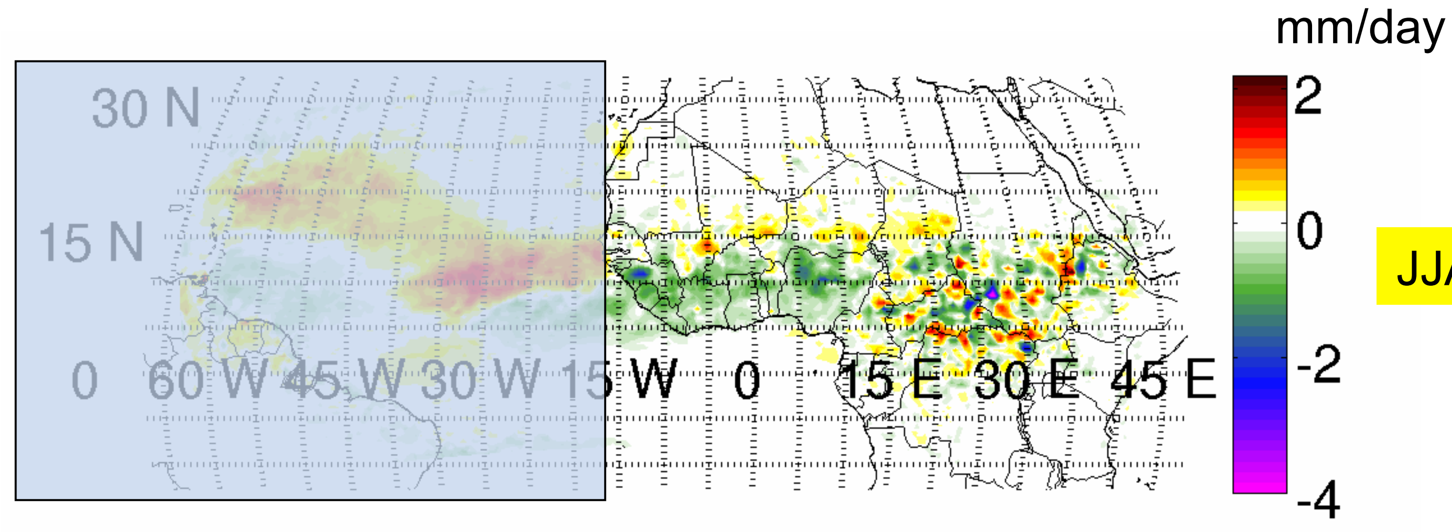

JJA 1996-2006

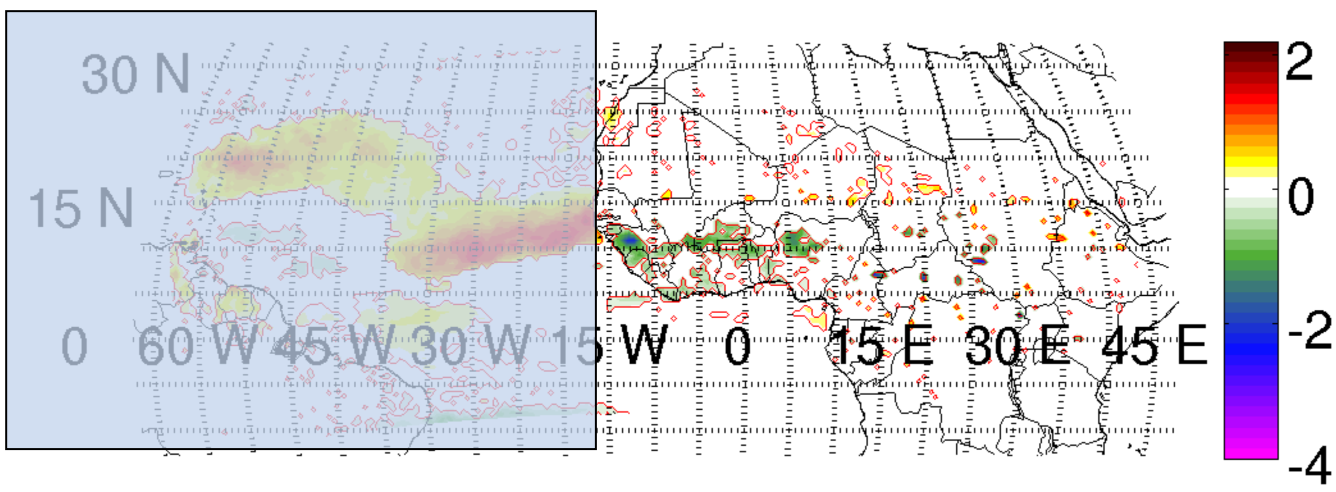

JJA 1984-2006

+ 95 % sig.

Consider zapping …

Dust Radiative forcing effect over the the ocean ?

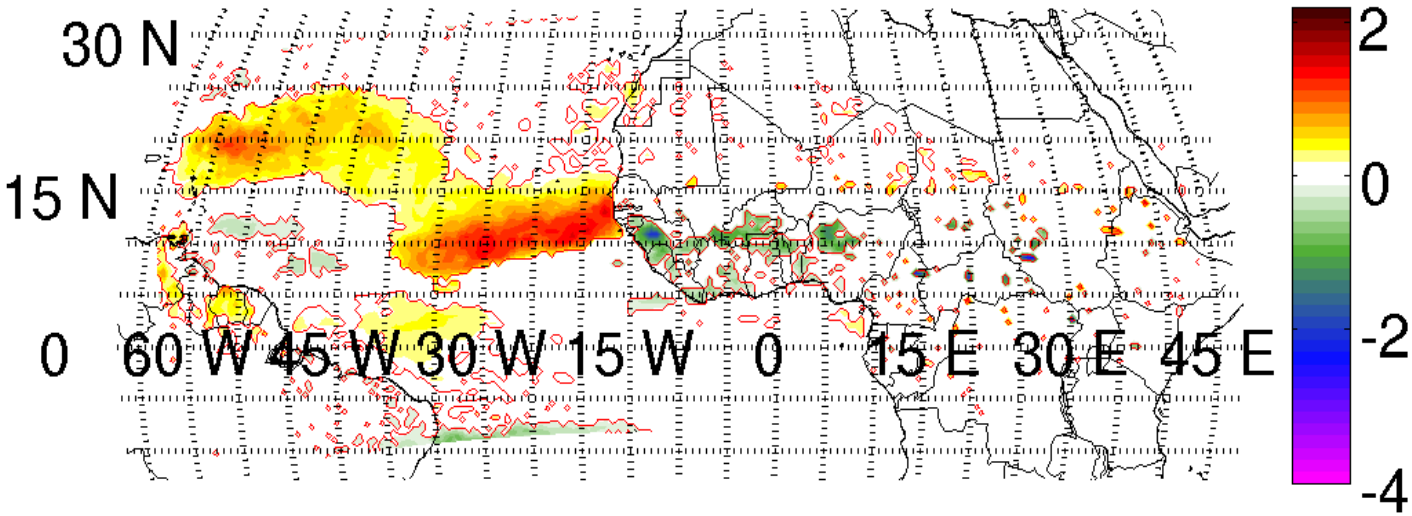

Over ocean only diabatic heating contribution is efficient since SST are forced (only diurnal variation is accounted for).

Can it affect results obtained over the Sahel ?

Can we trust RegCM climate/dust simulations over the ocean ?

Beyond the diurnal cycle : Seasonal cooling of the ocean mixed layer

Simple experiment : SST* = SST - 0.8 x AOD

as a result of less SW absorbed in ocean mixed layer due to dust extinction

(consistent with ***Avila et al., 2007***, ***Evan et al., 2009***, ***Yoshioka et al.,2007 studies using observation and coupled ocean models***)

T2m (temperature difference)

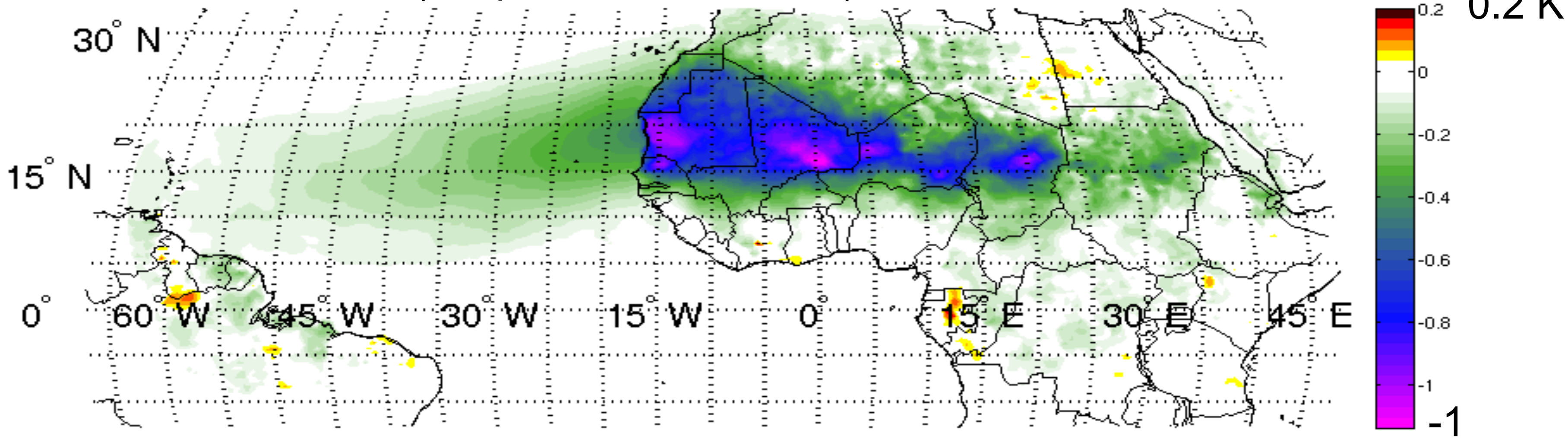

Limits of the hypothesis: SST anomaly is applied instantaneously

JJA 85-06

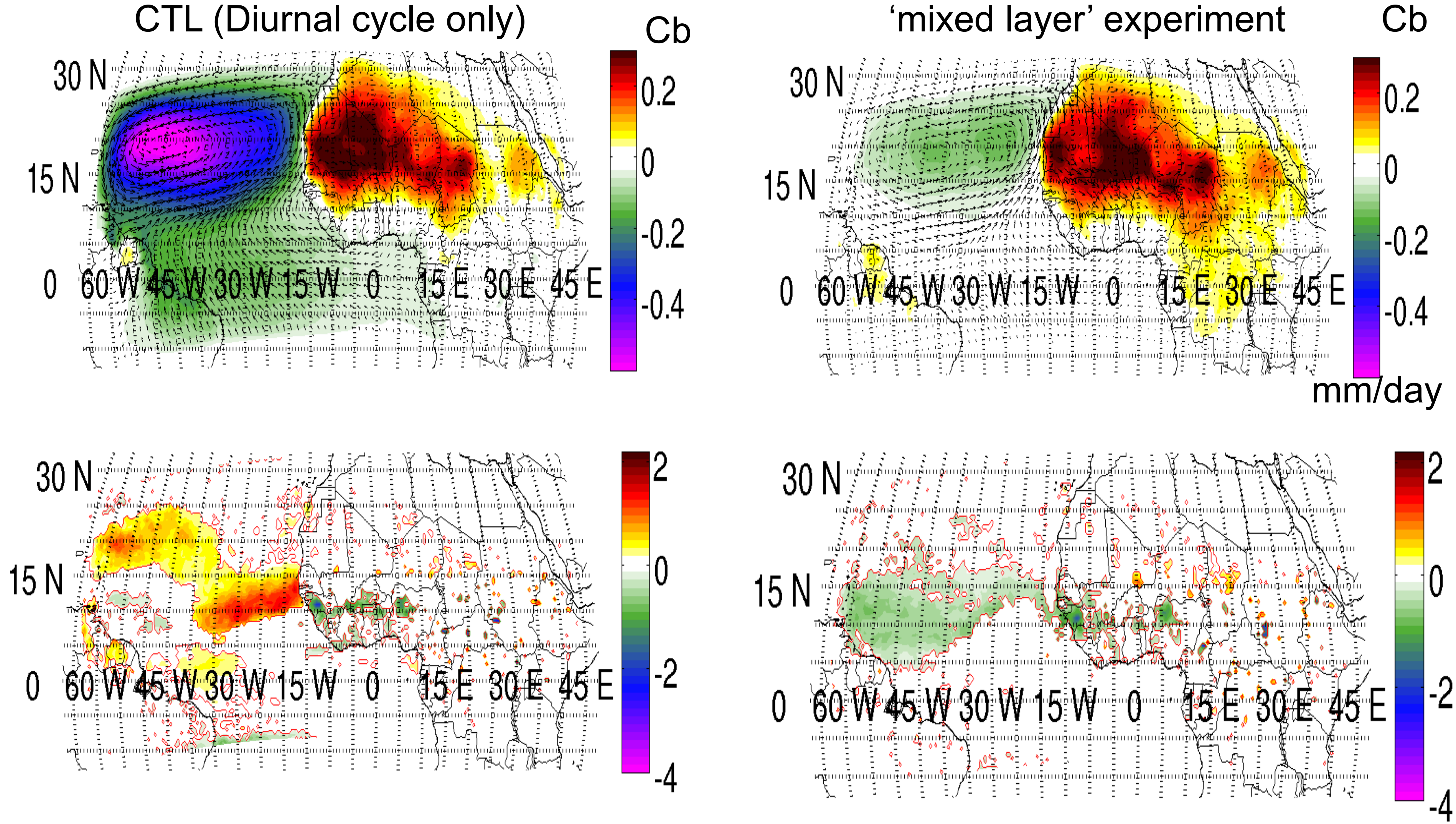

⇨ Robustness of Sahel drying signal

Over the Ocean : Where is the truth ?

Type of response A :

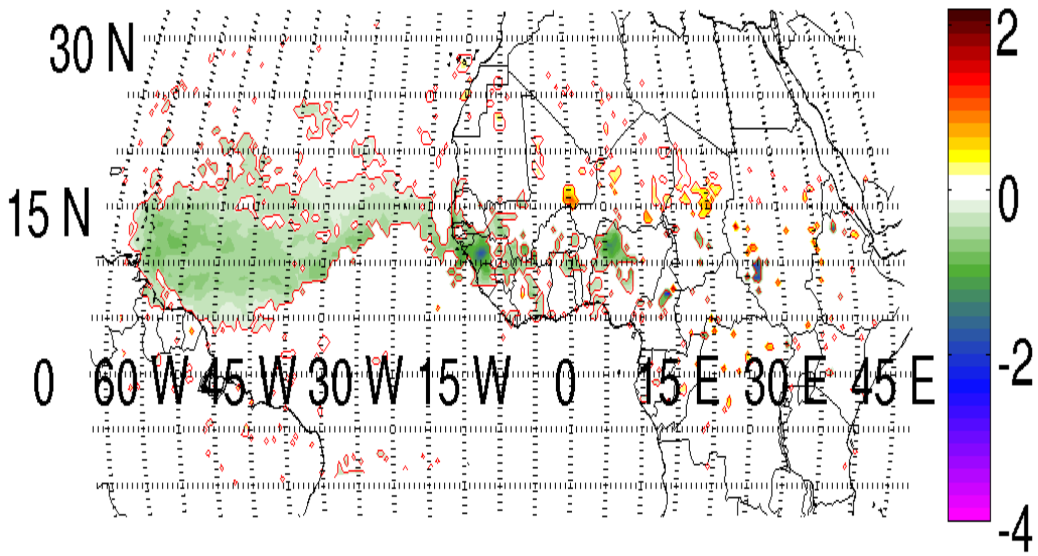

consistent with lower cyclonic activity during ‘anomalous’ high dust season
(Lau and Kim, 2007 comparing 2005 and 2006)

Type of response B :

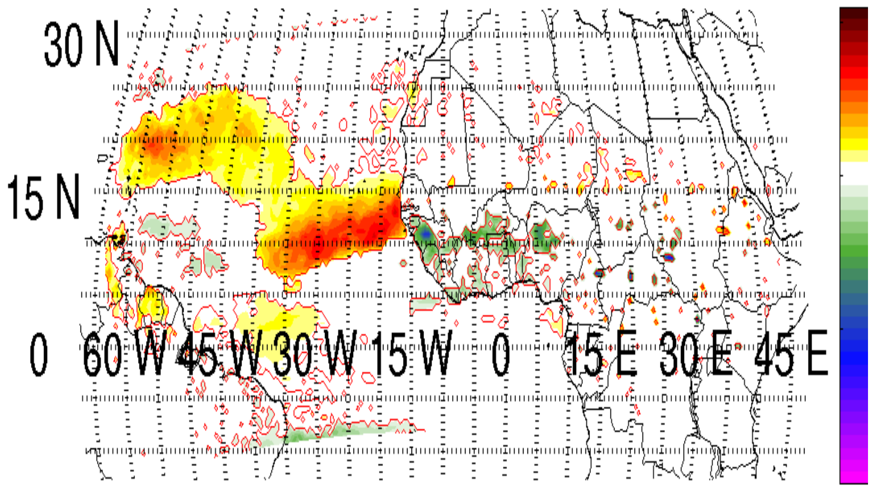

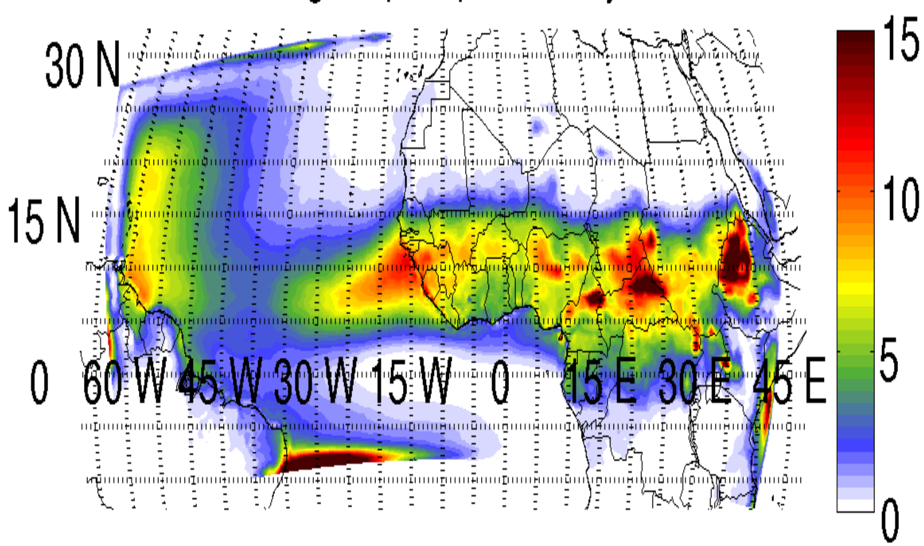

Wilcox et al., 2009 GRL

(using modis and TRMM observation)

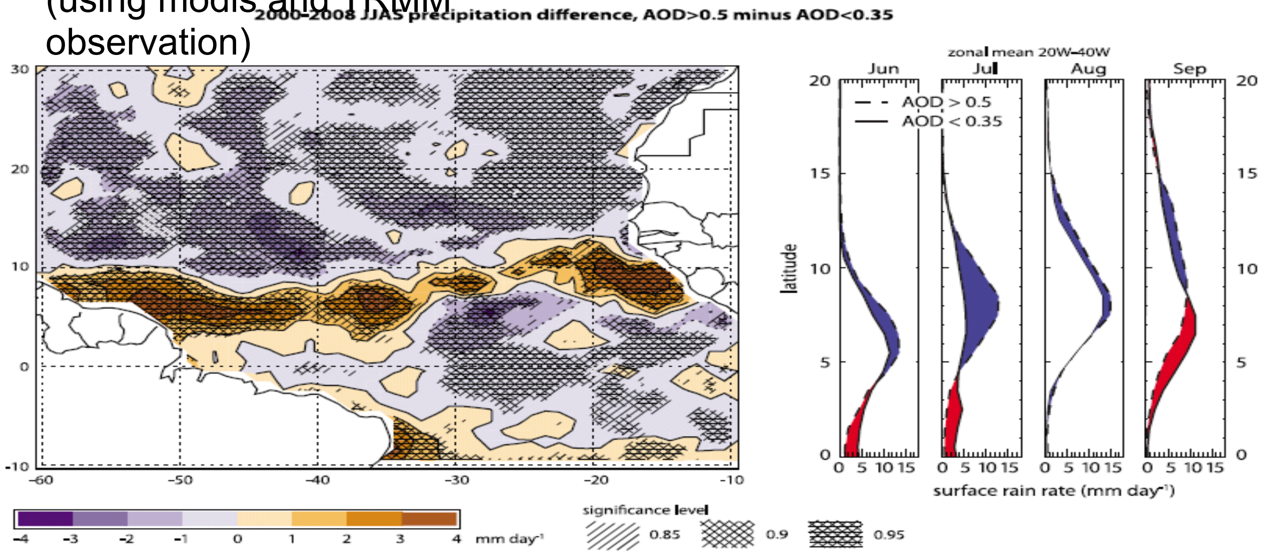

Figure 4. Difference in P (in mm d^{-1}) between dust outbreak conditions and low dust conditions. (left) Spatial distribution where the degree of hatching indicates level of significance of the difference compared to variability of pentad averages. The mean position of the ITCZ during the JJAS season is 8°N latitude. (right) Zonal-mean averaged 20° to 40° W by latitude of P during dust outbreak conditions (dashed) and low dust conditions (solid). Higher values during dust outbreaks denoted in blue, and lower values in red.

Saharan dust layer induce a northward shift of ITCZ

(the diabatic warming effect would be predominant)

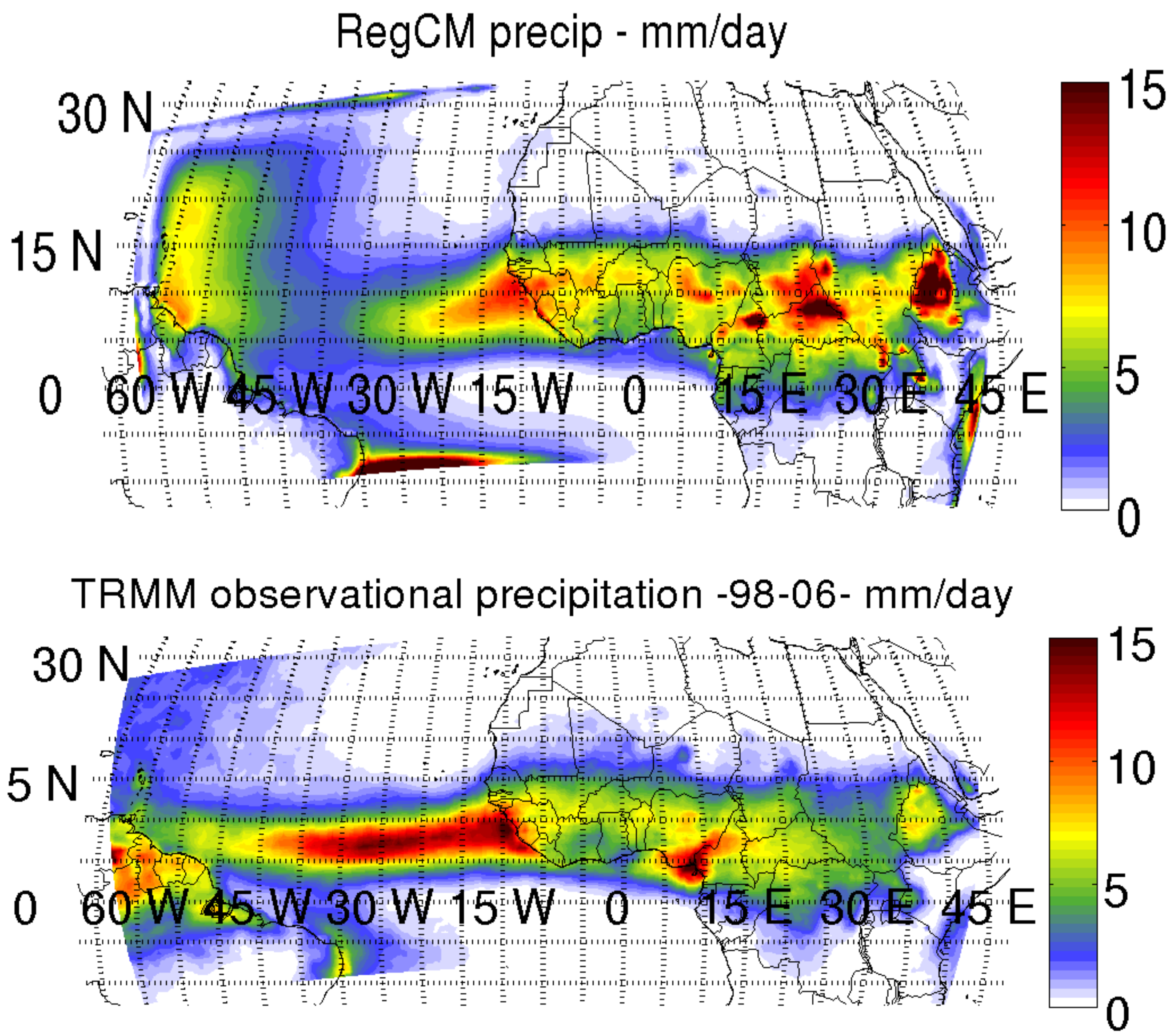

RegCM precip - mm/day
30 N
15 N
0
60 W
45 W
30 W
15 W
0
15 E
30 E
45 E
15
10
5
0
TRMM observational precipitation -98-06- mm/day
30 N
15 N
0
60 W
45 W
30 W
15 W
0
15 E
30 E
45 E
15
10
5
0

STD case SST* case

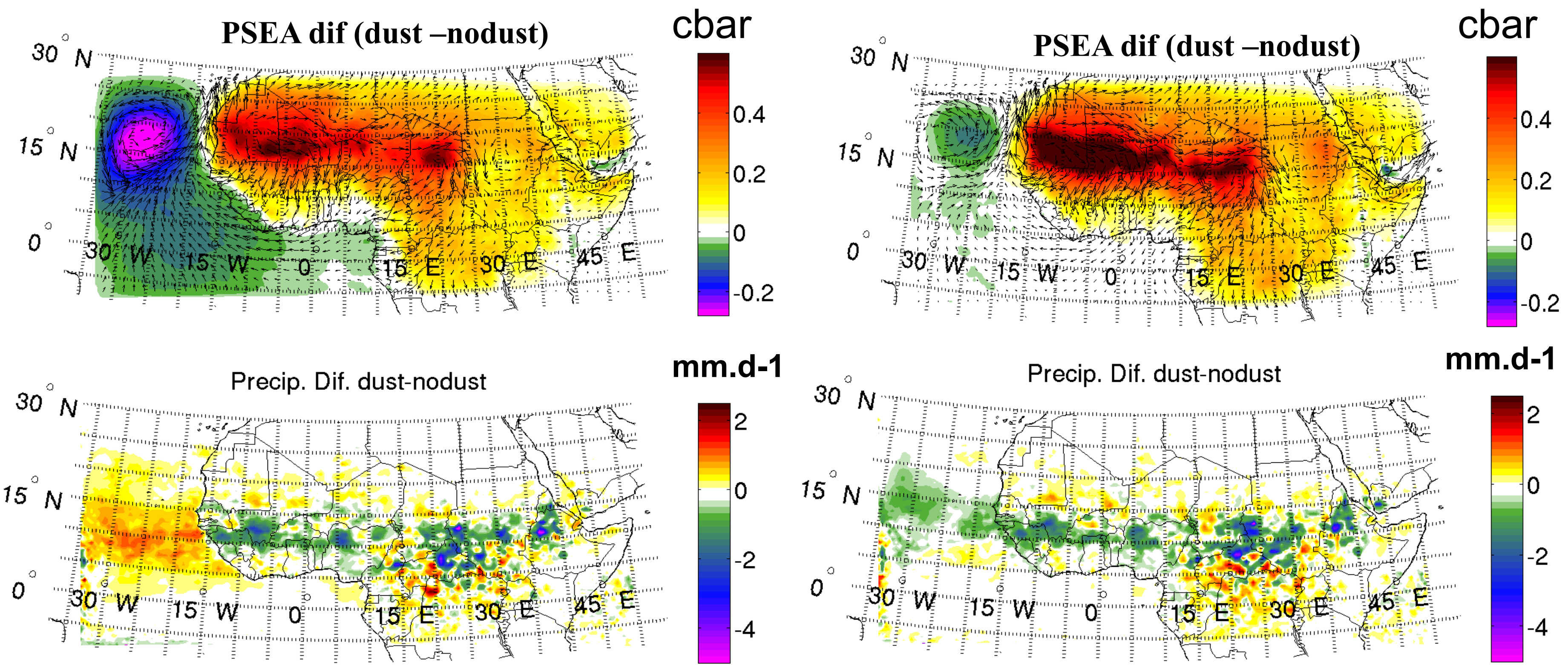

With SST correction : dust induced cyclonic anomaly but less precipitation over the ocean …

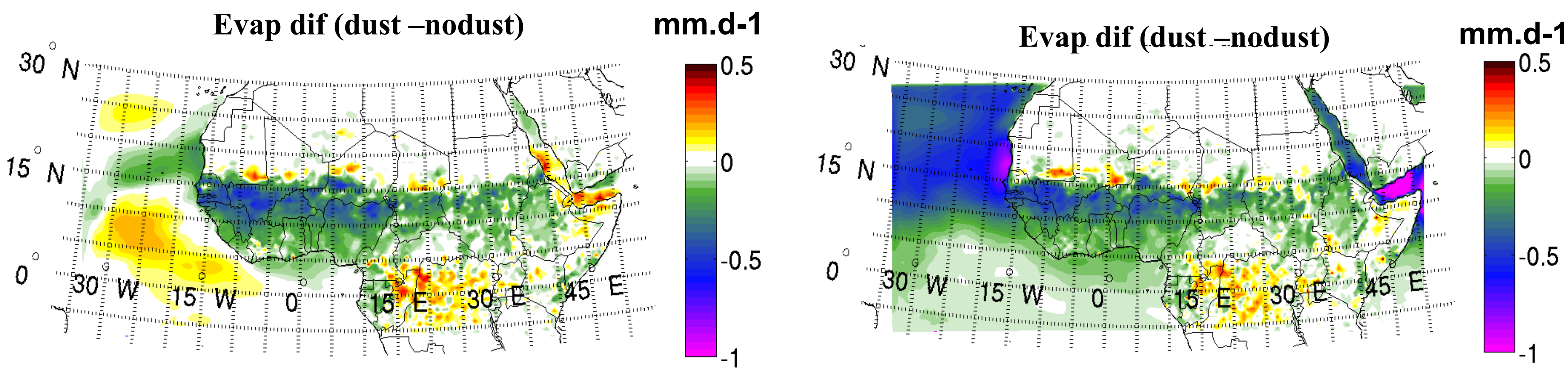

Climate sensitivity to dust absorption properties

STD

Dust bins size diameter (µm)	0.01-1	1-2.5	2.5-5	5-20
K_{ext} ($m^2.g^{-1}$)	2.45	0.85	0.38	0.17
g	0.71	0.76	0.81	0.87
SSA	0.95	0.89	0.80	0.70

A close up of a field of view of Fine Particles collected on the East Mediterranean Shore. Most particles are either spherical sulfates (similar to ammonium sulfates in appearance) or short aggregates of diesel particles.

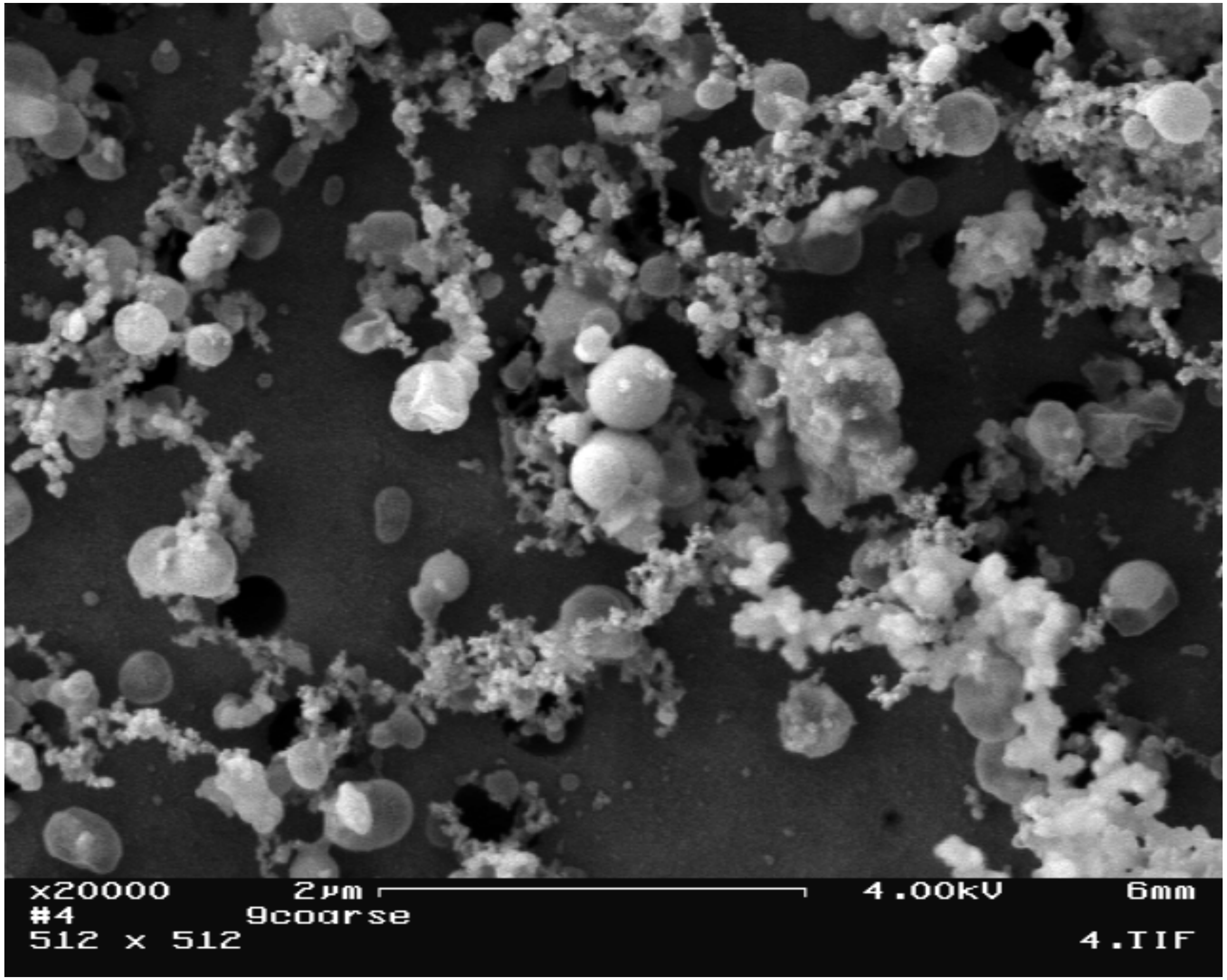

Thanks to
Prof. Mamane

Cubes of 3-7 μm <u>sea salt particles</u>, attached to a <u>mineral</u>, from the coarse fraction. Sea salt (Na, Cl) particles were found at both particle size fractions.

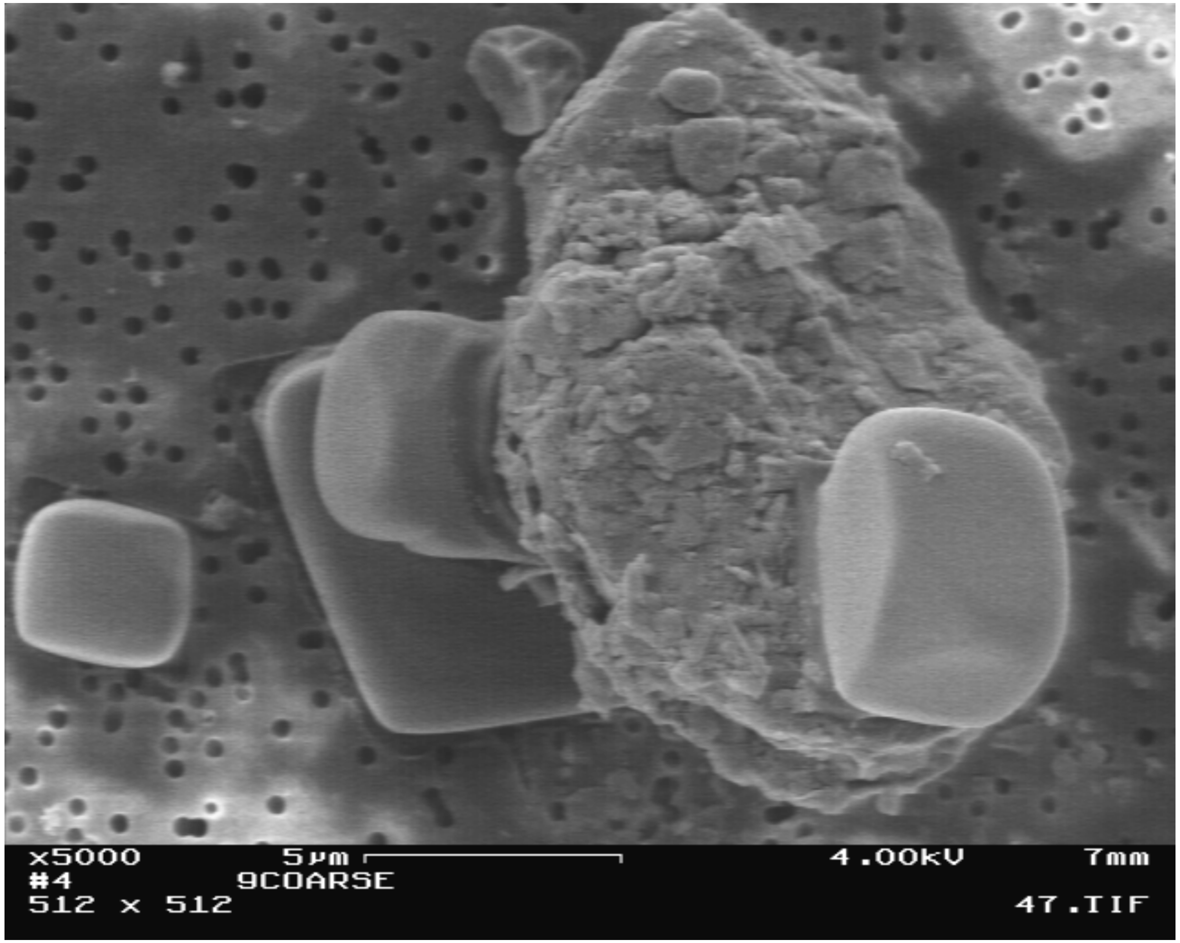

Typical Irregular Mineral with very rough porous surfaces collected at the coarse fraction. A spherical 1.5 μm coal fly ash is seen at the top, and a "crushed" spore at the upper left corner.

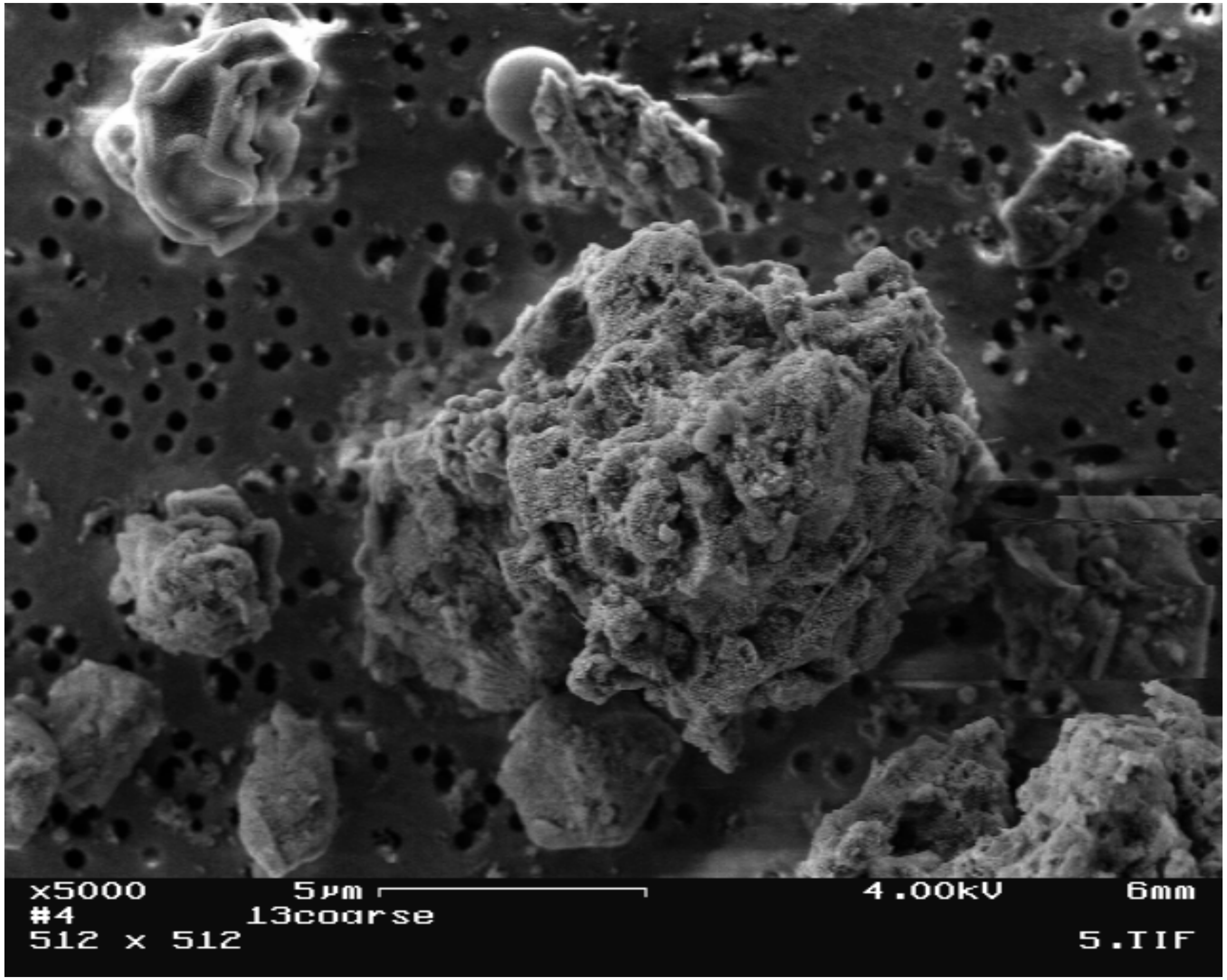

Oil Combustion Cenosphere rich in Ni and V collected in the coarse fraction. These are typical particles emitted from combustion of heavy oil.